Studies on reactivity of amino acid Schiff bases and formation of multinuclear Cu(II) complexes

A
Thesis Submitted
In Partial Fulfillment of the Requirement
for the Degree of

DOCTOR OF PHILOSOPHY

By

Rajesh C M

Department of Chemistry
Indian Institute of Technology Guwahati
Guwahati-781039
October-2015

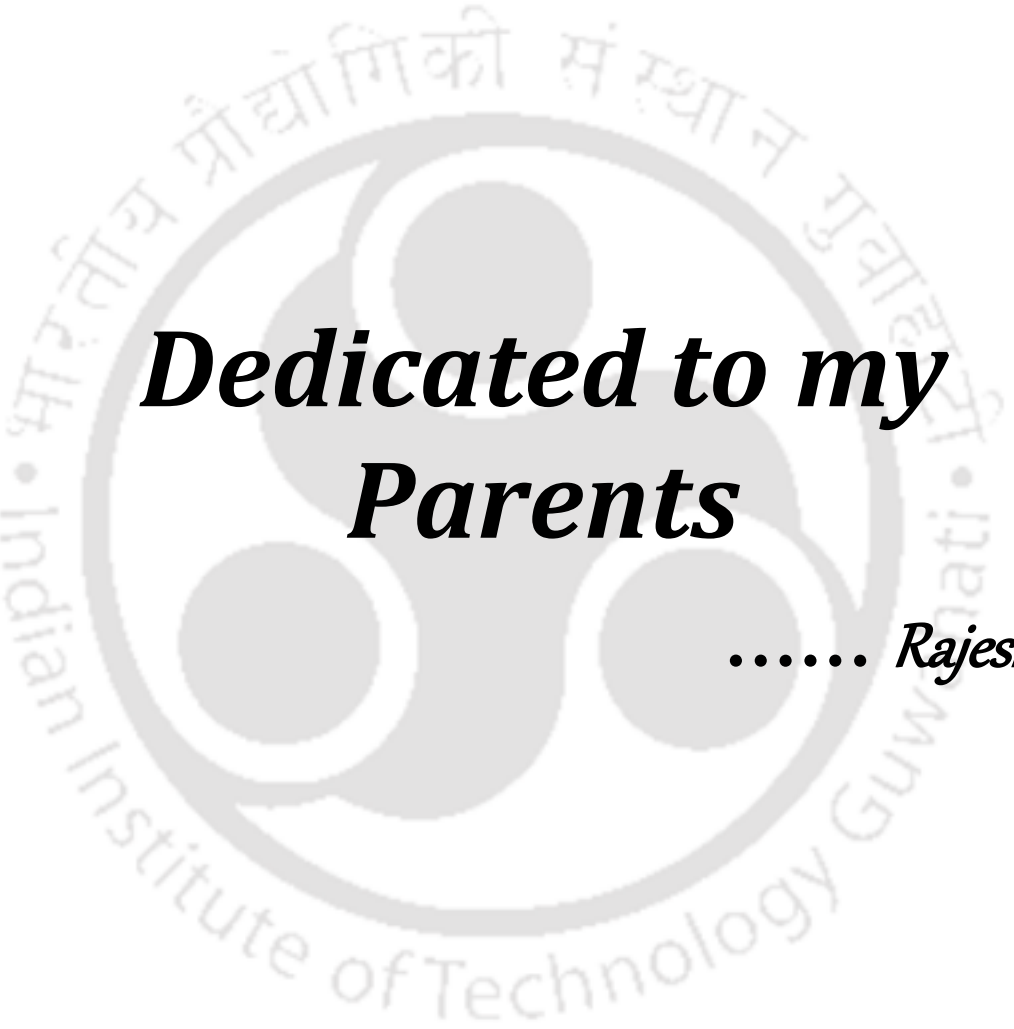

Dedicated to my Parents

…… Rajesh C M

INDIAN INSTITUTE OF TECHNOLOGY GUWAHATI

Department of Chemistry

STATEMENT

I hereby declare that the matter embodied in this thesis is the result of investigations carried out by me in the Department of Chemistry, Indian Institute of Technology Guwahati, India under the supervision of Prof. Manabendra Ray, Professor, Department of Chemistry, Indian Institute of Technology Guwahati, India.

In keeping with the general practice of reporting observations, due acknowledgements have been made wherever the work described is based on the findings of other investigations.

October, 2015

I. I. T. Guwahati Rajesh C M

Prof. Manabendra Ray
Professor
Indian Institute of Technology Guwahati
Department of Chemistry
Tel. 91 361 258 2310
Fax.91 361 258 2349

CERTIFICATE

This is to certify that Mr. Rajesh C M has been working under my supervision since July 2010. I am forwarding his thesis, entitled, "**Studies on reactivity of amino acid Schiff bases and formation of multinuclear Cu(II) complexes"** being submitted for the degree of Doctorate of Philosophy of this Institute. I certify that he has fulfilled all the requirements according to the rules of this Institute, and that the investigations embodied in this thesis have not been submitted elsewhere for a degree.

October, 2015
I. I. T. Guwahati

Prof. Manabendra Ray
Supervisor

I take this opportunity to express my deep sense of gratitude and indebtedness towards my supervisor **Prof. Manabendra Ray**, *Department of Chemistry, IIT Guwahati for his guidance, tireless efforts, perpetual encouragements and moral supports at each and every step of my research work, which enable me to complete my thesis work. He helped me to recognize what was important, and made many contributions to this work. I am fortunate enough to have his teaching about how to cultivate scientific thoughts.*

I would like to acknowledge my sincere gratitude to all my doctoral committee members, Prof. Gopal Das, Prof. V. Manivannan and Dr. Chandan Mukherjee for their insightful advices and valuable suggestions.

I express my sincere appreciation to Dr. Chandan. K. Jana, Assistant Prof., Department of Chemistry, I.I.T. Guwahati for his valuable suggestions.

I also express my sincere thanks to all faculty members, Department of Chemistry, IIT Guwahati for their help and encouragement.

I am thankful to the Institute, Indian Institute of Technology Guwahati for providing me with the state of the art infrastructure and facilities for advanced research.

I am grateful to all non-teaching staffs of the Department for their technical support.

I would like to thank DST under FIST program for providing single crystal XRD instrument facility and B. Das for mounting the crystal.

The financial support from Department of Science and Technology (DST), New Delhi is duly acknowledged.

I express my deep sense of gratitude to Prof. N. S. Nagarajan and Professor Abraham Jhon (Gandhigram Rural University, Dindigul, Tamil Nadu) for inspiring me to continue with chemistry.

I would like to thank my former and present group members Dr. Subash Chandra Sahoo, Dr. Mrigendra Dubey, Dr. S.H. Faizi and Chandani Rani Das for their timely help, support and for the wonderful time we shared during this period.

I am thankful to all research scholars and M.Sc students, Department of Chemistry, IIT Guwahati for their help.

I extend my sincerest special thanks to Mrigendra Dubey, S.H. Faizi, Chandani Rani Das, K. Radhakrishnan, M. Kannan, S. Baskar, Vasanth, Sivaramakrishnan and Vinoth Kumar for their constant help, motivation, enthusiastic company and all the wonderful time we spent in various events.

I wish to thank my childhood friend Dhakshnamurthy for accompanying me in my harder days of my life.

I wish to thank from the bottom of the heart to my closest well wisher K. Rajarajeswari for her constant support in every aspect to achieve this level.

At last but not least, I want to express my sincere thanks to all of my family members, especially to my Father (Shri- Mahalingam Chinnian), Mother (Smt. Vasantha Mahalingam) and Sister (M. Banu Priya) for their constant encouragements and moral supports during my research work.

Rajesh C M

Schiff bases are imines bearing a hydrocarbyl group on the nitrogen atom $R_2C=NR'$ ($R' \neq H$) and is formed by the condensation reaction between a primary amine and an aldehyde or ketone. Formation and reactions of Schiff bases are important both in terms of their relevance to biology and widespread use as ligands in coordination chemistry. We were especially interested in using Schiff bases, formed between natural amino acids and salicylaldehyde, as ligand. Schiff base formation and dissociation plays an important role in the amino acid transformations in biology, such as, racemization of amino acids, transamination, decarboxylation and C-C cleavage reactions catalyzed by pyridoxal phosphate (PLP, a co-factor or the active form of vitamin B6) dependent enzymes.[1] L-Amino acid derived Schiff bases with either salicylaldehyde derivatives or pyridoxal have been used as model compounds to mimic and understand the biological reactions. This is due to their structural similarity with that of the PLP derived amino acid Schiff bases. In the past there had been several reports published on the reactivity of amino acids in presence of aromatic aldehydes and base, and in the presence and absence of transition metal ions.[2] Mostly all these studies were done with an aim of understanding or elucidating the mechanism of amino acid transformations in biology. The products of the reactions were mostly characterized in solution state. Structural characterization was seldom used.

Schiff bases as ligands are versatile and well used in the literature.[3] However, well-characterized multinuclear complexes of amino acid derived ligands are relatively fewer. Multinuclear cages, capsules of different sizes and shapes have been synthesized in view of their potential use as selective hosts for anion sensing, catalysis, selective recognition and

[1] (a) J. Olivard, D. E. Metzler and E. E. Snell, *J. Biol. Chem.*, 1952, **199**, 669**;** (b) H. E. Sauberlich, in *The Enzymes***,** ed. W**.** H. Sebrell and R. S. Harris, Academic Press, New York, 1968, Vol. 11**,** pp. 44-74**;** (c) R. H. Holm, in *Inorganic Biochemistry*, ed. G. L. Eichhorn, Elsevier, New York, 1973, p. 1137.

[2] (a) D. E. Metzler, M. Ikawa and E. E. Snell, *J. Am. Chem. Soc*., 1954, **76**, 648; (b) G. N. Weinstein, M. J. O'connor and R. H. Holm, *Inorg. Chem*., 1970, **9**, 2104; (c) Y. N. Belokon, I. E. Zeltzer, V. I. Bakhmutov, M. B. Saporovskaya, M. G. Ryzhov, A. I. Yanovsky, Y. T. Struchkov and V. M. Belikov, *J. Am. Chem. Soc*., 1983, **105**, 2010; (d) M.-D. Tsai, H. J. R. Weintraub, S. R. Byrn, C.-J. Chang and H. G. Floss, *Biochemistry*, 1978, **17**, 3183.

[3] P. A. Vigato and S. Tamburini, *Coord. Chem. Rev.*, 2004, **248**, 1717 and references there in.

separation of guest molecules.[4] Addition of chirality to the design, in principle, can extend their utility further towards chiral recognition. Incorporation of chirality through Schiff-base ligands derived from amino acid is attractive due to their ease of synthesis and excellent metal binding properties.

However, very few attempts were made to incorporate a chiral centre within a metallo-organic assembly or a chiral host using such ligands. Schiff bases of amino acids are also one of the cheapest and easiest ways to incorporate chirality within a ligand as L-Amino acids occur in nature in enantiopure form and thus commercially cheap. In this thesis we chose to study Cu(II) complexation of multiple L-amino acid derived Schiff bases under various conditions. The Schiff bases between salicylaldehyde and L-alanine, L-threonine and L-serine were chosen as ligand. While our primary goal was to synthesize enantiopure chiral assemblies, to our surprise we observed reactions ranging from racemization, C-C bond cleavage and C-C bond formation occurred during complexation. Both Solid (structural) and solution state evidences for the observed reactivities were presented.

The thesis has been divided in to four chapters. Brief synopsis of each chapter has been provided below.

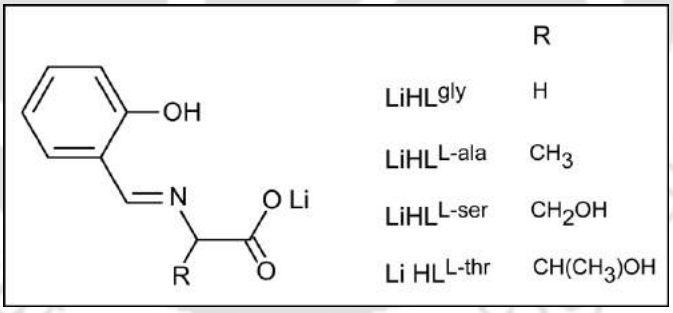

Scheme 1. Schematic representation of the amino acid Schiff bases used in this thesis.

[4] (a) Md. Akhtarul Alam, M. Nethaji and M. Ray, *Angew. Chem., Int. Ed.*, 2003, **42**, 1940; (b) D. H. Leung, R. G. Bergman and K. N. Raymond, *J. Am. Chem. Soc.*, 2007, **129**, 2746; (c) J. S. Seo, D. Whang, H. Lee, S. I. Jun, J. Oh, Y. J. Jeon and K. Kim, *Nature*, 2000, **404**, 982; (d) E. Lee, J. Kim, J. Heo, D. Whang and K. Kim, *Angew. Chem., Int. Ed.*, 2001, **40**, 399; (e) J. M. Rivera, T. Martin and J. Rebek Jr., *Science*, 1998, **279**, 1021.

Chapter 1. This chapter summarizes the literature on the biological relevance of amino acid derived Schiff bases and the use of salicylidene and pyridoxilidene amino acid Schiff bases, and its metal complexes as model compounds in understanding the mechanism of biological amino acid transformations. A summary of literature on the salicylidene amino acid Schiff base metal complexes and Cu(II) trinuclear Schiff base complexes have been presented and the objective of the thesis was defined.

Chapter 2. In this chapter, a chiral Schiff base, lithium salicylidenealaninate ($LiHL^{L\text{-}ala}$) was synthesized and characterized structurally. The structure is notable because of coordination of lithium. Lithium ion is coordinated to carboxylate and phenolate oxygens and tetrahedral in geometry (Figure **1**). Carboxylates acting as bridges between lithium ions forms a zigzag two dimensional network (Figure **1**), a pattern which is rare.[5]

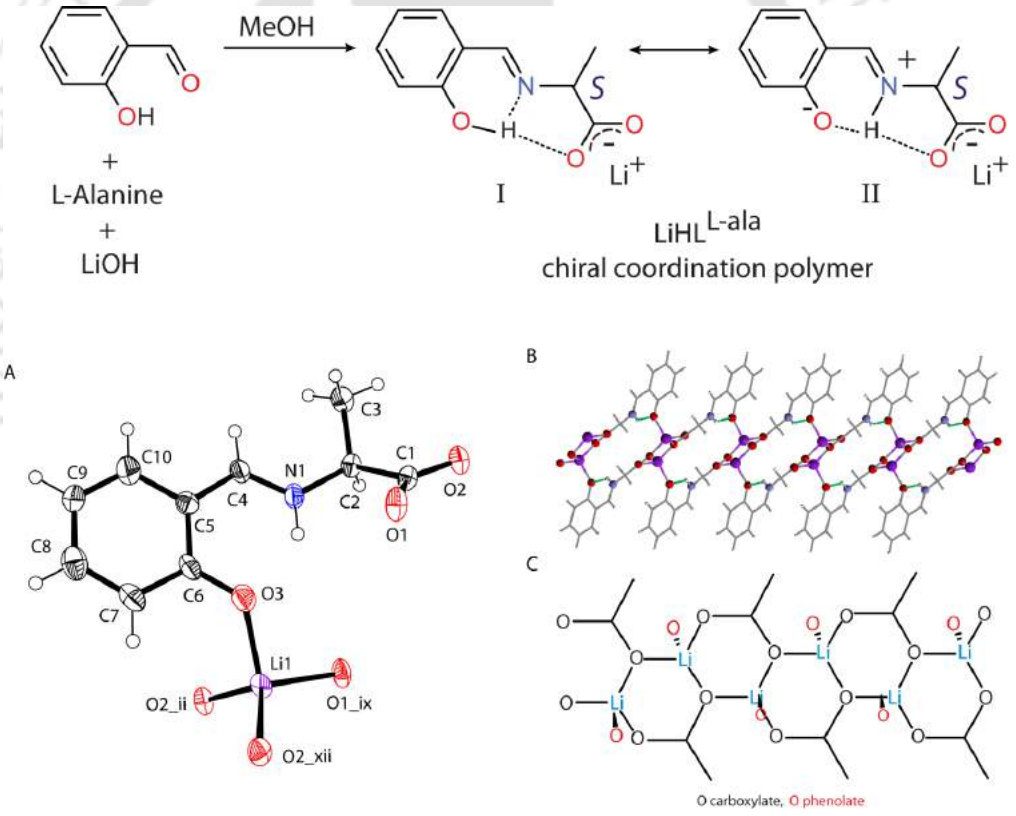

Figure 1. Scheme for the synthesis of $LiHL^{L\text{-}ala}$, (A) ORTEP diagram of the asymmetric unit of $LiHL^{L\text{-}ala}$ with thermal ellipsoids set to 40% probability, (B) and (C) showing the representations of 2D network of $LiHL^{L\text{-}ala}$.

[5] G. Miiller, G.-M. Maier and M. Lutz, *Inorg. Chim. Acta.*, 1994, **218**, 121

We have explored the complexation reaction between the above Schiff base and Cu(II) in presence of base ($LiOH•H_2O$). Quantities of base as well as metal:ligand ratios were varied to isolate structurally characterizable complex and we were successful in isolating a new hexanuclear Cu(II) cage **1**. The cage has several interesting structural features (Figure **2**). The Structure of the complex was solved under an achiral space group (*R*-3), which indicates that racemization of the amino acid has taken place during the reaction. The molecule of **1** has two tricopper units face to face with an ammonia molecule at the centre. The chirality of the ligands in tricopper units is identical but two tricopper half of hexanuclear assemblies have opposite chirality. Thus the hexanuclear assembly can be considered as a meso-isomer. By reducing the reaction temperature (up to 5 ^oC) we could able to isolate crystals **1b** (bulk) which contained more of one chiral isomer, showing optical activity. CD spectrum of **1b** in MeOH showed the presence of chiral enantiomer in the bulk by giving a negative cotton effect (Figure **3**). Variable temperature magnetic susceptibility measurements of the complexes showed that the complexes have interesting ferromagnetic property at low temperature (10-20 K).

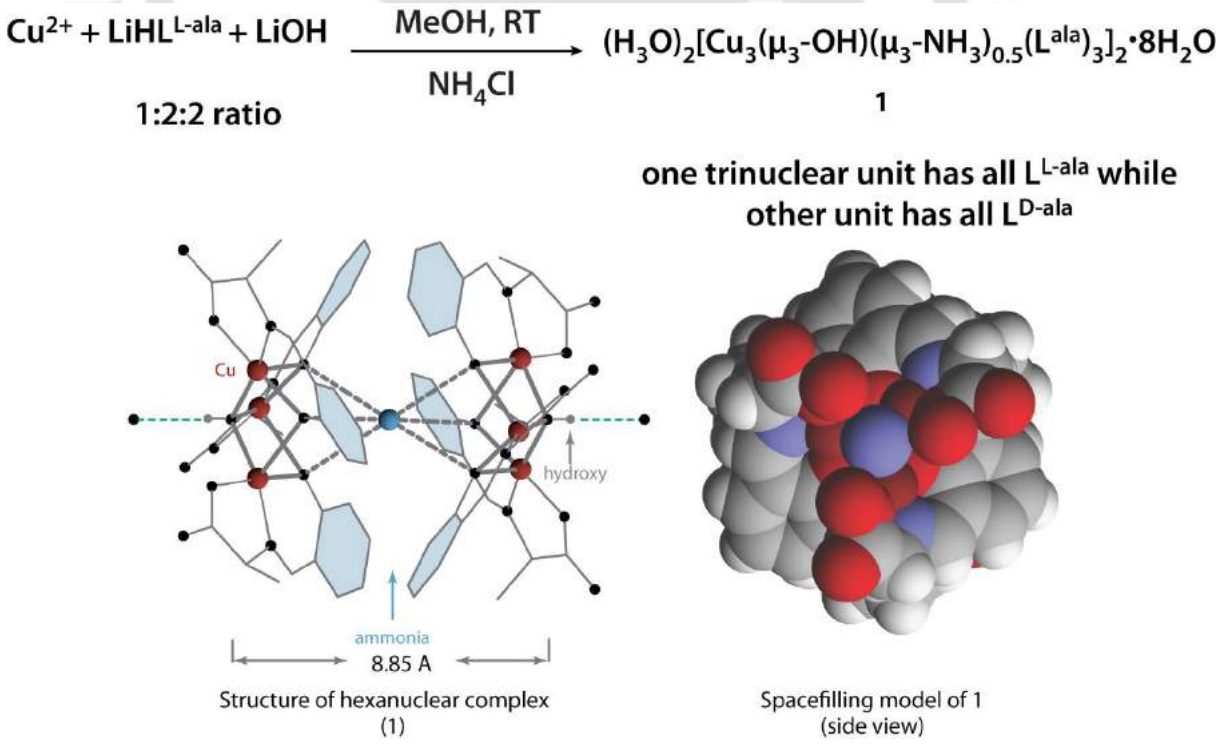

Figure 2. Scheme for the synthesis of **1** and different structural representations of the cage **1**.

Following the results of the structural analysis of the complex, the effect of base on the Schiff base's chirality in the absence of metal was studied in solution through polarimeter and CD (circular dichroism) experiments. The results of the solution state experiments indicated that racemization takes place in the absence of Cu(II), also (Figure **3**). Base or Cu(II) induced racemization of amino acid derivatives has been indicated in a number of cases in the past but structural characterization of the products or formation of this type of hexanuclear architecture was never reported.2

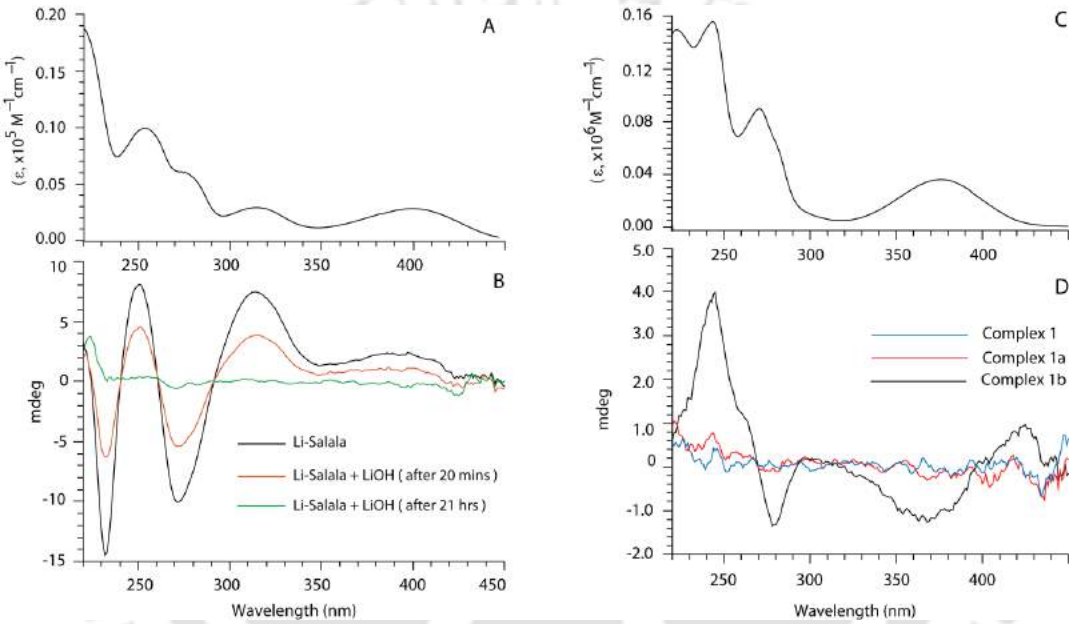

Figure 3. (A) UV-vis spectrum of $LiHL^{L\text{-}ala}$, (B) CD spectra of $LiHL^{L\text{-}ala}$ in presence and absence of LiOH, (C) UV-vis spectrum of **1** and (D) CD spectra of the complexes.

Chapter 3. Reactivity of L-alanine derived Schiff base and its Cu(II) hexanuclear cage formation were done in chapter 2. This chapter deals about the reactivity of salicylidene-L-threoninate and L-serinate Schiff bases in presence of base and Cu(II) and its Cu(II) tinuclear complex formation. The metal:ligand ratio was fixed to 1:1, whereas the base ($LiOH{\bullet}H_2O$) quantity was varied to isolate structurally characterizable complex (Figure **4**). The complexation of L-threonine and L-serine derived Schiff bases in presence of 2.33 equiv. $LiOH{\bullet}H_2O$ gave a structurally characterizable complex **2**, and a green powder which is insoluble in DMF, DMSO, water, MeOH and acetonitrile, respectively. Similarly the above

ligands in presence of 1.33 equiv. LiOH•H_2O gave a green viscous/colloidal substance with few crystals of **2** and a structurally characterizable complex **4**, respectively.

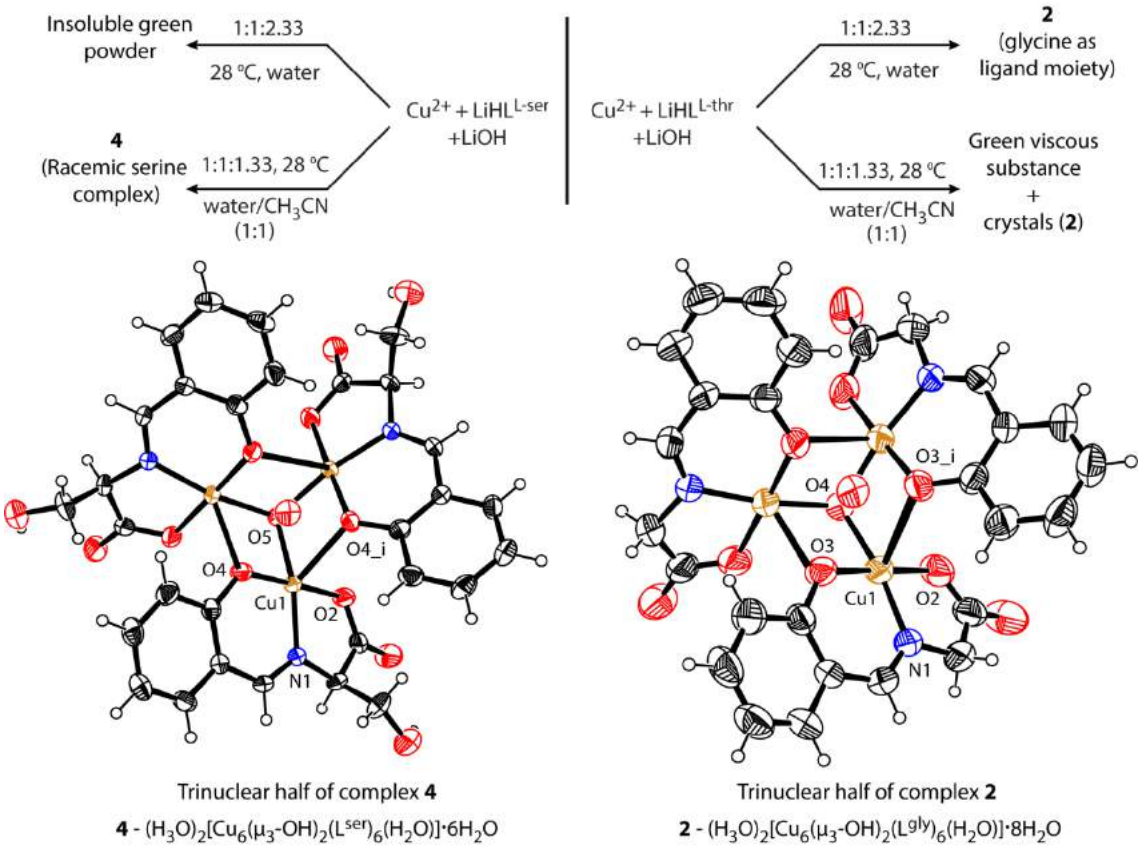

Figure 4. Scheme for the synthesis of complexes in chapter 3 and the ORTEP diagrams of the trinuclear half of the complexes **4** and **2**, with thermal ellipsoids set to 40% probability.

All the structurally characterized complexes were solved under the achiral space group (*R*-3) and the structural features of the complexes are similar to that of the complex in chapter 2. Structural characterization of **2** showed the presence of glycine in the ligand moiety of the complex indicating the occurrence of C-C cleavage in the threonine's side arm during the reaction, whereas structure of **4** showed that the serine's side arm was intact in the ligand moiety of the complex indicating the non-occurrence of C-C cleavage in the serine's side (Figure **4**). Alternatively complex **2** can also be synthesized directly from salicylideneglycinate ligand. The above results indicate that the reactions are sensitive to base quantities. In the case of L-threoninate Schiff base the extent of C-C cleavage is more when the base quantity is more and vice versa.

Apart from the structural characterization, solution state experiments were performed to know whether the C-C cleavage is happening before or after complexation in the reaction. UV-vis, ^{1}H-NMR and CD experiments were performed. A solution of ligand and base (2 equiv.) in water (D_2O, for ^{1}H-NMR) was taken for the study. Both UV-vis and ^{1}H-NMR study of the test solution showed the occurrence of dissociation of the Schiff base, whereas there is no symptom of C-C cleavage (Figure **5**).

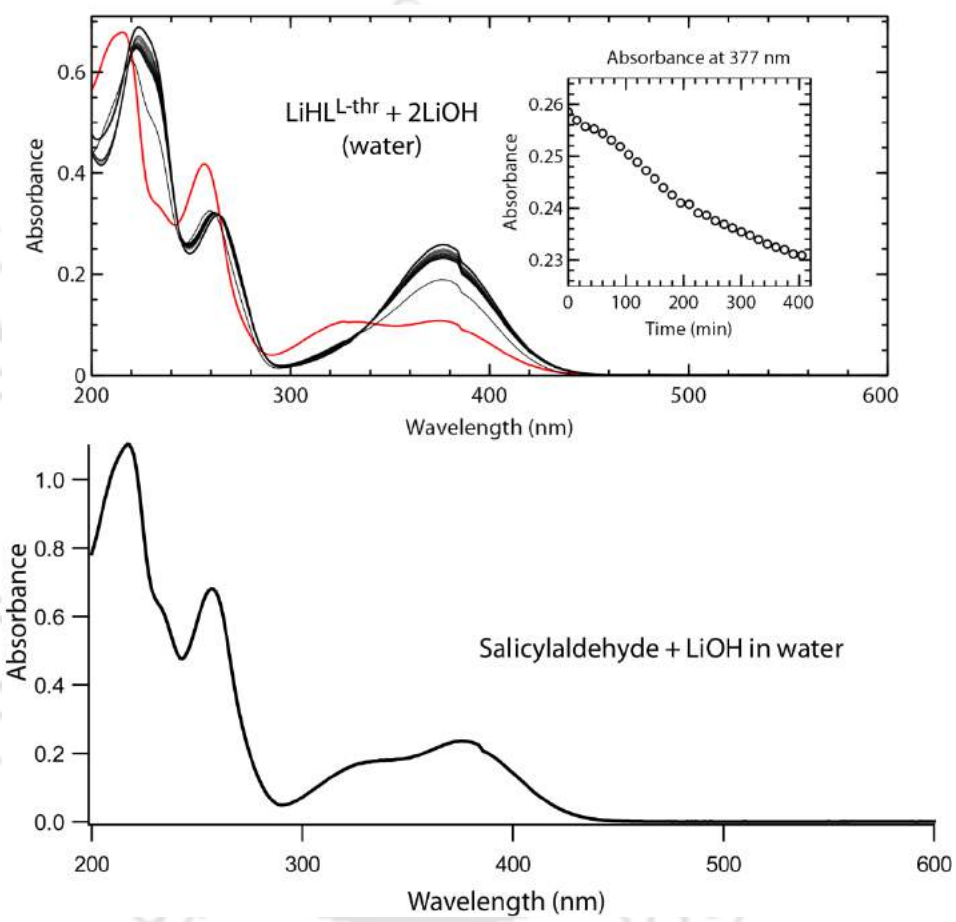

Figure 5. UV-vis spectra of $LiHL^{L\text{-}thr}$ with 2 equiv. of $LiOH{\bullet}H_2O$ monitored continuously for about 7 h (black) and (red) after about 36 h in water. The inset is the absorbance vs time plot for the same at 377 nm. (4.54×10^{-5} M) (above) and UV-vis spectra of salicylaldehyde with LiOH in water (below).

The peak corresponding to the threonine's side arm was intact in the ^{1}H-NMR spectrum of the test solution. CD spectra of the test solutions showed no bands when compared to the ligand, indicating the occurrence of racemization without C-C cleavage.

Chapter 4. In this chapter we present the isolation and structural characterization of a Cu(II) mononuclear complex of a new organic molecule which has been formed in situ within the applied reaction conditions. While exploring different conditions to isolate crystallizable Cu(II) complexes with amino acid derived Schiff bases, we have tried the use of three alkali metal hydroxides individually ($LiOH•H_2O$, NaOH and KOH) with lithium salicylideneglycinate, Cu(II) and anhydrous $CaCl_2$ with different ratios with respect to each other.

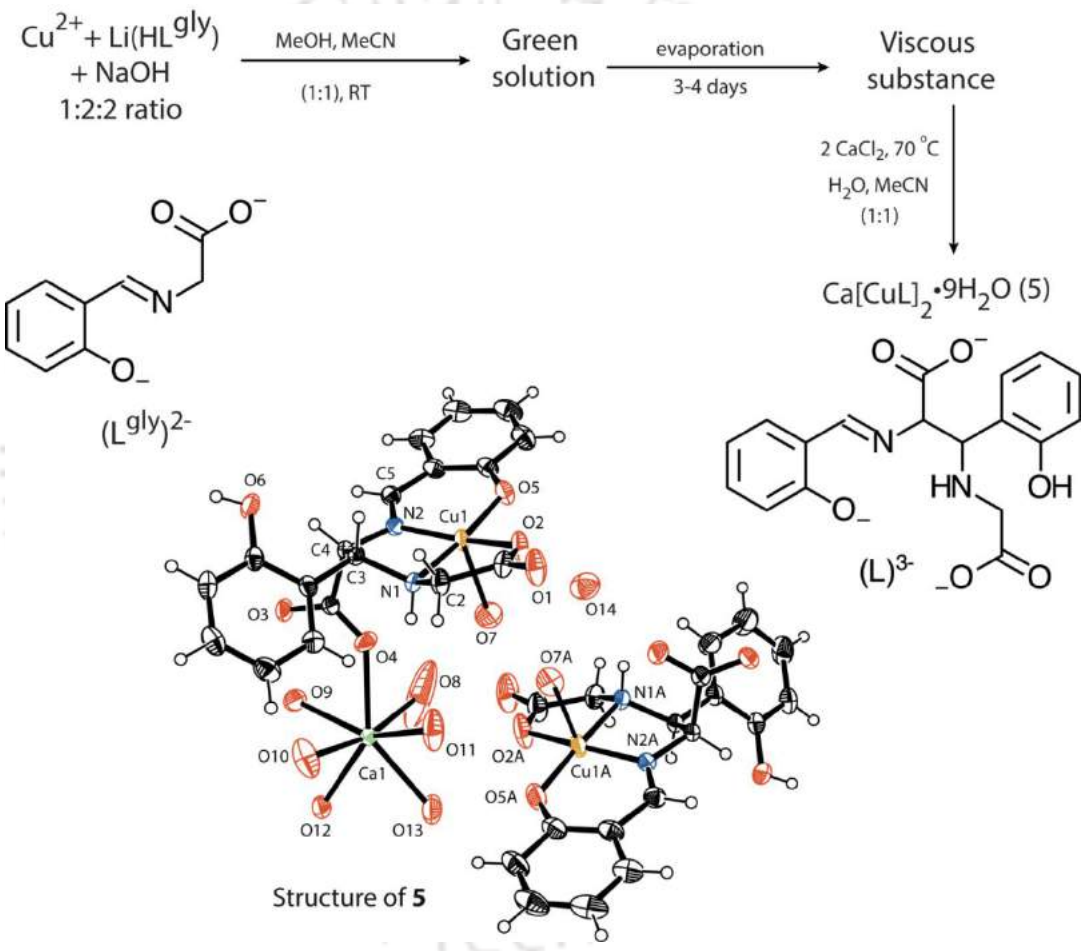

Figure 6. Synthesis of Complex **5** containing new ligand (L^{3-}) formed during complexation and the ORTEP diagram of the complex, with thermal ellipsoids set to 40% probability.

In one of the reaction we have isolated a blue crystal **5** different from the trinuclear complexes described in the earlier chapters. Structural analysis of the complex revealed the formation of a new organic molecule through C-C bond formation between two salicylideneglycinate units

in in situ within the reaction condition (Figure **6**). Such C-C bond formations in amino acid Schiff bases were not previously known. The structure was solved under *P*-1 space group. The asymmetric unit contains two mononegative molecules of the complex with one Ca(II) neutralizing the charge.

Contents

Chapter I

Introduction

Schiff bases are imines bearing a hydrocarbyl group on the nitrogen atom $R_2C=NR'$ ($R' \neq H$) and is formed by the condensation reaction between a primary amine and an aldehyde or ketone. The chemistry of Schiff bases have been well established in literature since its origin. They are large in number and variety, depending on the type of aldehyde or ketone and amines used for synthesis. In the context of chirality, Schiff bases can be classified as achiral and chiral Schiff bases. Chiral Schiff bases are relatively less in number when compared to achiral Schiff bases due to its complexity in synthesis and resolution. L-Amino acids get its priority with respect to incorporation of chirality in Schiff bases, due to its natural occurrence with enantiopurity, its ease of synthesis and relatively lower cost. Formation and reactions of Schiff bases are important both in terms of their relevance to biology and widespread use as ligands in coordination chemistry.

1.1 Relevance of Schiff bases in Biology

A number of chemical reactions take place in biology now and then. These reactions are often catalyzed by enzymes. For example, amino acid transformations in biology are essential for several metabolic processes taking place in living organisms. Some of the amino acid transformations taking place in biology are racemization, transamination, C-C cleavage, decarboxylation, α-β elimination and deamination. Most often, these reactions are catalyzed by pyridoxal 5'-phosphate (PLP) dependent enzymes. PLP the co-factor or the active form of vitamin-B_6, assist enzymes in their catalytic process by the formation and dissociation of L-amino acid derived Schiff base, between the L-lysine amino acid residue of the enzyme and the PLP, having an aldehyde group (Figure **1.1**). This is called an internal aldimine[1] formation in biology. When a substrate amino acid is ready to undergo transformation, it forms a Schiff base with PLP, by replacing the lysine residue of the enzyme in the internal aldimine. The new substrate amino acid Schiff base is called an external aldimine[1] in biology and this Schiff base formation catalyzes the amino acid transformations. Once the transformation is attained by the substrate amino acid the external aldimine dissociates and releases the transformed amino acid, which is required for other biological processes. The PLP dissociated from the external aldimine again forms a Schiff base with an enzyme, to involve in next catalytic process.

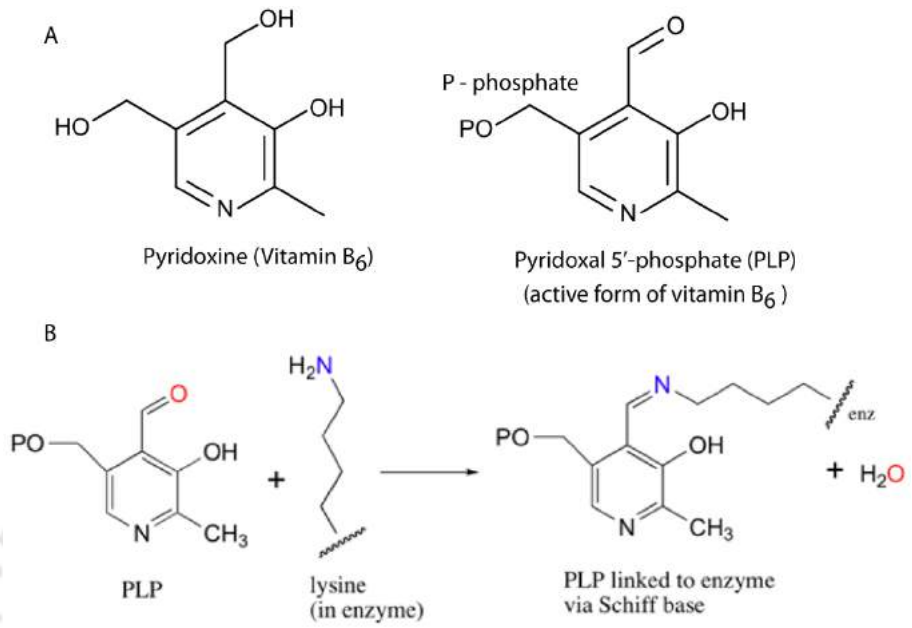

Figure 1.1. (A) The schematic representations of pyridoxine and PLP and (B) The schematic representation of a Schiff base formation between an enzyme and PLP.

A solid state example, for the amino acid derived Schiff base in biology was reported by Sun and his co-workers.[2] They have solved the crystal structure of the PLP dependent enzyme, called *serine dehydratase* (SDH), isolated from a human liver in the Schiff base form (an internal aldimine) (Figure **1.2**). It catalyzes the deamination of L-amino acids, yielding ammonia and pyruvic acid.

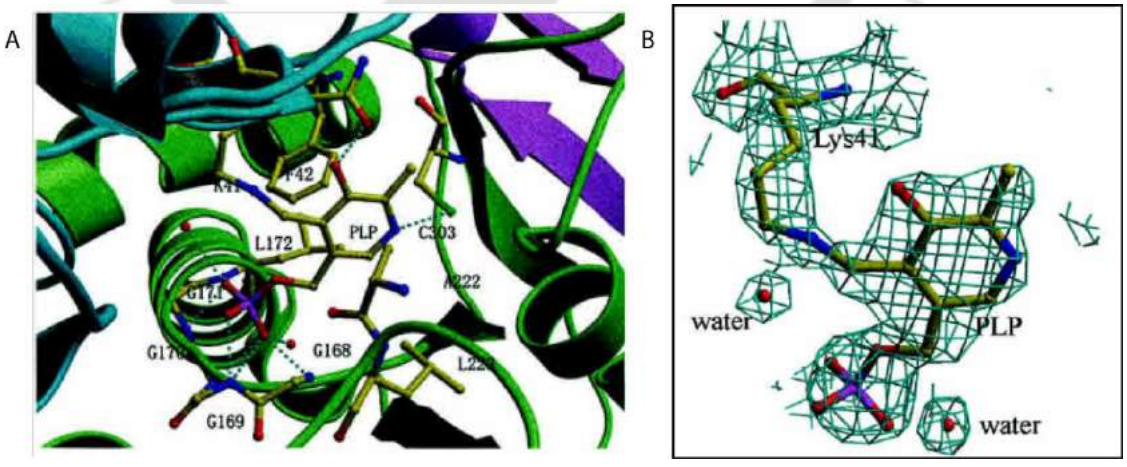

Figure 1.2. (A) Stereospecific view of the active site region of SDH and (B) Electron density peaks of the PLP-aldimine Schiff base and water molecules in the active site (ref. 2).

1.2 Amino acid derived Schiff bases as model compounds

In biology, enzyme catalyzed reactions are common but their mechanisms are appreciated only to a certain extent. Most of these reactions are catalyzed by Schiff bases that are formed between amino acids and PLP. In non-enzymatic amino acid transformations, pyridoxal, salicylaldehyde and their substituted analogs were used in the place of PLP, due to their structural similarity with that of PLP. In the past, there had been several reports on elucidating or appreciating the mechanisms of enzyme catalyzed biological reactions through the study of reactions of model compounds.[3,4] Examples of some of the enzyme catalyzed biological reactions are racemization, C-C cleavage, transamination, deamination and decarboxylation of amino acids.

Snell and his co-workers have proposed some probable mechanisms for non-enzymatic amino acid transformation reactions.[3b] In their study they have used pyridoxal and metal salts as catalyzing agents in non-enzymatic amino acid transformation reactions. They have proposed that, pyridoxal forms a Schiff base with amino acids through the formyl group and the metal salts helps in the formation of chelates. Chelate formation of Schiff bases with the metal salts gives a planar configuration to the Schiff base and also assists in activating the bonds around α-C of the amino acid moiety by pulling the electron density around the α-C towards it. The results of their experiments reveal that the presence of the hydroxyl group next to the formyl group in pyridoxal is important for the catalyzing action of pyridoxal. They have found that, substitution of the hydroxyl group by methoxy group reduces the catalytic activity by a large amount. Similarly, para-nitrobenzaldehyde lacks the catalytic activity due to the absence of hydroxyl group, whereas 4-nitrosalicylaldehyde was found to increase the catalytic activity.

In their proposed mechanistic pathways for non-enzymatic amino acid transformation reactions, a general starting point for all amino acid transformations is the cleavage of an appropriate bond around the α-C, leading to the formation of a carbanion intermediate. The negative charge formed on the α-C delocalizes with the conjugated system of the Schiff base for stabilization. Depending upon the type of the amino acid transformation reaction, appropriate products were formed from the carbanion intermediate.

1.2.1 α-C-H acidity of L-amino acids and Racemization

Belokon and his co-workers have studied about the factors which influence the α-C-H acidity of amino acids in its Schiff bases.[5] The results of their experiments reveal that esterification of the carboxylate group of the amino acids in their Schiff bases increase the α-C-H acidity by 4 folds when compared to the unesterified (free carboxylate) amino acid Schiff bases. They have also stated that, L-amino acid derived Schiff bases having bulky group in their side arm might affect the racemization rate constant by the effect of steric overlap of the bulky group with the aldimine proton in the transition state for α-proton ionization. Inclusion of ortho-methoxy group to aromatic aldehydes reduces the α-C-H acidity of amino acids in their Schiff bases, when compared to the unsubstituted aromatic aldehydes.

The effect of nature of metal ions on the α-C-H acidity of amino acids in their Schiff base metal complexes was studied by Snell *et al.*[6] The results of their study indicates that increase in the covalency of metal-ligand bond increases the α-C-H acidity. For example, Co(III) and Rh(III) increase the α-C-H acidity more, than Cr(III).

Belokon and his co-workers have done a comparative study of α-C-H acidity of alanine, its Schiff bases with different aromatic aldehydes, and Cr(III), Co(III), Rh(III) and Cu(II) Schiff base complexes of alanine.[7] Their study using pyridine analogue of alanine Schiff bases revealed certain facts, (a) both protonation at the pyridine nitrogen and the carboxylate group of amino acid increases the α-C-H acidity, (b) the α-C-H exchange rate of glycine in presence of base is found to be far less than the amino acid Schiff bases with salicylaldehyde or pyridoxal, indicating the importance of these aldehydes in the catalysis of α-C-H exchange rate, (c) racemization rate constants of Schiff bases of amino acids of 3-hydroxy-4-formylpyridine and salicylaldehyde are found to be of same order, (d) Role of the metal ions is to increase the concentration of the reactive species, i.e, the carbanion which is formed after deprotonation of the α-C-H proton of the amino acid and (e) increase in the temperature increases racemization rate constant.

Byrn *et al.* has studied the relationship between conformation of N-C_α bond and the reactivity of α-C-H bond towards racemization rate in pyridoxal Schiff bases of amino acids.[8]

The outcome of their study is that, the order of racemization rates of Schiff bases does not parallel the predictions solely based, either on electronic or steric effect, whereas it depends on the proportion of the reactive conformers (conformer with α-C-H bond orthogonal to the pi-system) estimated by the CPK (Corey-Pauling-Koltun) models. Their experimental results are consistent with the theoretically estimated results of CPK models. One of the observations during their study is that the reactivity of α-C-H bond is very sensitive to the number of β substituents on the amino acid. For example, they have not observed any detectable racemization rate in the case of valine and isoleucine Schiff bases, which have β substituents, whereas alanine Schiff base racemizes rapidly which does not have any β substituent.

1.2.2 alpha-beta C-C Cleavage

Snell et al, has reported reversible α-β C-C cleavage of threonine in presence of pyridoxal, and Al(III), Cu(II) and Fe(III) salts at 100 ^{o}C in aqueous media and in a pH range of 4-10.[9] Products of deamination reaction were anticipated before the analysis of the results of their experiments. The products of the reaction were characterized at the solution state. The major product obtained was glycine, while negligible amount of deaminated products of threonine were also observed. Serine also undergoes this type of cleavage to give glycine but very less when compared to threonine.

In the above all studies the amino acid Schiff bases and its associated metal complexes were not synthesized beforehand for the studies, instead they were generated *in situ.* The products of the amino acid transformation reactions were characterized at the solution state and none was structurally characterized.

1.3 Schiff bases as ligands in coordination chemistry

Importance of Schiff bases are well established in chemistry, due to their use in understanding coordination chemistry. There is no boundary for the number and types of Schiff bases, and so is the case with its metal complexes. However, a survey of literature showed that the both the amino acid Schiff bases and its complexes are relatively less when compared to others.[10] Mostly salicylidene-amino acid Schiff bases and their substituted analogs were studied in the past. They were generated *in situ* and characterized mostly at the solution state, and are directly used for complexation mostly with transition metals.

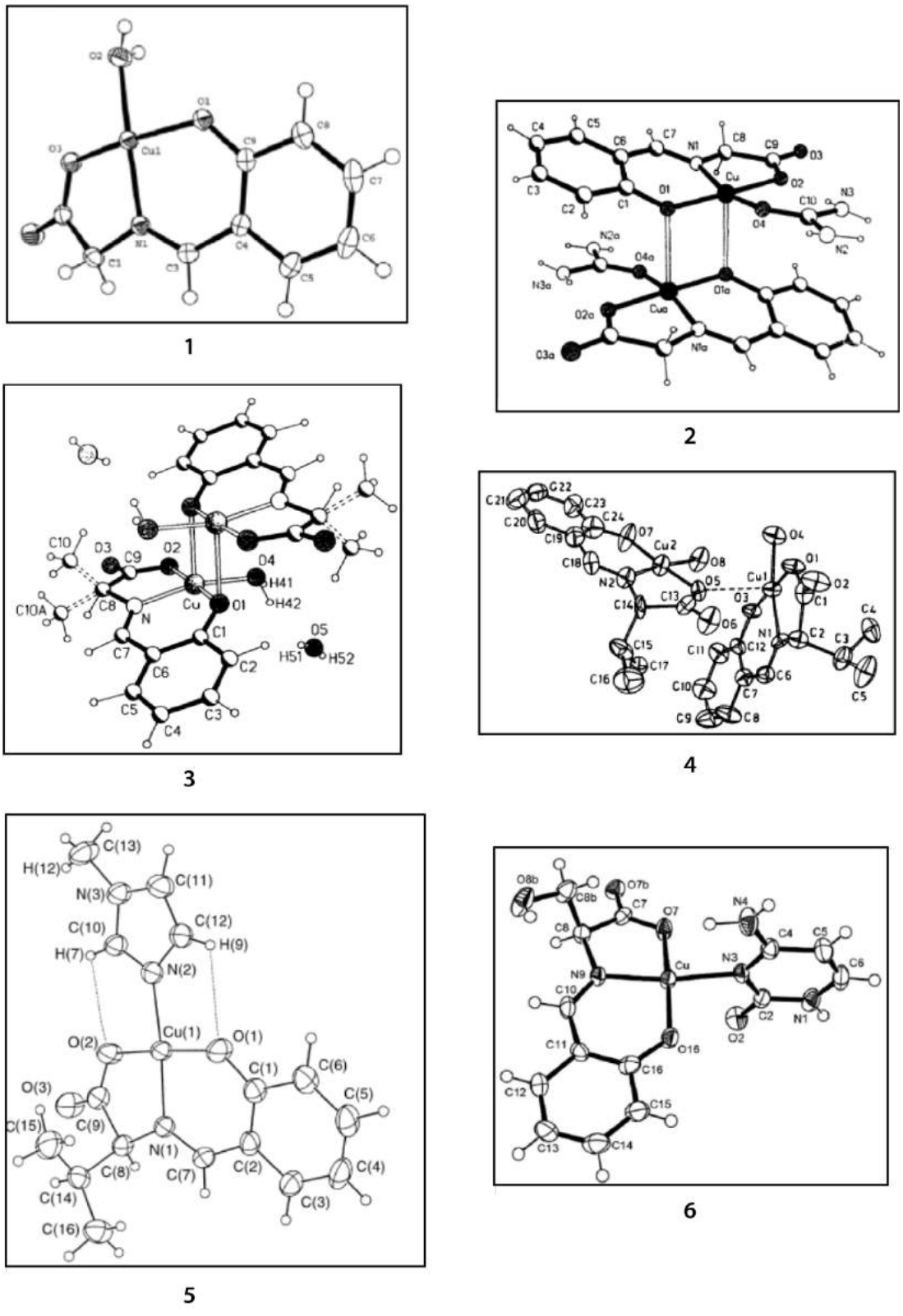

Figure 1.3. Representative structural examples of Cu(II)salicylideneaminoacidate complexes. [1-6, taken from references 17b, 11c, 13a, 16a, 13d and 14b, respectively]

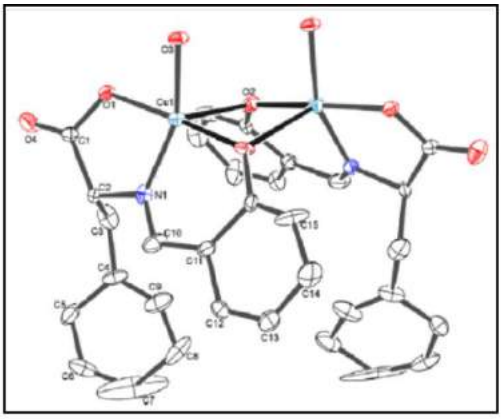

7

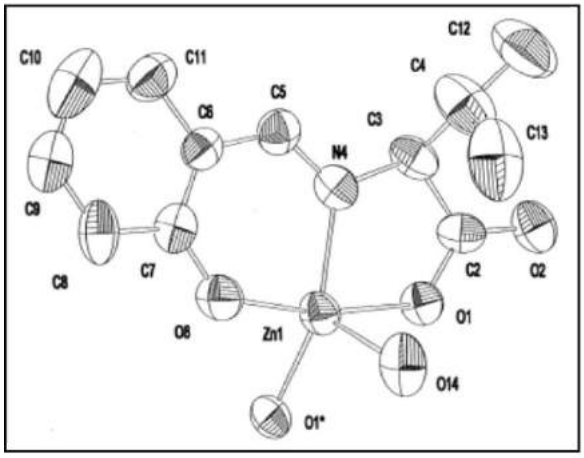

8

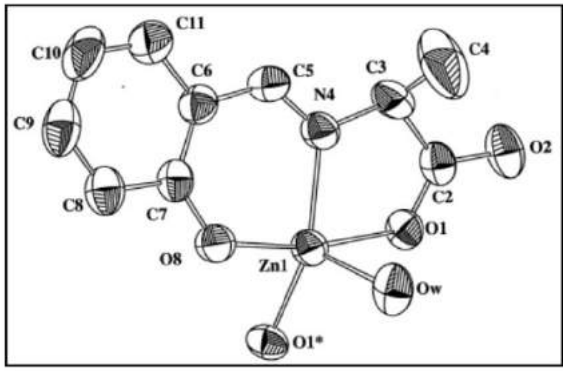

9

Figure 1.4. Representative structural examples of Cu(II) and Zn(II)salicylideneaminoacidate complexes. [7 - ref. 17b and 8-9 - ref. 13f]

Mononuclear and binuclear transition metal complexes of salicylidene-amino acid Schiff bases are known and some are structurally characterized (Figure **1.3** and **1.4**). Recently, there is only one report with glycine-acetylacetone Schiff base Cu(II) trinuclear complex (amino acid Schiff base trinuclear complex).[27] The known salicylideneaminoacidate mononuclear and dinuclear complexes are given in table **1.1**. Trinuclear Cu(II) complexes of Schiff bases from literature are given in table **1.2**. The ligands used in the synthesis of Cu(II) trinuclear complexes are displayed in figures **1.5** and **1.6**. Representative examples of Cu(II) trinuclear complexes are shown in figure **1.7**.

Table 1.1. Transition metal complexes of salicylideneaminoacidate ligands and their substituted analogs from literature

S.No	Amino acid derived Schiff base ligands with salicylaldehyde and its substituted analogs	Metal Complexes	Comments	References
1.	Amino acid: glycine	Cu(II), Zn(II), Ni(II), Fe(III), Co(III), Bi(V) and V(IV and V)	Ligand was generated *in situ* and followed by complexation Ligand isolated as K-salt: 11d and 12e	**Structurally characterized** Mononuclear Cu(II), Zn(II) and Ni(II): 11a-d, 11g V(V): 11e Bi(V): 11f Dinuclear Cu(II): 16b **Not structurally characterized** Mononuclear Cu(II): 12a-c V(IV): 12f Fe(III) and Co(III): 12d Dinuclear Fe(III): 12e
2.	Amino acid: L-alanine and D/L-alanine	Cu(II), Zn(II), V(V), Fe(III) and Ru(III)	Ligand was generated *in situ* and followed by complexation Ligand isolated as K-salt: 12e	**Structurally characterized** Mononuclear Zn(II): 13f Dinuclear Cu(II): 13a-d

				Polymer Cu(II): 13g **Not structurally characterized** Mononuclear Cu(II): xa, 13e Fe(III): 12d, 16g V(IV and V): 11e, 12f Ru(III): 18c Dinuclear Fe(III): 12e
3.	Amino acid: L-valine and D/L- valine	Cu(II), Zn(II), Ni(II), Fe(III), Co(III), Bi(V) and V(IV and V)	Ligand was generated *in situ* and followed by complexation Ligand isolated as K-salt: 12e	**Structurally characterized** Mononuclear Cu(II) and Zn(II): 13d, 13f V(V): 18b Binuclear Cu(II): 16a-b **Not structurally characterized** Mononuclear Cu(II), Zn(II), Ni(II), Co(II): 16c-f, 18a V(IV and V): 11e, 12f Fe(III) and Co(III): 12d, 16g Ti(IV): 16h Ru(III): 18c Dinuclear Fe(III): 12e

4.	Amino acid: L-serine	Cu(II) and Ru(III)	Ligand was generated *in situ* and followed by complexation	**Structurally characterized** Mononuclear Cu(II): 14a-b Polymer Cu(II): 14c **Not structurally characterized** Mononuclear Cu(II): 18a Ru(III): 18c
5.	Amino acid: L-threonine	Cu(II) and V(IV and V)	Ligand was generated *in situ* and followed by complexation	**Structurally characterized** Mononuclear Cu(II): 15a V(V): 18b **Not structurally characterized** Mononuclear V(IV): 12f
6.	Amino acid: L-phenylalanine and D/L- phenylalanine	V(IV and V), Cu(II), Fe(III) and Ru(III)	Ligand was generated *in situ* and followed by complexation Ligand isolated as K-salt: 12e	**Structurally characterized** Dinuclear Cu(II): 16b, 17a-c **Not structurally characterized** Mononuclear Cu(II): 13e, 17d, 18a Zn(II): 17e V(IV and V): 11e, 12f Fe(III): 12d, 16g Ru(III): 18c Dinuclear

				Fe(III): 12e
7.	Amino acid: L-leucine and D/L- leucine	V(IV and V), Cu(II) and Fe(III)	Ligand was generated *in situ* and followed by complexation Ligand isolated as K-salt: 12e	**Structurally characterized** Mononuclear V(V): 18b **Not structurally characterized** Mononuclear Cu(II): 16d, 18a Zn(II): 17e V(IV): 12f Dinuclear Fe(III): 12e

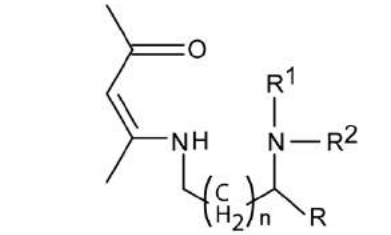

	R	R^1	R^2
L^1	H	H	H
L^{2*}	H	H	H
L^3	H	H	Me
L^4	Me	H	H
L^5	H	H	Et
L^6	H	Me	Me

* L^2 : n = 1 $L^{1, 3-6}$: n = 0

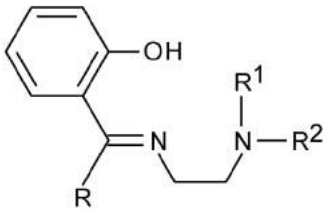

	R	R^1	R^2
L^7	H	H	H
L^8	H	Me	H
L^9	H	Me	Me
L^{10}	Me	Me	Me
L^{11}	Me	Et	Et

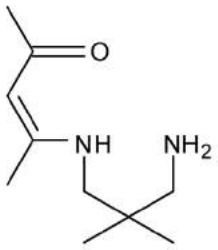

L^{12}

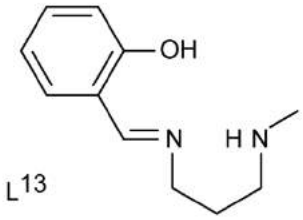

L^{13}

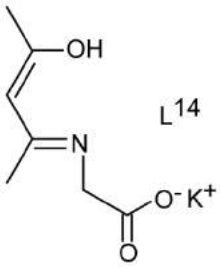

L^{14}

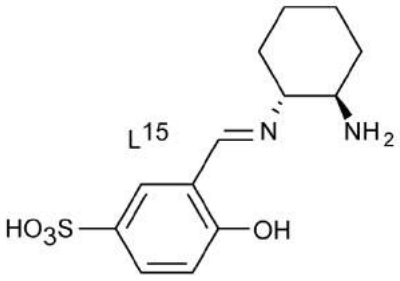

L^{15}

Figure 1.5. Schematic representation of the ligands used in the synthesis of Cu(II) trinuclear complexes.

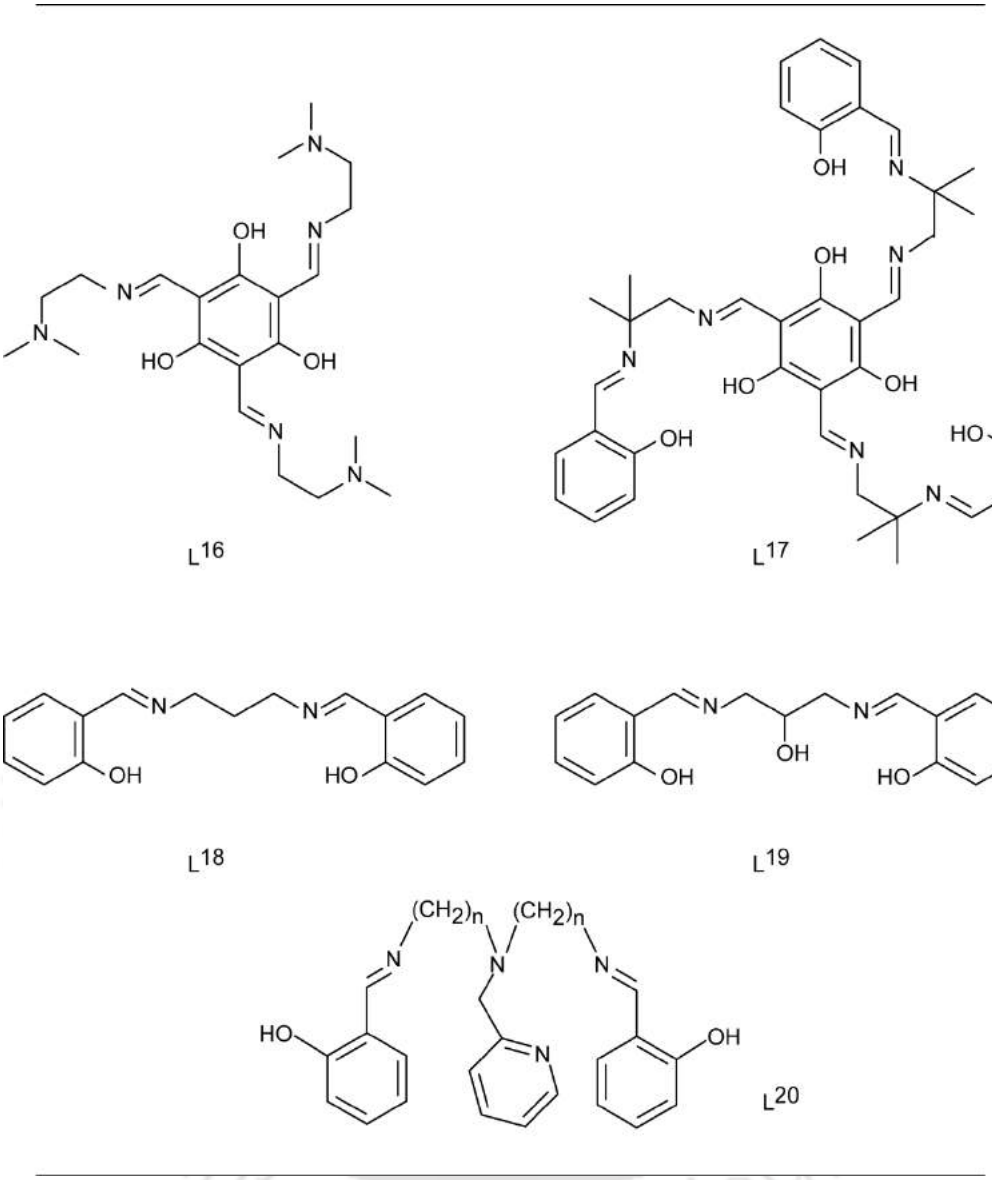

Figure 1.6. Schematic representation of the ligands used in the synthesis of Cu(II) trinuclear complexes.

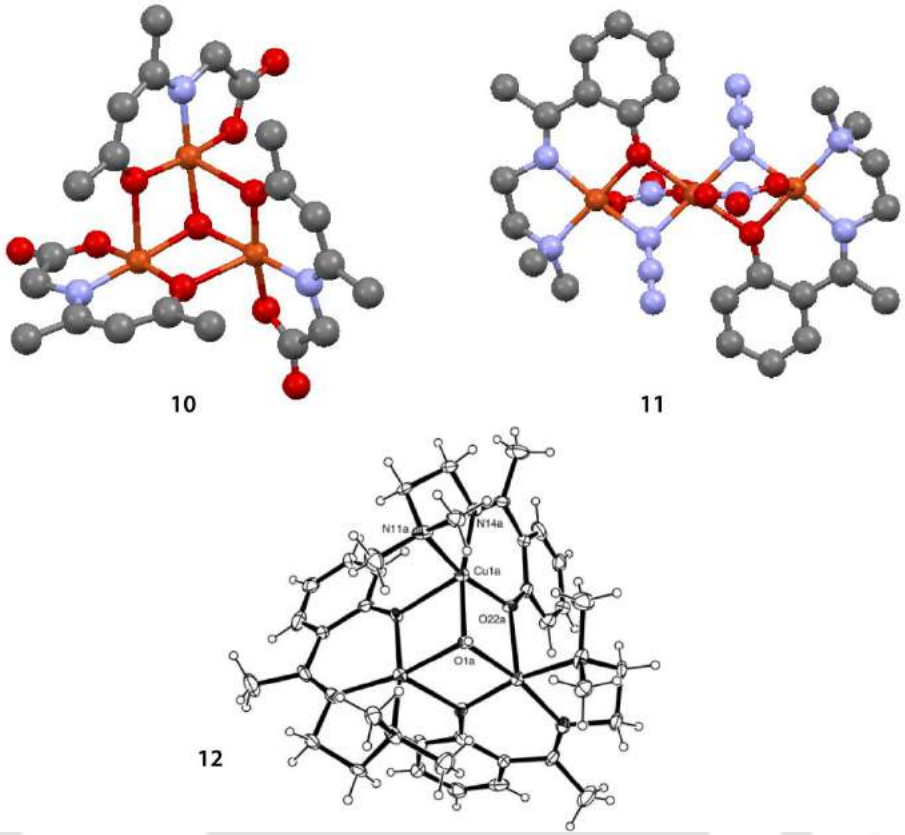

Figure 1.7. Represenative structural examples of trinuclear Cu(II) Schiff base complexes [10-12, taken from references 28, 25 and 24, respectively]

Table 1.2. Cu(II) trinuclear complexes from literature

Ligands	Comments	References
$L^1 – L^6$ and L^{12}	Ligands were synthesized from acetylacetone and, substituted and unsubstituted aliphatic diamines Trinuclear Cu(II)-μ_3-hydroxo complexes having partial cubane structure were obtained	19-23
$L^7 – L^{11}$, $L^{13}$and L^{15}	Ligands were synthesized from salicylaldehyde, substituted salicylaldehyde, 2-hydroxyacetophenone and, substituted and unsubstituted aliphatic diamines Trinuclear Linear, angular and μ_3-hydroxo Cu(II) complexes were obtained	24-27

	Complex of L^{15} was used as catalyst in the synthesis of 1,2,3-triazoles	
L^{14}	Ligand were synthesized from acetylacetone and glycine	28
L^{16} - L^{17}	Ligands were synthesized from salicylaldehyde, 2,4,6-trihydroxybenzene-1,3,5-tricarbaldehyde, and substituted aliphatic diamines Only planar trinuclear Cu(II) complexes were obtained	29-30
L^{18} - L^{19}	Ligands were synthesized from substituted and unsubstitited aliphatic diamines and slaicylaldehyde Only planar trinuclear Cu(II) complexes were Obtained and they are used as models for the active site of mutlicopper oxidases	31-32, 34
L^{20}	Ligands were synthesized from salicylaldehyde, Pyridine-2-carboxaldehyde and aliphatic triamines Linear trinuclear Cu(II) complexes were obtained	33

1.4 Conclusions from the literature survey and objectives of the thesis

From the survey of literature, it was observed that the reactivities of amino acid Schiff bases were characterized at the solution state and there is lack of structural evidence for the observed reactivities. Synthesis and structural characterization of multinuclear amino acid Schiff base complexes were found to be rare in literature.

. In this thesis we chose to study Cu(II) complexation of multiple L-amino acid derived Schiff bases under various conditions. The Schiff bases formed between salicylaldehyde and L-alanine, L-threonine and L-serine were chosen as ligands. While our primary goal was to synthesize enantiopure chiral assemblies, to our surprise we observed reactions ranging from racemization, C-C bond cleavage and C-C bond formation occurred during complexation. Both Solid (structural) and solution state evidences for the observed reactivities were presented.

References

1. E. F. Oliveira, N. M. F. S. A. Cerqueira, P. A. Fernandes and M. J. Ramos, *J. Am. Chem. Soc.*, 2011, **133**, 15496.
2. L. Sun, M. Bartlam, Y. Liu, H. Pang, Z. Rao, *Protein Science*, 2005, **14**, 791.
3. (A) E. E. Snell, P. M. Fasella, A. Braunstein and A. R. Fanelli, *Chemical and Biological Aspects of Pyridoxal Catalysis*, Pergamon Press, New York, 1963; (B) D. E. Metzler, M. Ikawa and E. E. Snell, *J. Am. Chem. Soc.*, 1954, **76**, 648; (C) J. Olivard, D. E. Metzler and E. E. Snell, *J. Biol. Chem.*, 1952, **199**, 669**;** (D) H. E. Sauberlich, in *The Enzymes***,** ed. W**.** H. Sebrell and R. S. Harris, Academic Press, New York, 1968, Vol. 11**,** pp. 44-74**;** (E) R. H. Holm, in *Inorganic Biochemistry*, ed. G. L. Eichhorn, Elsevier, New York, 1973, p. 1137.
4. (A) A. E. Martell, *Acc. Chem. Res.*, 1989, **22**, 115; (B) G. N. Weinstein, M. J. O'connor and R. H. Holm, *Inorg. Chem.*, 1970, **9**, 2104; (C) Y. N. Belokon, I. E. Zeltzer, V. I. Bakhmutov, M. B. Saporovskaya, M. G. Ryzhov, A. I. Yanovsky, Y. T. Struchkov and V. M. Belikov, *J. Am. Chem. Soc.*, 1983, **105**, 2010.
5. Y. N. Belokon, V. M. Belikov, V. A. Maksakov, N. G. Faleev and E.A. Paskonova, *Izv. Akad. Nauk SSSR, Ser. Khim.*, 1978, **5**, 1026.
6. Y. N. Belokon, V. A. Karginov, V. I. Tararo, and V. M. Belikov, *Izv. Akad. Nauk SSSR, Ser. Khim.*, 1976, **1**, 63.
7. V. M. B elikov, Yu. N. Belokon, V. A. Karginov, N. S. Martinkova and M. B. Saporovskaya, *Izv. Akad. Nauk SSSR, Ser. Khim.*, 1976, **6**, 1276.
8. M. –D. Tsai, H. J. R. Weintraub, S. R. Byrn, C.-j. Chang and H. G. Floss, *Biochemistry*, 1978, **17**, 3183.
9. D. E. Metzle, J. B. Longenecker and E. E. Snell, *J. Am. Chem. Soc.*, 1953, **75**, 2786; (B) D. E. Metzle, J. B. Longenecker and E. E. Snell, *J. Am. Chem. Soc.*, 1954, **76**, 639.
10. P. A. Vigato and S. Tamburini, *Coord. Chem. Rev.*, 2004, **248**, 1717 and references there in.
11. (A) T. Ueki, T. Ashida, Y. Sasada and M. Kakudo, *Acta Crystallogr*., 1967, **22**, 870; (B) T. Ueki, T. Ashida, Y. Sasada and M. Kakudo, *Acta Crystallogr., Sect. B: Struct. Sci., Cryst. Eng. Mater.*, 1969, **B25**, 328; (C) S. A. Warda, P. Dahlke, S. Wocadlo, W. Massa, C. Friebel, *Inorg. Chim. Acta*, 1998, **268**, 117; (D) Y. H. Xing, J. Han, G. H.

Zhou, Z. Sun, X. J. Zhang, B. L. Zhang, Y. H. Zhang, H. Q. Yuan and M. F. Ge, *J. Coord. Chem.*, 2008, **61**, 715; (E) S. Mondal, S. P. Rath, K. K. Rajak and A. Chakravorty, *Inorg. Chem.*, 1998, **37**, 1713; (F) G. C. Wang, J. Xiao, Y. N. Lu, L. Yu, H. B. Song, J. S. Li, J. R. Cui, R. Q. Wang, F. X. Ran and H. G. Wang, *Appl. Organometal. Chem.*, 2005, **19**, 113; (G) Y. Zou, Y. Z. Jiang and W. Z. Wang, *Acta Crystallogr., Sect. E: Struct. Rep. Online*., 2010, E**66**, m455.

12. (A) A. Nakahara, *Bull. Chem. Soc. Jpn.*, 1959, **32**, 1195; (B) M. Kishita, A. Nakahara and M. Kubo, *Aust. J. Chem.*, 1964, ***17,*** 810; (C) M. R. Wagner and F. A. Walker, *Inorg. Chem.*, 1983, **22**, 3021; (D) R. C. Burrows and J. C. Bailar, Jr., *J. Am. Chem. Soc.*, 1966, **88**, 4150; (E) V. P. Garcia, R. O. Latorre, E. Spodine, *Polyhedron*, 2004, **23**, 1869; (F) J. C. Pessoa, I. Cavaco, I. Correia, M. T. Duarte, R. D. Gillard, R. T. Henriques, F.J. Higes, C. Madeira, I. Tomaz, *Inorg. Chim. Acta*, 1999, **293**, 1.
13. (A) S. A. Warda, *Z. Kristallogr. - New Cryst. Struct.*, 1998, **213**, 771; (B) S. A. Warda, *Acta Crystallogr., Sect. C: Struct. Chem*., 1998, **54**, 304; (C) S. A. Warda, *Z. Kristallogr. - New Cryst. Struct.*, 1999, **214**, 1999, 77; (D) G. Plesch, C. Friebel, S. A. Warda, J. Sivy and O. Svajlenova, *Transition Met. Chem.*, **22**, 1997, 433 and references there in; (E) G. N. Weinstein, M. J. Oconnor and R. H. Holm, *Inorg. Chem.*, 1970, **9**, 2104; (F) A. G. Raso, J. J. Fiol, A. L. p. Zafra, I. Mata, E. Espinosa, E. Molins, *Polyhedron*., 2000, **19** , 673.
14. (A) A. G. Raso, J. J. Fiola, A. L. Zafra,J. A. Castro, A. Cabrero, I. Mata, E. Molins, *Polyhedron*., 2003, **22** ,403; (B) A. G. Raso, J. J. Fiola, A. L. Zafra, A. Tasada, I. Mata, E. Espinosa, E. Molins, *Polyhedron*., 2006, **25** , 2295; (C) A. G. Raso, J. J. Fiola, A. L. Zafra, A. Cabrero, I. Mata, E. Molins, *Polyhedron*., 1999, **18** , 871.
15. K. Korhonen and R. Hamalainen, *Acta Crystallogr., Sect. B: Struct. Sci., Cryst. Eng. Mater.*, 1981, B**37**, 829.
16. (A) K. Korhonen,R. Hamalainen, *Acta Chem. Scand. Ser. A*, 1979, A**33**, 569; (B) J. Vanco, Z. Travnicek, J. Marek, R. Herchel, *Inorg. Chim. Acta*, 2010, **363**, 3887; (C) G. O. Carlisle, A. Syamal, K. K. Ganguli, L. J. Theriot, *J. Inorg. Nucl. Chem.*, 1972, **34**, 2761; (D) H. Chakraborty,N. Paul,M. L. Rahman, *Transition Met. Chem.*, 1994, **19**, 524; (E) R. K. Ray, G. B. Kauffman, *J. Therm. Anal.*, 1989, **35**, 1603; (F) M. E. M. Emam, I. M. M. Kenawy, M. A. H. Hafez, *Thermochim. Acta*., 1995, **249**, 169; (G)

L. Casella, M. Gullotti, A. Pintar, L. Messori, A. Rockenbauer and M. Gyorl, *Inorg. Chem.*, 1987, **26**, 1031; (H) S. Colonna, A. Manfredi, M. Spadoni, L. Casella, M. Gullotti, *J. Chem. Soc., Perkin Trans. 1*, 1987, **1**, 71; (I) J. L. B. Royles, D. C. Sherrington, *J. Mater. Chem.*, 2000, **10**, 2035; (J) B. J. L. Royles, D. C. Sherrington, *Chem. Commun.*, 1998, **3**, 421; (K) M. Nath, Kamaluddin, J. Cheema, Indian J. Chem., Sect A., 1993, **32A**, 108 .

17. (A) J. E. Davies, *Acta Crystallogr., Sect. C: Cryst. Struct. Commun.*, 1984, **40**, 903; (B) B. Das, K. O. Medhi, *Spectrochim. Acta, Part A.*, 2013, **104**, 352; (C) R. Hamalainen, U. Turpeinen, M. Ahlgren, M. Rantala, *Acta Chem. Scand. Ser. A.*, 1978, A**32**, 549; (D) H. S. Laurie, *Aust. J. Chem.*, 1967, **20**, 2597; (E) M. Gharagozlou, D. M. Boghaei, *Spectrochim. Acta, Part A.*, 2008, **71**, 1617.
18. (A) Y. Nakao, K. Sakurai and A. Nakahara, *Bull. Chem. Soc. Jpn.*, 1967, **40**, 1536; (B) L. Krivosudsky, P. Schwendt, R. Gyepes, Z. Zak, *Polyhedron*, 2014, **81**, 421; (C) M.M. T. Khan, R.I. Kureshy and N.H. Khan, *Tetrahedron: Asymmetry*, 1991, **2**, 1015.
19. H.-D. Bian, J.-Y. Xu, W. Gu, S.-P. Yan, P. Cheng, D.-Z. Liao and Z.-H. Jianga, *Polyhedron*, 2003, **22**, 2927.
20. M. S. Ray, S. Chattopadhyay, M. G. B. Drew, A. Figuerola, J. Ribas, C. Diaz and A. Ghosh, *Eur. J. Inorg. Chem.*, 2005, **2005**, 4562.
21. B. Sarkar, M. Sinha Ray, M. G. B. Drew, A. Figuerola, C. Diaz and A. Ghosh, *Polyhedron*, 2006, **25**, 3084.
22. P. Mukherjee, M. G. B. Drew, M. Estrader, C. Diaz and A. Ghosh, *Inorg.Chim. Acta*, 2008, **361**, 161.
23. C. Biswas, M. G. B. Drew and A. Ghosh, *Inorg. Chem.*, 2008, **47**, 4513.
24. C. Biswas, M. G. B. Drew, A. Figuerola, S. G. Coca, E. Ruiz, V. Tangoulis and A. Ghosh, *Inorg. Chim. Acta*, 2010, **363**, 846.
25. C. Biswas, M. G. B. Drew, E. Ruiz, M. Estrader, C. Diaz and A. Ghosh, *Dalton Trans.*, 2010, **39**, 7474.
26. S. Naiya, B. Sarkar, Y. Song, S. Ianelli, M. G. B. Drew, A. Ghosh, *Inorg. Chim. Acta*, 2010, **363**, 2488.
27. Y.-B. Cai, L. Liang, J. Zhang, H.-L. Sunc and J.-L. Zhang, *Dalton Trans.*, 2013, **42**, 5390.
28. B. L. Guennic, S. Petit, G. Chastanet, G. Pilet, D. Luneau, N. Ben Amor and V. Robert, *Inorg. Chem.*, 2008, **47**, 572.

29. A. E. Ion, S. Nica, A. M. Madalan, F. Lloret, M. Julve and M. Andruh, *Cryst. Eng. Comm*., 2013, **15**, 294.
30. T. Glaser, M. Heidemeier, S. Grimme and E. Bill, *Inorg. Chem.* 2004, **43**, 5192.
31. W. Li, R. H. Hui, P. Zhou, P. Hou and Z.L. You, *Synth. React. Inorg. Met-Org. Nano-Met. Chem.*, 2012, **42**, 256.
32. S. Gupta, A. Mukherjee, M. Nethaji, A. R. Chakravarty, *Polyhedron*., 2004, **23**, 643.
33. N. A. Bailey, D. E. Fenton, Q. –Y. He, N. Terry, W. Haase and R. Werner, *Inorg.Chim. Acta*., 1995, **235**, 273.

Chapter II

Racemization of salicylidene-L-alaninate Schiff base and formation of Cu(II) hexanuclear complex

Compilation of literature in Chapter 1 pointed out the relevance of Schiff bases formed between natural amino acids and aromatic aldehydes. These are easy to synthesize and served as multi-dentate chelate ligands in coordination chemistry. The racemization process of the Schiff bases and associated metal complexes in presence of base has been utilized to better understand the functioning of Vitamin B6.[1-6] Salicylaldehyde owing to its structural similarity often substitute pyridoxal-5'-phosphate (PLP), the active form of vitamin B6, in model complexes. The simplest of this type of ligand, N-salicylidene glycinate, acts as a tridentate ligand which binds readily with transition metals such as Co(II) and Co(III), Ni(II), Cu(II), Zn(II), Fe(II) and Fe(III), and V(IV) and V(V)[7-9]. Structurally, the reported complexes are mostly mononuclear[8] with few reports on binuclear or coordination polymers[10]. We could find three reports of hexanuclear Cu(II) complexes with Schiff base.[11] However, none of these used salicylidene aminoacidate ligands or any other chiral ligands in the synthesis of hexanuclear Cu(II) complexes.

Our interest with these types of Schiff bases originates from their use as ligand in synthesizing large chiral assembly to facilitate chiral recognition. Multinuclear cages, capsules of different size and shapes have been synthesized in view of their potential use as selective hosts for anion sensing, catalysis, selective recognition and separation of guest molecules.[12] Addition of chirality to the design, in principle, can extend their utility further towards chiral recognition. Incorporation of chirality through Schiff-base ligands is attractive due to their ease of synthesis and excellent metal binding property. However, very few attempts were made to incorporate chiral centre within a metalloorganic assembly or chiral host using such ligands.[12b,d,e] Very few of the reported structurally characterized complexes utilize chiral amino acids beyond alanine or phenyl alanine.[10b,13,14] Most of these did not have a chiral pocket or cleft suitable for binding chiral guest. None of the reported hexanuclear complexes are chiral.

In this chapter, we have explored the complexation reaction between L-alanine derived Schiff base and Cu(II) in presence of base. Quantities of base as well as metal:ligand ratios were varied to isolate structurally characterizable complex. We were successful in isolating a new hexanuclear Cu(II) cage.[15] The cage has several interesting structural features. Formation of this type of chiral hexanuclear architecture was never reported.

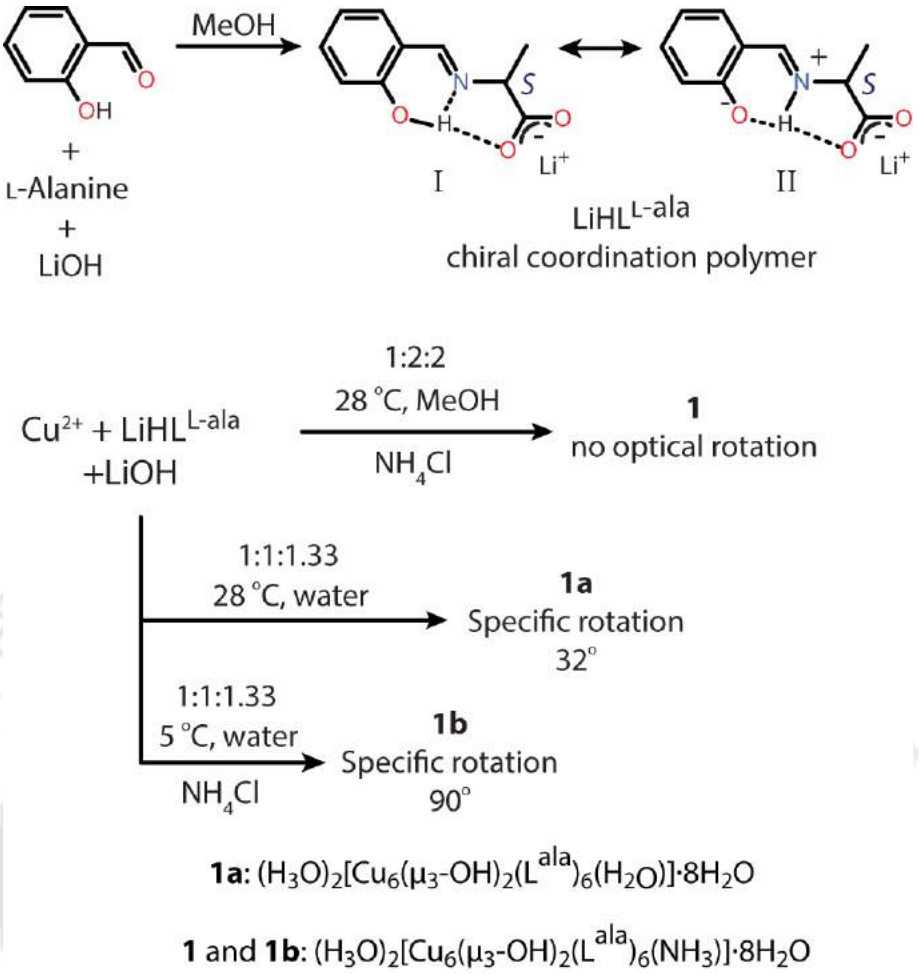

Scheme 2.1. The synthesis of the ligand and the complexes.

2.1 Experimental section

2.1.1 Materials and Methods

Solvents and reagents were obtained from commercial sources and used without further purification unless otherwise stated. Salicylaldehyde and L-alanine were purchased from Aldrich Chemical Co. and Sisco Research Laboratories Pvt. Ltd. (SRL), India, respectively and used as received.

The IR spectra were recorded on Nicolet FT-IR spectrophotometer with KBr discs in the range 4000-400 cm^{-1}. UV-vis spectra were recorded on Perkin-Elmer Lambda 25 UV-vis spectrophotometer. ^{1}H NMR spectra were recorded using a Brucker 600 MHz instrument. Ionization mass (ESI-MS) spectra were recorded on Agilent 6500 Q-TOF LC/MS mass spectrometer. Solid-state magnetic susceptibility of the complexes at room temperature was

recorded using Sherwood Scientific Magnetic balance MSB-1. Solution electrical conductivity measurements were made with a Eutech Instruments CON 5/TDS 5 Conductivity Meter calibrated with 0.01 N KCl solutions as calibrant. Optical rotation measurements were done using Rudolph and Perkin Elmer Polarimeter. Elemental analyses were done using Thermo Finnigan FLASH EA 1112 and by EuroEA elemental analyzer instruments. X-Band EPR spectra were recorded at room temperature with a Jeol JES-FA series spectrometer. The spectra were calibrated with an internal manganese marker. Thermogravimetric analyses were performed with Mettler Toledo SDTA 851e and TA SDT Q600 instruments, with a heating rate of 5 ^{o}C per minute under N_2 atmosphere using 5-10 mg of sample per run. Powder X-Ray diffraction patterns were obtained using a MAKE Bruker, D2 phaser with Cu–Kα radiation (λ =1.5418 Å) equipped with an integrated PC and DIFFRAC. SUITE software. The diffraction patterns were collected over a 2θ range of 5–55° at a step scan rate of 0.02°. Variable temperature magnetic susceptibility data were collected by using a Quantum Design MPMS SQUID magnetometer over a temperature range of 2 to 300 K at a fixed field of 1 T. CD spectra were recorded on a JASCO J-815 spectrophotometer.

2.2 Syntheses and characterization

2.2.1 $LiHL^{L\text{-}ala}$

The amino acid, L-alanine (4.00 g, 0.045 mol) in 35 mL of MeOH was stirred for about 10-15 min, to form white slurry. Partially grinded $LiOH{\bullet}H_2O$ (1.88 g, 0.045 mol) was added to this slurry and stirred for about 30-40 min. The solution turned clear with few white undissolved particles. The reaction mixture was decanted to remove the undissolved particles. Dropwise addition of salicylaldehyde (5.50 g, 0.045 mol) to this solution, under stirring, produced a clear yellow solution. After about 15-20 min, a yellow precipitate started appearing. The reaction mixture was allowed to stir for another one and half hour, while the last 30 min the reaction mixture was heated on water bath at 50-55 °C. The precipitate was filtered through Büchner funnel. The solid was washed with ethanol followed by diethyl ether. Finally, it was dried in a vacuum desiccator. Yield 7.31 g (82%). Anal. Calcd. for $C_{10}H_{10}NO_3Li$: C, 60.31; H, 5.06; N, 7.03; found C, 60.35; H, 4.93; N, 7.30. ^{1}H NMR (600MHz, CD_3OD, ppm): 8.38 (imine, s, 1H), 7.30-7.27(Ph-H, m, 2H), 6.77(Ph-H, d, 1H, *J* =

8.8 Hz), 6.77(Ph-H, t, 1H, *J* = 7.8 Hz), 4.09 (C-H, q, 1H, *J* = 6.8 Hz), 1.54(CH_3, d, 3H, *J* = 6.8 Hz). ESI-MS ($[M+H]^+$): calcd 194.0817; found 194.0816. $[\alpha]_D^{25}$ = +109° in MeOH, *c* = 1. UV/Vis (MeOH): λ_{max}, nm (ε, M^{-1} cm^{-1}): 216 (19000), 254 (9900), 277sh (5900), 316 (2900), 402 (2800). IR (KBr, cm^{-1}): 1648s, 1620s, 1525 s, 1405m, 1369m. Λ_M (ohm^{-1} cm^2 mol^{-1}): 50 in MeOH.

2.2.2 $(H_3O)_2[Cu_6(\mu_3\text{-}OH)_2(L^{ala})_6(NH_3)]\bullet 8H_2O$ (1)

$LiHL^{L\text{-}ala}$ (0.100 g, 0.502 mmol) and $LiOH\bullet H_2O$ (0.021 g, 0.502 mmol) were stirred in ~8 mL of MeOH to give a clear yellow solution. To this, $Cu(ClO_4)_2\bullet 6H_2O$ (0.093 g, 0.251 mmol) in ~5 mL of MeOH was added dropwise, which initially gave a dull green solution without any precipitation but the green color was considerably intensified at the end of addition. The reaction mixture was stirred continuously for 1 h, during which, there was no precipitation. Ammonium chloride (0.014 g, 0.251 mmol) was added as solid and stirred continuously for another 1 h, during which, there was no observable change in the reaction mixture. Equal volume of acetonitrile was added to the resulting reaction mixture and kept in air. After 5-7 days, most of the solvent was evaporated leaving small cube like, deep blue crystals along with green viscous solution. The crystals were isolated, and washed first with minimum volume of ice cold water (0.5 mL × 2) and then with water-acetone (1:2) mixture. The crystals were dried under vacuum and weighed. Yield 0.033 g (44%). Anal. Calcd. for $(H_3O)_2[Cu_6(\mu_3\text{-}OH)_2(L^{ala})_6(NH_3)]\bullet 8H_2O$: C, 40.91; H, 4.63; N, 5.57; found C, 40.74; H, 4.33; N, 5.35. UV/Vis (MeOH): λ_{max}, nm (ε, M^{-1} cm^{-1}, /Cu_6 unit): 221 (149000), 241 (155000), 268 (89000), 368 (36000), 651 (700). $[\alpha]_D^{25}$ = 0° in MeOH, *c* = 0.1. IR (KBr, cm^{-1}): 3384(broad and weak), 1639(s), 1600(s), 1541(s), 1470(m), 1442(s), 1404(m), 1377, 1351, 1291(s), 1198 (s), 911, 799, 781, 770, 575 and 547. μ_{eff} (powder, 298K): 1.83 μ_B/Cu. Λ_M (ohm^{-1} cm^2 mol^{-1}): 58 in MeOH. EPR in DMF at 298K: g_{av} 2.151, A_{av} 90G. EPR in DMF at 77K: $g_\parallel$ 2.303, $g_\perp$ 2.064 and $A_\parallel$ 196 G.

2.2.3 $(H_3O)_2[Cu_6(\mu_3\text{-}OH)_2(L^{ala})_6(H_2O)]\bullet 8H_2O$ (1a)

$LiOH\bullet H_2O$ (0.056 g, 1.33 mmol) was added as solid to a clear yellow solution of $LiHL^{L\text{-}ala}$ (0.200 g, 1.00 mmol) in ~4 mL of H_2O. Addition of lithium hydroxide did not give any observable change to the yellow solution. This solution was added dropwise to a solution

of $Cu(ClO_4)_2$•$6H_2O$ (0.371 g, 1.00 mmol) in ~2-3 mL of H_2O under stirring condition. Initially, it gave a light green solution, which on further addition of ligand gradually formed a pale blue-green precipitate (fluffy). The beaker containing the ligand solution was washed with acetone for complete transfer of ligand solution into the reaction mixture. Acetone was used to avoid adding more water to the mixture. The reaction mixture was stirred continuously for another 1 h and then filtered through frit. The filtrate along with acetone (half volume of filtrate) was kept in air. After 4-5 days, most of the solvent was evaporated leaving very fine bluish crystalline solid (cubes under microscope) along with green viscous soln. The crystalline solid was isolated, and washed first with minimum volume of ice cold water (0.5 mL × 3) and then with water-acetone mixture in the ratio (1:2). The crystals were dried under vacuum and weighed. Yield 0.098 g (33%). Anal. Calcd. for $(H_3O)_2[Cu_6(\mu_3\text{-}OH)_2(L^{ala})_6(H_2O)]$•$8H_2O$: C, 40.89; H, 4.57; N, 4.77; found C, 40.33; H, 4.34; N, 4.37. $[\alpha]_D^{25}$ = +32° in MeOH, *c* = 0.1. UV/Vis (MeOH): λ_{max}, nm (ε, M^{-1} cm^{-1} /Cu_6 unit): 221 (143000), 241 (146000), 268 (86000), 367 (34000), 655 (670). IR (KBr, cm^{-1}): 3404 (broad and weak), 1639(s), 1600(s), 1541(s), 1470(m), 1443(s), 1403(m), 1380, 1352, 1291(s), 1198(s), 911, 799, 770, 577 and 547. μ_{eff} (powder, 298K): 1.83 μ_B/Cu. Λ_M (ohm^{-1} cm^2 mol^{-1}): 102 in MeOH. EPR in MeOH at 298K: g_{av} 2.153, A_{av} 83G. EPR in MeOH at 77K: $g_{\parallel}$ 2.317, $g_{\perp}$ 2.072 and $A_{\parallel}$ 181 G.

2.2.4 $(H_3O)_2[Cu_6(\mu_3\text{-}OH)_2(L^{L\text{-}ala})_6(NH_3)]$•$8H_2O$ (1b)

$LiHL^{L\text{-}ala}$ (0.500 g, 2.512 mmol) and $LiOH$•H_2O (0.140 g, 3.340 mmol) were stirred in ~5 mL of H_2O at 5 °C to give a clear yellow solution, followed by formation of a pale yellow precipitate. To this, $Cu(ClO_4)_2$•$6H_2O$ (0.931 g, 2.512 mmol) in ~3 mL of H_2O was added dropwise to give a green solution along with precipitation. The reaction mixture was stirred continuously for 1 h at 5 °C and then ammonium chloride (0.134 g, 2.512 mmol) in ~2 mL of H_2O was added dropwise. Slight decrease in the intensity of the green color was observed and the reaction mixture was further stirred for 1 h at 5 °C. The reaction mixture was filtered and the filtrate was kept for slow evaporation. After 6-8 days, most of the solvent was evaporated leaving fine deep blue crystalline solid along with green viscous solution. The crystals were isolated, and washed first with minimum volume of ice cold water (0.5 mL × 2) and then with water-acetone (1:2) mixture. The isolated crystals were dried under vacuum and weighed.

Yield 0.180 g (24%). Anal. Calcd. for $(H_3O)_2[Cu_6(\mu_3\text{-}OH)_2(L^{ala})_6(NH_3)]\bullet 8H_2O$: C, 40.91; H, 4.63; N, 5.57; found C, 40.73; H, 4.30; N, 5.76. UV/Vis (MeOH): λ_{max}, nm (ε, M^{-1} cm^{-1}, /Cu_6 unit): 223 (108000), 242 (152000), 268 (66600), 368 (26700), 650 (670). $[\alpha]_D^{25}$ = 90° in MeOH, *c* = 0.1. IR (KBr, cm^{-1}): 3382(broad and weak), 1639(s), 1599(s), 1540(s), 1470(m), 1443(s), 1400(m), 1384, 1354, 1292(s), 1200 (s), 911, 799, 779, 676, 576 and 546. μ_{eff} (powder, 298K): 1.79μ_B/Cu. Λ_M (ohm^{-1} cm^2 mol^{-1}): 37 in MeOH.

2.3 X-ray data collection, Structure solution and Refinement

The crystal structures of **LiHL$^{L\text{-}ala}$**, **1** and **1a** were obtained by single crystal X-ray diffraction method. Single crystals of **LiHL$^{L\text{-}ala}$** were obtained from the mixture of methanol and diethyl ether solution of the ligand by slow evaporation. Single crystals of **1** were obtained by the slow evaporation of a mixture of the reaction mixture and acetonitrile (1:1). Single crystals of **1a** were obtained by the slow evaporation of a mixture of the reaction mixture and acetone (2:1).

Single crystal X-ray structural studies of **LiHL$^{L\text{-}ala}$**, **1** and **1a** were performed on a CCD Oxford Diffraction XCALIBUR-S diffractometer. The intensities of the X-ray reflections were collected at room temperature [296(2) K] using graphite-monochromated Mo Kα radiation (λα = 0.71073 Å). The strategy for the intensity data collection was evaluated by using the CrysAlisPro CCD software. The intensities data were recorded by the standard φ-ω scan techniques, and were scaled and reduced using CrysAlisPro RED software.[16a] The structures were solved by direct methods using SHELXS-97 and refined by full-matrix least-squares with SHELXL-97, refining on F^2.[16b] All non-hydrogen atoms were refined anisotropically. The hydrogen atoms were located from the difference Fourier maps and were refined isotropically. Perspective view of the complex was obtained by ORTEP.[17]

2.4 Results and Discussion

2.4.1 Ligand Synthesis

Majority of the other reports utilizes in situ condensation of Schiff base without isolation.[7-9,18] The ligand was synthesized by condensing salicylaldehyde and L-alanine in presence of one equiv. of LiOH. Base was used to deprotonate the zwitterion form of amino

acid to free amine form. This is similar to the procedure reported by Heinart and Martell using KOH as base.[19] The ligand was isolated as a monolithium salt ($LiHL^{L\text{-}ala}$) with 82% yield. Analytical data and ESI-Mass support the formula (Experimental section).

Schiff-base of amino acids can have more than one tautomeric form (Scheme **2.1**).[19] The FT-IR showed a pair of strong vibration at 1648 and 1620 cm^{-1} indicating the formation of imine. Appearance of these two bands along with one at 1405 cm^{-1} indicates the tautomeric form in the solid state being type II (Scheme **2.1**).[19] UV-vis spectrum of $LiHL^{L\text{-}ala}$ showed two characteristic imine absorption bands between 300 and 410 nm, at 316 and 402 nm in MeOH (Figure **2.11**).[19b] The molar conductance was found to be almost half of what is expected for 1:1 electrolyte suggesting significant association in solution.[20] In ^{1}H NMR spectra, the aromatic protons appeared between 6.77 and 7.30 ppm. The appearance of imine hydrogen at 8.38 ppm and methyl protons at 1.54 ppm are as expected. Detailed assignments based on both position and integration has been provided in experimental section.

2.4.2 Crystal Structure of the Lithium salt of the ligand

Crystallographic characterization of Schiff bases of amino acids are rare.[8d,10a,21] The $LiHL^{L\text{-}ala}$ was crystallized in the chiral space group of *C*2 in monoclinic crystal system. Although the structure did not show any significant disorder, the R-value was found to be high at 9% (Table **2.1**). As a supportive measure, the powder diffraction of the sample and simulated from X-ray were compared and found to be consistent with each other (Figure **2.2**). The asymmetric unit contains lithium salt of ligand (Figure **2.1**). The bond N1-C4 at 1.289(7) Å is shorter due to its double bond nature. The hydrogen attached with N1 was located from difference Fourier map. Forcible attachment of this to oxygen leads to increase in R-value. Thus attachment of this hydrogen with N1 is justified. This support the tautomeric form II (Scheme **2.1**) identified from FTIR spectra. Heinart and Martell proposed occurrence of this tautomeric form based on IR analysis.[19] The present structure supports that proposition. The only other closely related structure that we could find is a potassium salt of salicylidene-β-alaninate which unfortunately did not have the hydrogen refined.[21] The structure is also notable because of coordination of lithium. Lithium ion is coordinated to carboxylate and phenolate oxygens and is tetrahedral in geometry (Figure **2.1A**). Carboxylates acting as bridges between lithium ions forms a zigzag chain network (Figure **2.1D**), a pattern which

was seen earlier in lithium salt of glycine.[22] The coordination network formed around lithium ion is two-dimensional (2D) in structure and each 2D layer has a hydrophilic core sandwiched between hydrophobic aromatic rings (Figure **2.1B-C**). Partial retention of this network or coordination of lithium with the ligand in methanol perhaps reduced the conductance value substantially. The chirality at *C*2 was found to be *S* which is expected as it was synthesized from L-alanine (*S*-isomer). Specific rotation measured in methanol was found to be +109° (experimental section).

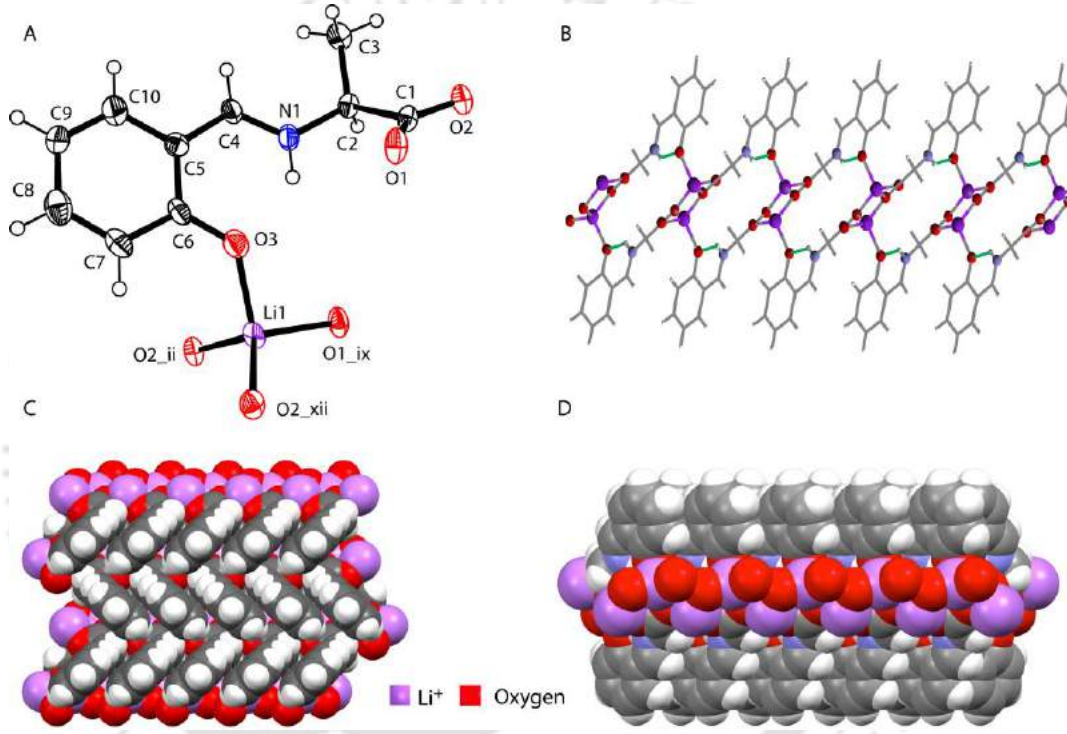

Figure 2.1. (A) ORTEP diagram showing the $LiHL^{L\text{-}ala}$ with thermal ellipsoids set to 40% probability along with lithium coordination. The atoms O1_ix, O2_xii and O2_ii were generated using symmetry operations (1 - x, y, 1 - z), (1 - x, 1 + y, 1 - z) and (-1/2 + x, 1/2 + y, z) respectively, (B) 2D coordination network formed by $LiHL^{L\text{-}ala}$, (C) and (D) Space filling model of the coordination network along different axes. Selected bond distances (Å): N1–C4 1.289(7), N1–C2 1.511(8), O3–C6 1.296(8), C4–C5 1.409(9), C5–C6 1.418(9), C6–C7 1.419(9), C7–C8 1.379(8), C8–C9 1.431(11), C9– C10 1.336(11), C10–C5 1.427(8), Li1–O1 1.944(12), Li1–O2 1.922(12), Li1– O2 2.016(12), Li1–O3 1.949(13), Li1–Li1 3.153(15). H-bond d(D···A) (Å): N1···O3 2.594(9).

Table 2.1. Selected crystallographic data for **LiHL$^{L\text{-}ala}$, 1 and 1a.**[a]

Compounds	LiHL$^{L\text{-}ala}$	**1**	**1a**
Empirical formula	$C_{10}H_{10}LiNO_3$	$C_{60}H_{77}Cu_6N_7O_{29}$	$C_{60}H_{78}Cu_6N_6O_{30}$
M	199.13	1741.56	1744.56
Wavelength (Å)	0.71073	0.71073	0.71073
Crystal system	Monoclinic	Trigonal	Trigonal
Space group	*C*2	$R\bar{3}$	$R\bar{3}$
a/Å	14.561(5)	16.4342(9)	16.3913(7)
b/Å	5.1031(14)	16.4342(9)	16.3913(7)
c/Å	14.153(5)	22.5159(15)	23.2922(12)
α/°	90	90	90
β/°	114.57(4)	90	90
γ/°	90	120	120
V/Å^3	956.4(6)	5266.4(8)	5419.6(6)
Z	4	3	6
ρ/g cm^{-3}	1.383	1.627	1.583
μ/mm^{-1}	0.101	1.873	1.821
Flack parameter	-1(4)	-	-
Reflections collected	3500	4611	8704
Independent reflections	2449	3043	3142
Goodness of fit	0.989	1.054	1.016
R_{int}	0.0806	0.0252	0.0377
Final *R* indices [$I > 2\sigma(I)$]	*R*1 = 0.0906	*R*1 = 0.0522	*R*1 = 0.0564
	*wR*2 = 0.1109	*wR*2 = 0.1393	*wR*2 = 0.1480
R indices (all data)	*R*1 = 0.1910	*R*1 = 0.0844	*R*1 = 0.0867
	*wR*2 = 0.1534	*wR*2 = 0.1604	*wR*2 = 0.1664

[a] Refinement method: full-matrix least-squares on F^2

Table 2.3 H-bonding distances (Å) and angles (°) for **1** and **1a**.[a]

D-H…A	*d*(D-H) (Å)	*d*(H…A) (Å)	*d*(D…A) (Å)	∟D-H…A (°)
		Complex **1**		
O4-H1…O5	0.83(7)	1.90(7)	2.73(11)	180
O6-H2…O1	1.01(12)	1.80(13)	2.73(9)	152(11)
[a]O5…O6	-	-	2.80	-
[a]N2…O3	-	-	3.02(4)	-
		Complex **1a**		
O4-H1…O5	0.73(7)	1.99(7)	2.72(10)	180
O6-H2…O1	1.0(7)	2.1(6)	2.73(11)	119(-1)
[a]O5…O6	-	-	2.87	-
[a]O8…O3	-	-	3.11	-

[a] Hydrogen on O5, N2 and O8 could not be found from difference Fourier map.

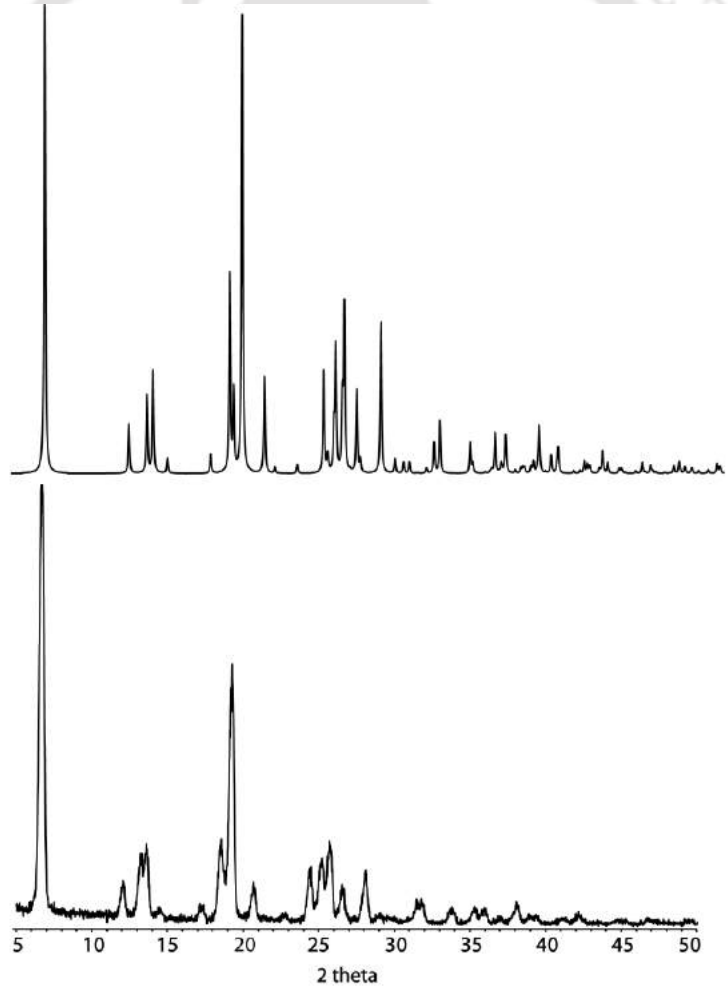

Figure 2.2. Simulated (above) and experimental (below) powder XRD pattern of $LiHL^{L\text{-ala}}$.

2.4.3 Hexanuclear Cu(II) complex

A dark green crystalline complex (**1)** was isolated from room temperature mixing of metal salt, ligand and base in the 1:2:2 ratios in methanol. Reaction is sensitive to reagent ratios and additives. Addition of NH_4Cl before isolation improves the yield by 5-10% and larger crystals. Only microcrystals were isolated without addition of NH_4Cl, which were unsuitable for single crystal X-ray diffraction study. Changing, the metal, the ligand and the base ratios to 1:1:1.33 resulted in microcrystals of **1a**. The **1a** is nearly identical to **1** with respect to powder diffraction pattern (Figure **2.5**) and FT-IR spectra. Analysis on both supports identical formulation except that one ammonia molecule in **1** was replaced by water in **1a** (experimental section).

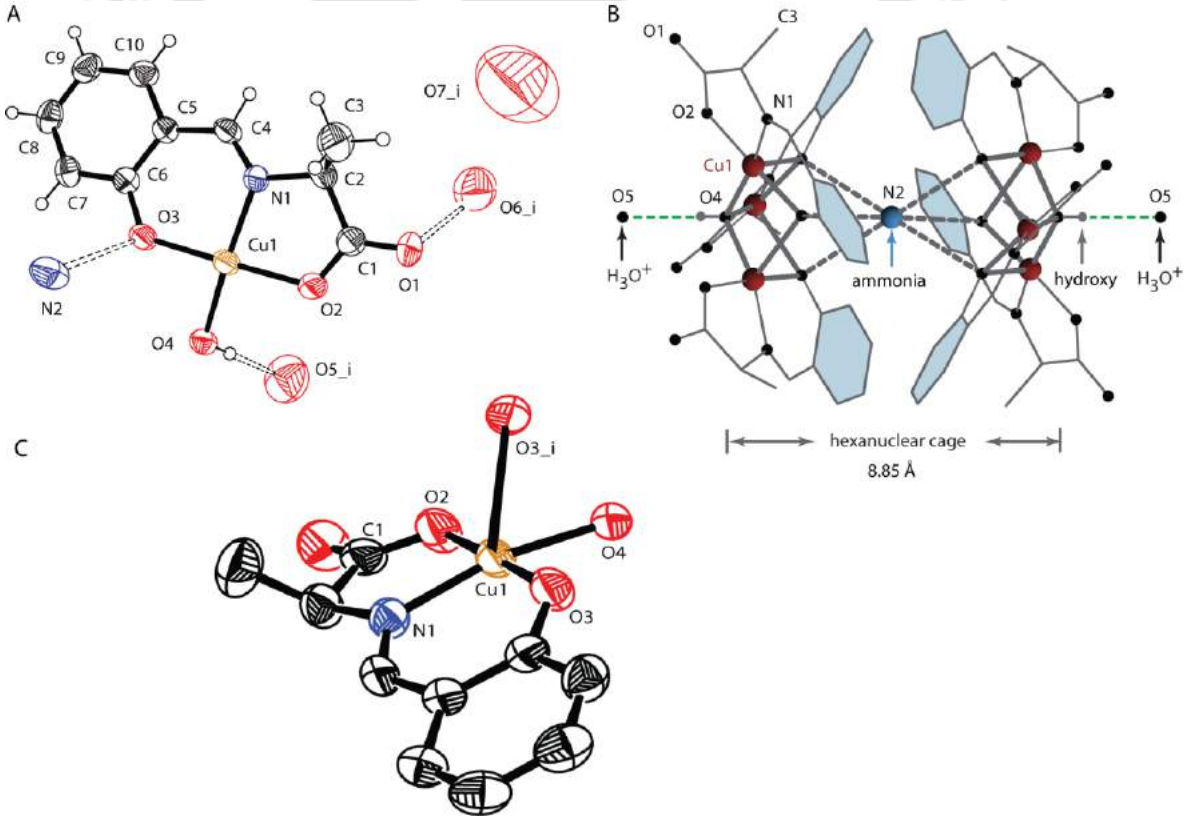

Figure 2.3. (A) ORTEP diagram of the asymmetric unit of **1** with thermal ellipsoids set to 40% probability. The atoms O5_i, O6_i and O7_i were generated using symmetry operations (x, y, -1 + z), (x, y, -1 + z), and (x, y, -1 + z) respectively, (B) Schematic presentation of the

hexanuclear molecule of **1** and (C) ORTEP diagram showing the pentacoordinated Cu(II) in **1**, with thermal ellipsoids set to 40% probability. The atoms O3_i was generated using the symmetry operation (-x+ y, 1-x, z). Selected bond distances (Å): Cu1–O3 1.918(3), Cu1–N1 1.921(4), Cu1–O2 1.933(3), Cu1–O4 1.968(2), Cu1–O3_i 2.490(3), N1–C4 1.277(5), O3–C6 1.341(5). Angles (°): O3–Cu1–N1 94.20(13), N1–Cu1–O2 84.34(14), O2–Cu1–O4 94.13(16), O4–Cu1–O3 87.28(16), O3–Cu1–O2 178.54(14), N1–Cu1–O4 165.50(17), N1–Cu– O3_i 121.5(1), O4–Cu1–O3_i 72.9(2), Cu1–O4–Cu1 106.93(18). $\tau = 0.217$.

Another difference between the two is that while **1** is not optically active, bulk material of **1a** shows a specific rotation of +32° implying a mixture of both optically active and inactive form in the **1a**. Formulation based on analysis for both the complexes support metal:ligand ratio of 1:1 in the complexes. These results indicate that (a) NH_4Cl worked as a possible crystal habit modifier and (b) extra set of ligand and/or base was required for complete racemization. The complex **1** has been further characterized using the single crystal X-ray diffraction method.

The complex **1** was solved in achiral space group *R*-3 in the trigonal crystal system. The asymmetric unit contains one sixth of the molecule (Figure **2.3A**). The molecule of **1** has two tricopper units face to face with an ammonia molecule at the centre (Figure **2.3B**). Each tricopper unit consist of three five coordinated Cu(II) bound to a single terminal hydroxo bridge. Each Cu(II) is coordinated by one tridentate L^{2-}, hydroxo bridge (O4) and phenolate oxygen atom (O3_i) from the next Cu(II) in the axial position (Figure **2.3**). The geometry at the Cu(II) is slightly distorted square pyramidal (τ 0.217).[23] The in-plane bond length ranges from 1.918(3) Å for phenolate (O3) to 1.968(2) Å for bridging hydroxide and considerably a longer axial length of 2.490(3) Å for the phenolate bridge. The lengths and angles are comparable to other hydroxo-bridged trinuclear Cu(II) complexes.[24] The longer axial bond length due to Jahn-Teller effect, common for Cu(II).[25] The chirality of the ligands in tricopper units are identical but two tricopper half of a hexanuclear assembly have opposite chirality. Thus the hexanuclear assembly can be considered as a meso-isomer. Each of the trinuclear halves has a *C*3 symmetric chiral cavity accommodating the central ammonia molecule (Figure **2.4A & B**).

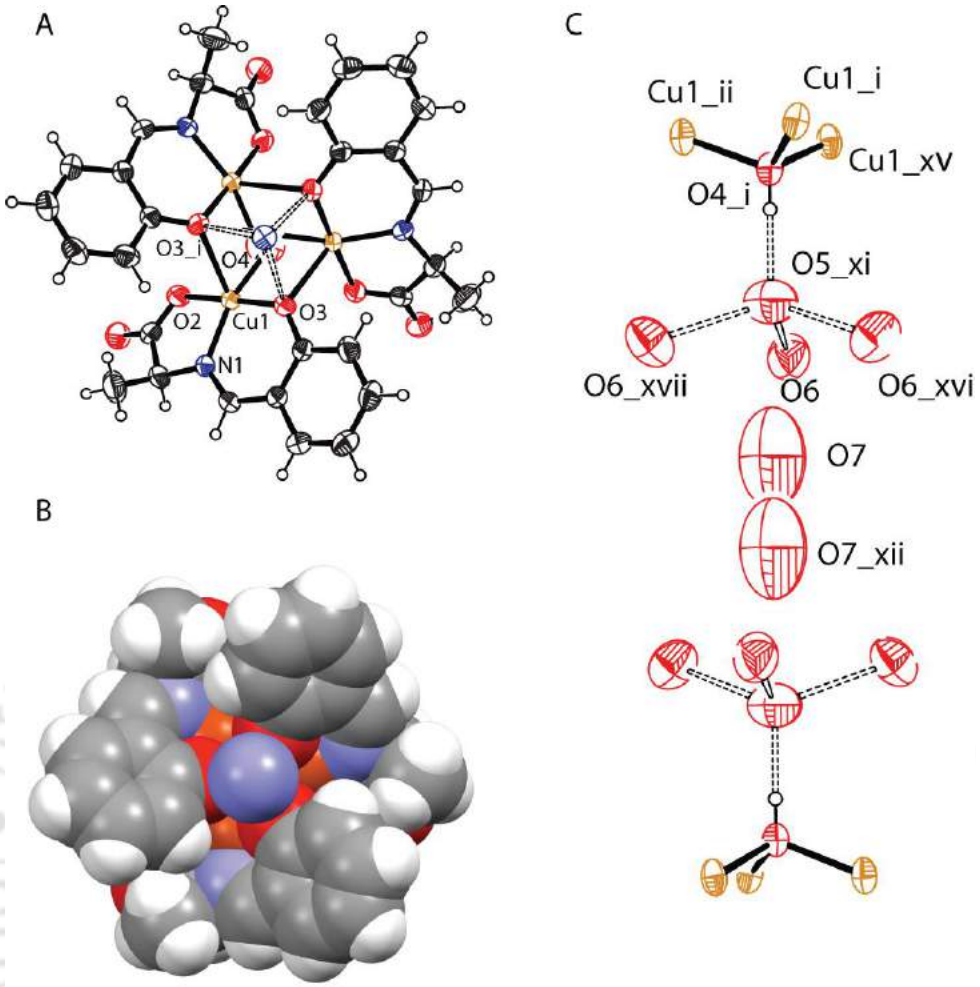

Figure 2.4. (A) ORTEP diagram of the trinuclear half of **1** with thermal ellipsoids set to 40% probability. The atom O3_i was generated using the symmetry operation (-x+ y, 1-x, z), (B) Space filling model of the same showing the *C*3 symmetric chiral cavity and (C) The cavity formed between two hydronium ions occupied by a disordered water molecule. The atoms Cu1_i, Cu1_ii, Cu1_xv, O4_i, O5_xi, O6, O6_xvi, O6_xvii, O7 and O7_xii were generated using the symmetry operations (1/3 - x, 2/3 - y, 2/3 - z), (1/3 + x - y, -1/3 + x, 2/3 - z), (-2/3 + y, -1/3 - x + y, 2/3 - z), (1/3 - x, 2/3 - y, 2/3 - z), (1/3 - x, 2/3 - y, 1.66 - z), (x, y, z), (-y, x - y, z), (-x + y, -x, z), (x, y, z) and (-x, -y, 2 - z), respectively.

The structure has two notable H-bonding at N2 and O5. The N2 at the centre, assigned as ammonia, is within H-bonding distance of six equivalent phenolate oxygens (N2…O3, 3.017(4) Å). Thus the H's on NH_3 is distributed over six equivalent sites. H's on N2 could not be located in the structure. The other position is around O5 (hydronium), which is within H-

bonding distances of O4 (bridging hydroxide) and three O6 (solvent water) (Figure **2.4**). The atom O6 is further H-bonded to carboxylate (O1) from the neighboring unit. H's on O5 and O6 could not be attached. The charge balance on the $[Cu_3L_3OH]^-$ unit requires two cation. No other counter cation could be located in the lattice. We tentatively assigned the O5 as a hydronium ion as it within H-bonding distance of three O6 symmetrically. This assignment augurs well with the charge of the trinuclear half. Alternatively, it is possible that one proton/per trinuclear unit is disordered over O5 and three O6. The known examples of hydronium ion within crystals usually bind to three water molecules with short H-bond distances of ~2.5 Å without any possibility of fourth H-bond on oxygen.[26] Thus, a total of four H-bond on O5 is difficult to explain. Thus it is not possible to pinpoint the location of the protons either on O5 or O6.

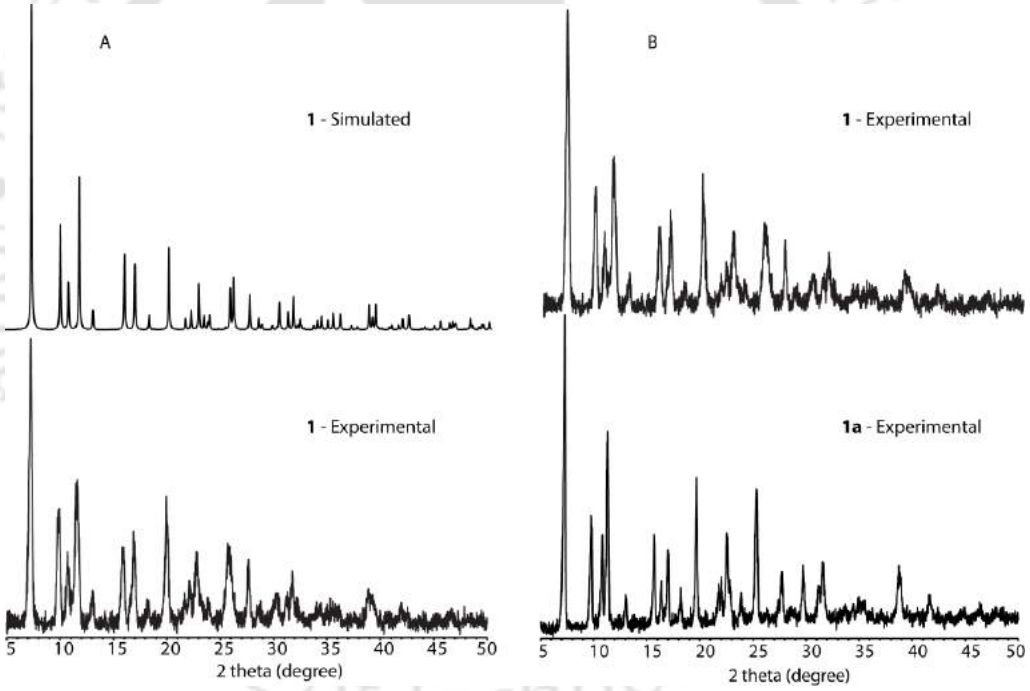

Figure 2.5. (A) Simulated and experimental powder XRD pattern of **1** and (B) Experimental powder XRD pattern of **1** and **1a**.

The lattice also contains a pocket, formed between six of the O6 from neighboring hexanuclear assembly (Figure **2.4C**). Electron density inside pocket was refined as oxygen atom (O7, water, 50% occupancy). Thermogravimetric analysis of **1** (TGA) between 25-180 °C showed weight loss of 11.02% which could be accounted for one NH_3 and 10 H_2O

molecules (calc. weight loss of 11.2 %)(Figure **2.6**). Thus TGA support the assignment of O7 as water. However, large thermal ellipsoids and short O7-O7 distance indicate disorder at this position.

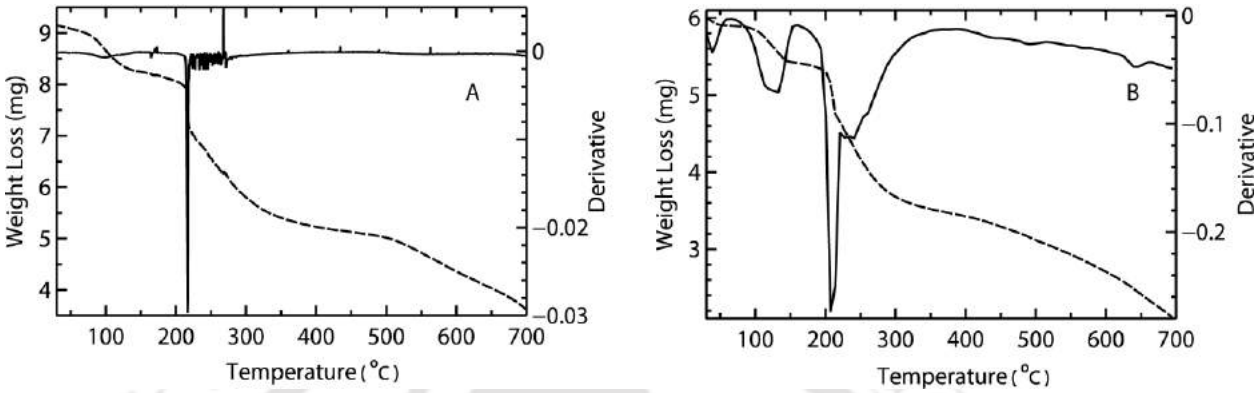

Figure 2.6. (A) and (B) are the TGA and DTA plot of **1** and **1a**, respectively.

Microcrystals of **1a** were uneven in size, mostly too small for mounting in X-ray diffractometer. However, we were able to mount a relatively larger one (0.2 mm x 0.1 mm x 0.1 mm) and collected data. The diffraction spots were weak. The crystal space group, parameters and structure are nearly identical with that of **1** with the exception of water, instead of ammonia, at the centre (Table **2.1**). This is supported by the elemental analysis. Thus, the crystal is of same meso isomer despite the bulk showing optical rotation. This indicates that the bulk contains both meso and chiral isomers. The relative ratio could not be determined. Interestingly, the solubility of **1** and **1a** differs significantly in MeOH. While **1a** is readily soluble in methanol, **1** takes ~18 h to dissolve on standing. We attempted the separation of isomers using the difference in solubility. Unfortunately the optical rotation measurement, although differs for both fractions, implies that, complete separation using this method is not possible.

Although the crystallographic parameters *a*, *b* and *c* of the complexes **1** and **1a** differ very slightly, they are found to be isostructural with respect to, the coordination geometry or the environment around Cu(II) ion. The bond lengths, angles and H-bonding pattern are found to be almost similar with each other.

The complexes were also characterized by FT-IR, UV-vis, EPR and room temperature magnetic susceptibility. The FT-IR spectra of all the complexes show a strong and sharp imine stretching frequency at 1639 cm^{-1}. The imine stretching frequency in the complexes moved about 9 cm^{-1} towards lower wave number when compared to the free imine, typical for the coordinated imine's to the metal centre.[27] Electronic spectra of all the complexes show essentially five absorption bands between 200 and 700 nm. Complexes **1, 1a** and **1b** show a broad band at 651, 655 and 650 nm, respectively, which are assigned for the d-d transition and is as expected for the usual distorted square pyramidal or tetragonal geometry around Cu(II) (Figure **2.11**).[6,28] The remaining four absorption bands between 200 and 380 nm are of ligand origin (experimental section). Room temperature magnetic susceptibility of all the complexes are in the range 1.79-1.86 μ_B.[29] Solution state EPR spectra of the complexes **1** and **1a** at room temperature and at 77 K, showed an axial spectra which is usual for the distorted square pyramidal geometry around Cu(II) (Figure **2.12**).[30]

2.4.4 Racemization of $LiHL^{L\text{-}ala}$

As the structure of **1** showed that the ligand underwent racemization before isolation of the complex, we did the following experiments to determine the factors responsible for it. The process of racemization of $LiHL^{L\text{-}ala}$ in presence of base was monitored using optical rotation at 589 nm over a time period of 12 h (Figure **2.7**). In methanol at room temperature (28 °C), optical rotation of $LiHL^{L\text{-}ala}$ decreases gradually over 4 h to about 40% of initial value and continue decreasing at a slower pace. The rate of decrease followed a first order behavior (Figure **2.8**). The observed rate/mole was found to be 0.110 min^{-1} M^{-1}. This is slower (1/5) than the rate reported for Cu(4-NO_2sal-L-val)1•5H_2O in presence of base in ethanol at 50 °C, where (4-NO_2sal-L-val)$^{2-}$ is the Schiff base of L-valine and 4-nitro-salicylaldehyde.[6] Electron withdrawing nitro substitution on salicylaldehyde stabilizes the intermediate necessary for racemization, hence the rate is higher for nitro derivative. However, it is not a requirement for racemization to occur as is shown for non-substituted salicylaldehyde & amino acid esters.[6] Thus the present result is consistent with the reported racemizations. The circular dichroism (CD) spectra of $LiHL^{L\text{-}ala}$ before addition of base, 20 min after and disappearance of it after 20 h in methanol clearly shows that racemization indeed took place (Figure **2.9**).

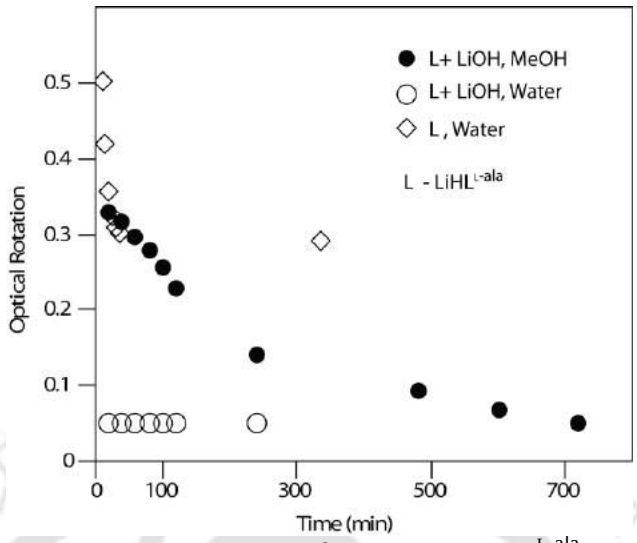

Figure 2.7. Plot of optical rotation vs. time for L (L – LiHL$^{L\text{-}ala}$) with LiOH in MeOH and water, and without LiOH in water.

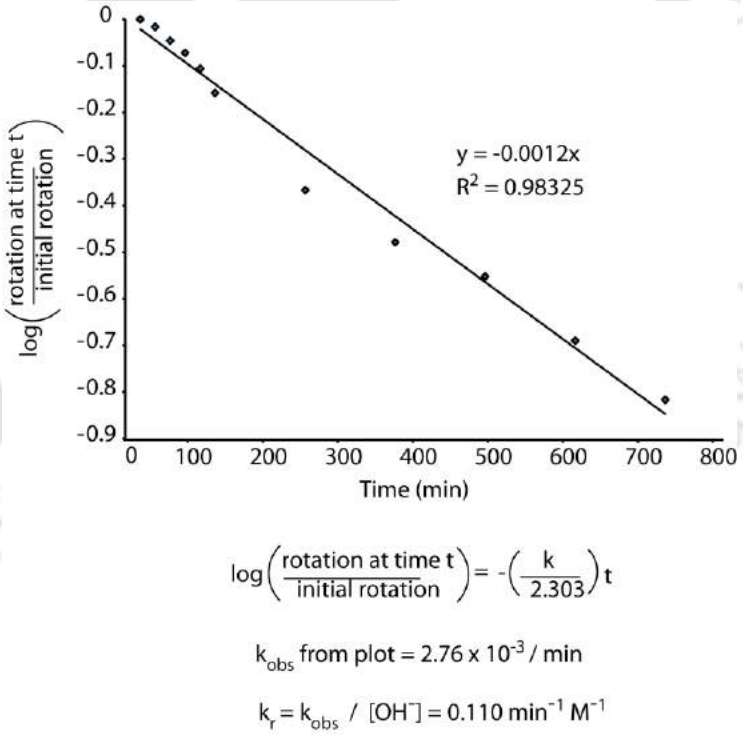

Figure 2.8. Determination of racemization rate constant (k_r) for L (L – LiHL$^{L\text{-}ala}$) with LiOH in MeOH.

In water at room temperature, even without base addition, the optical rotation initially decreases faster up to 30 min (40% decrease) but then remain constant for over 10 h. In

presence of 1 equiv. of base, it decreases to ~ 8% of initial value within 20 min and remain constant thereafter. From these observations, we infer that in presence of base, racemization occurs in both methanol and water. Racemization is much faster in water compared to methanol at room temperature.

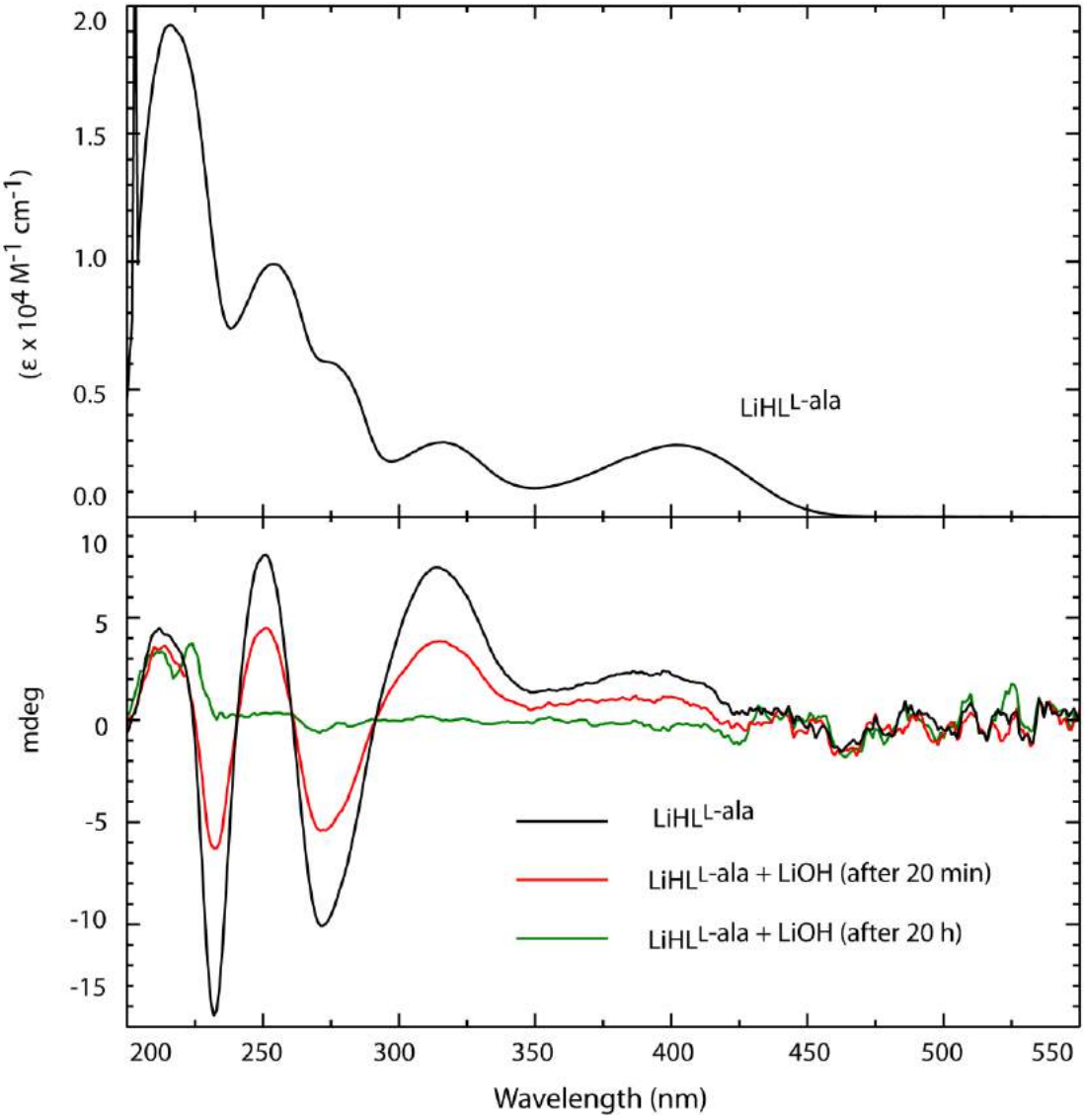

Figure 2.9. UV-vis spectrum of $LiHL^{L\text{-}ala}$ in MeOH (60.0 μM, above), and CD spectra of $LiHL^{L\text{-}ala}$ and $LiHL^{L\text{-}ala}$ with one equiv. of LiOH in MeOH at different time intervals (750.0 μM, below).

In order to check the effect of temperature, the optical rotation of $LiHL^{L\text{-}ala}$ in presence of 1 equiv. of base was measured at room temperature in methanol after stirring for 2 h at 0

°C, 28 °C and 80 °C before measurement to replicate the synthesis condition. The optical rotations were 0.313, 0.228 and 0 respectively. This means that racemization is faster at elevated temperature. Thus it is no wonder that complex **1a**, isolated from water in presence of base at room temperature is a mixture of isomers.

From these observations, we infer that in presence of base, racemization occurs in both methanol and water. Racemization is much faster in water compared to methanol at room temperature. This also means that at lower temperature, the racemization is quite slow. Thus we repeated the synthesis of complex **1a** at ice cold condition (~5 °C) and isolated the complex **1b**, which shows much higher specific rotation of 90° compared to **1a** (Scheme **2.1**). The higher quantity of chiral isomer in complex **1b** became more evident from CD spectra of the copper (II) complexes (Figure **2.10**). Out of three complex only complex **1b** showed spectrum with negative cotton effect, indicative of chirality in the sample. The reaction was attempted in methanol as well. However, in methanol, green amorphous solid precipitated immediately after reagents were added, perhaps due to lower solubility at low temperature, which shows specific rotation lower than **1b**. We suspect the purity of this solid. Hence the product from low temperature reaction in methanol has not been subjected to circular dichroism spectroscopy.

2.4.5 Magnetic property of the complexes

Magnetic properties of multinuclear paramagnetic complexes are important for multiple reasons. Although detail magnetic property studies are beyond our scope and expertise, we did measure temperature variable magnetic property of these two complexes with outside help. Temperature dependent magnetic studies on both **1** and **1a** were performed in the temperature range of 2-300 K at a fixed field of 1.0 T. The experimental data were corrected for underlying diamagnetism, calculated using Pascal's constants.[29b,d] From room temperature χ_M x T for trinuclear unit gradually rises up to 14 K and then sharply decreases (Figure **2.13**). This nature is consistent with ferromagnetic interaction within trinuclear unit but antiferromagnetic interaction between different trinuclear units.[31] Almost identical behaviour was observed for complex **1a** (Figure **2.13**). Similar observation were made by Suh and co-workers for a hydroxo bridged trinuclear Cu(II) complex with a macrocyclic ligand.[31a]

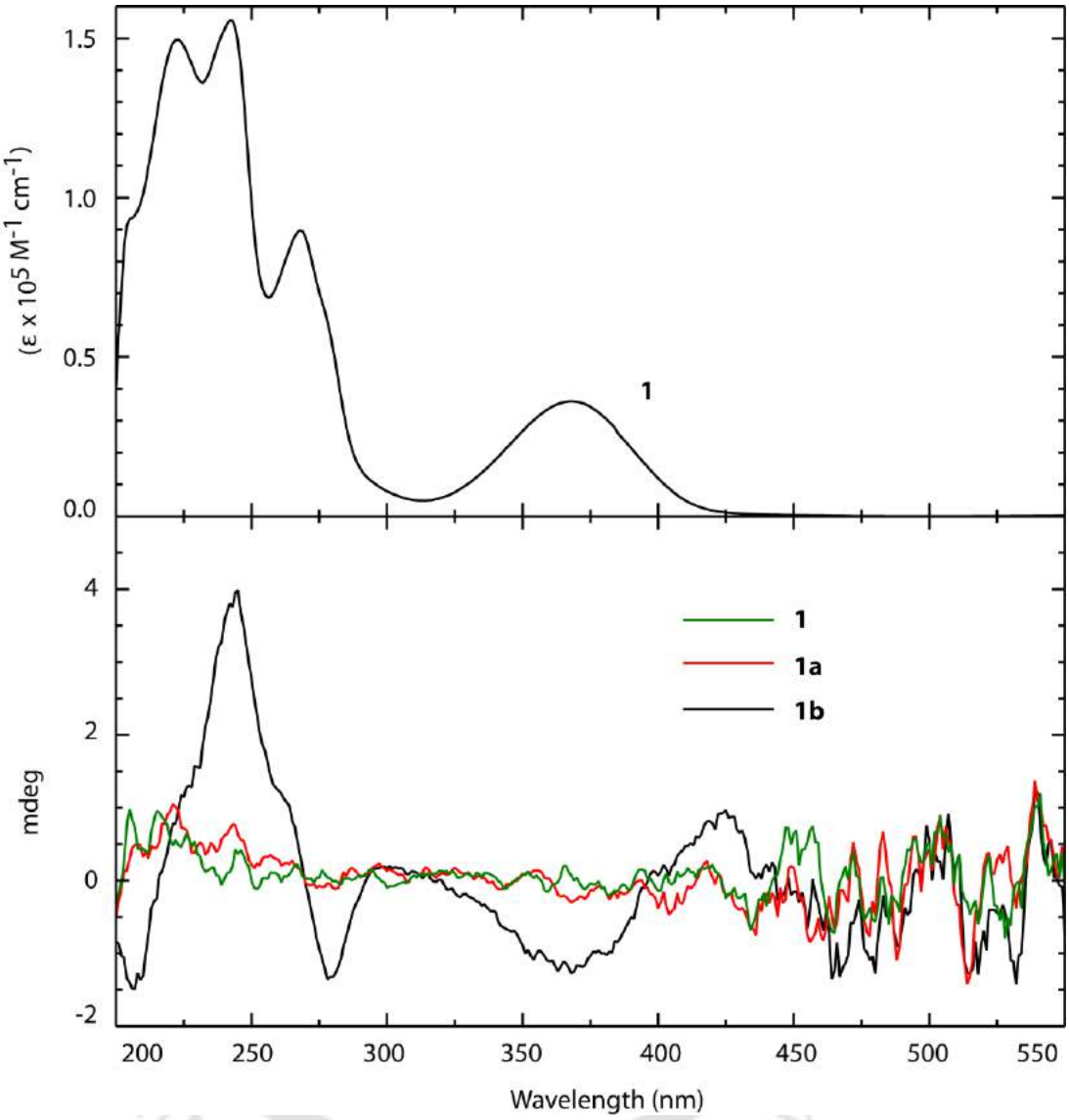

Figure 2.10. UV-vis spectrum of the complex **1** in MeOH (6.6 μM, /Cu6 unit, above) and CD spectra of the complexes **1, 1a** and **1b** in MeOH, same concentrations were maintained for all the complexes (43.0 μM, /Cu_6 unit, below).

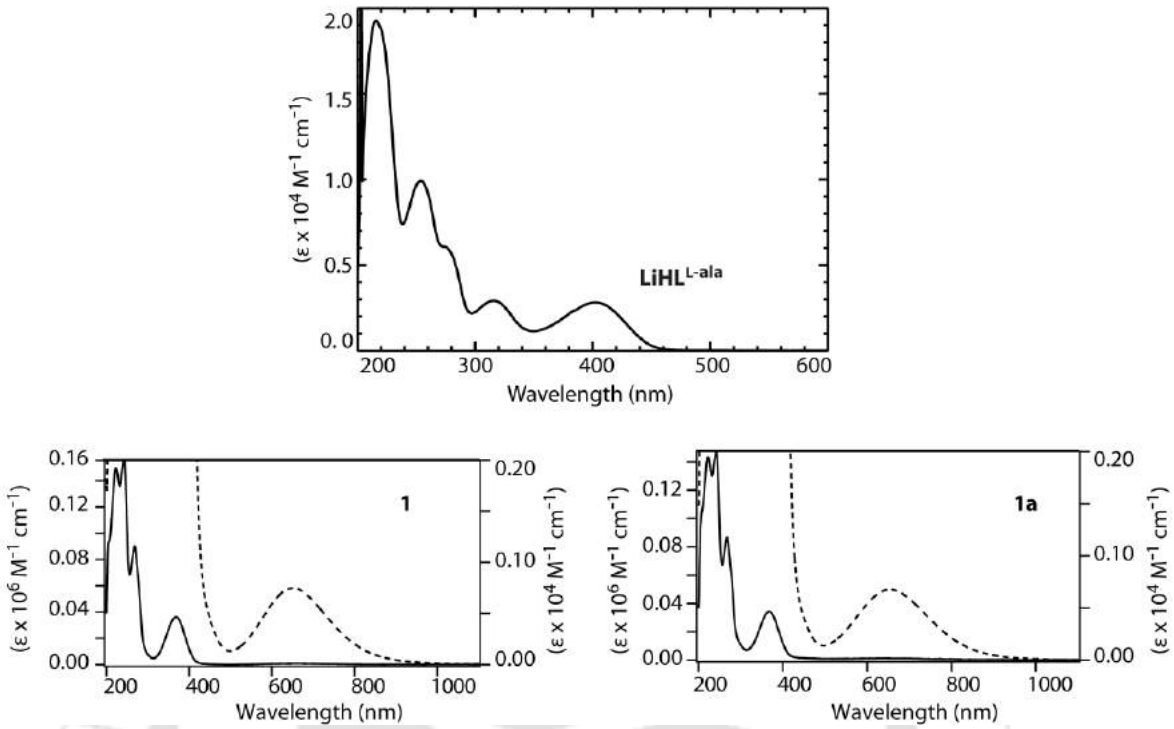

Figure 2.11. UV-vis spectra of the LiHL$^{L\text{-}ala}$ (60.0 µM), **1** [(- - - - 6.6×10^{-4} M, /Cu_6 unit) and (—— 6.6×10^{-6} M, /Cu_6 unit)] and **1a** [(- - - - 6.6×10^{-4} M, /Cu_6 unit) and (—— 6.6×10^{-6} M, /Cu_6 unit)] in MeOH.

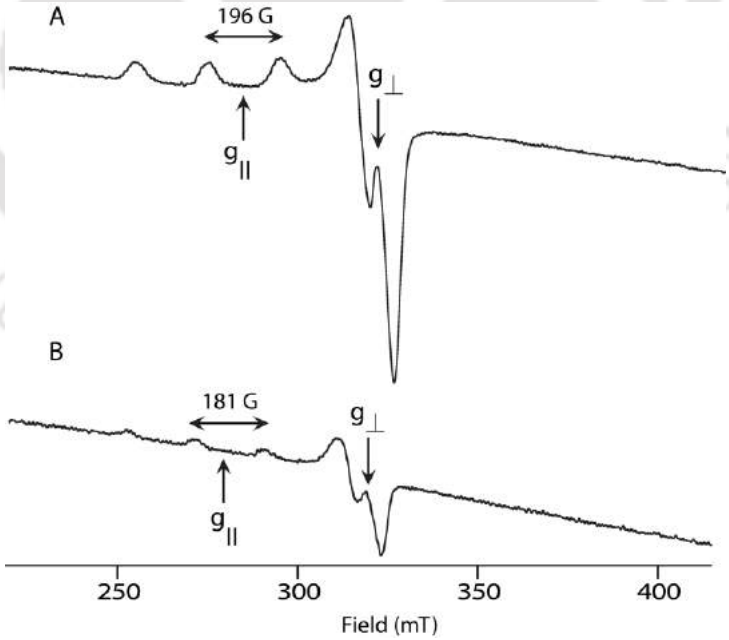

Figure 2.12. (A) and (B) are the solution state EPR spectra of **1** and **1a** in DMF and MeOH at 77 K, respectively.

The susceptibility data were further analyzed on the basis of the usual spin-Hamiltonian description for the electronic ground state by using the simulation package julX written by Eckhard Bill for exchange coupled systems of three s = ½ system.[32] The operator contained exchange Hamiltonian and Zeeman interaction. The zero-flied splitting option was not used. The ferromagnetic coupling constant *J* and Theta-Weiss constant in K for **1** was found from the fitted data and are 14 cm^{-1} and -0.8 K respectively. Same parameters for **1a** are 12 cm^{-1} and -0.6 K. Compared to this, complex reported by Suh and co-workers[31a] were *J* = 37.8 cm^{-1} and complex by Yan and co-workers[31b] were *J* = 7.83 cm^{-1}. Other than these two reported example and the complexes in this manuscript, rest of the reported trinuclear Cu(II) complexes shows anti-ferromagnetic behaviour.

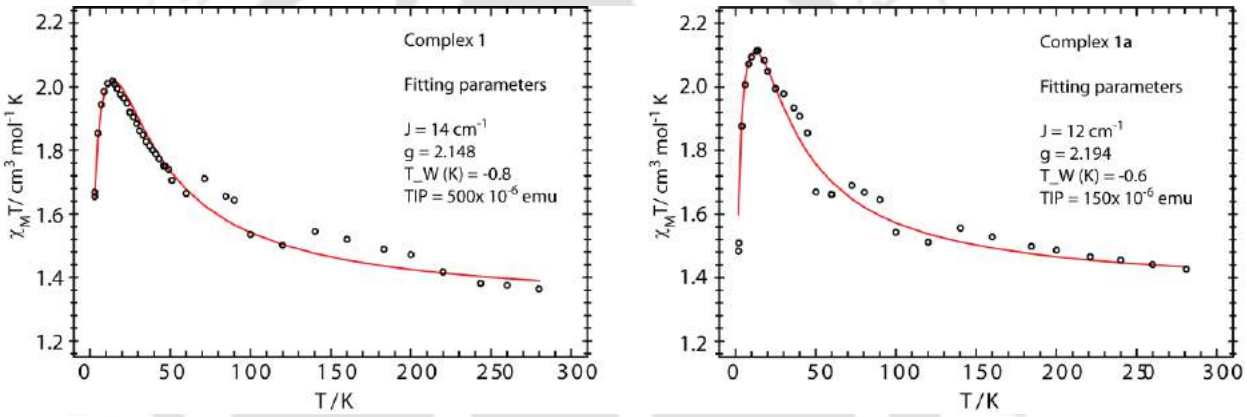

Figure 2.13. Plot of χ_M vs. T in the range 2–300 K for **1** and **1a**. The solid line is the best fit to the experimental data using the fitting parameters given in the figure.

Hatfield and others[33,34] had shown that for a set of hydroxo-bridged complexes, coupling depends on the Cu-OH-Cu angle. The Cu-OH-Cu angle >97.5° promote antiferromagnetic coupling, whereas angle of < 97.5° promotes ferromagnetic coupling. In the present set of complexes, Cu-OH-Cu angle is ~106° and Cu-$O_{phenolate}$-Cu is 90.4°. Thus, one of the bridges support antiferromagnetic coupling, while the other promotes ferromagnetism leading to an overall ferromagnetic coupling. Compared to present set of complexes, the reported trinuclear hydroxo complexes have Cu-$O_{phenolate}$-Cu angles between 96 to 99° (reported Cu-OH-Cu angles lies between 100 to 107°).[24,34] This shorter Cu-$O_{phenolate}$-Cu angle probably is the reason for overall ferromagnetism.

Conclusions

The isolation and characterization of **1** and **1a** are significant for multiple reasons. First of all it shows that simplicity in Schiff base formation could be utilized for synthesizing large chiral multinuclear cages/assemblies. Even though handful of trinuclear hydroxo bridged Cu(II) complexes have been reported, none of them used chiral ligand.[24f] The complex showed ferromagnetic interactions. Thus the complexes would be of interest for other researchers as well.

The structures of **1** and **1a** are unique in terms of H-bonding capability through both carboxylate and phenolate. Both of which contributed to the stabilization of protons as possible hydronium form within the lattice and the central ammonia in **1** or water in **1a**. The centre of the cage is especially notable as it is within H- bond distance (N2-O3, 3.017 Å) from six H-bond acceptors (phenolate) which resulted in a rather unique H-bonding situation for the central molecule, be it water (**1a**) or ammonia (**1**). Front to front organization of trinuclear units in to a hexanuclear capsular form in the solid state is another structural feature not seen before.

Apart from the structural aspect, observation of a meso-isomer showed that racemization of the amino acid took place. Racemization of amino acid derivatives in presence of base or Cu(II) have been reported.[1,3,6] Based on the solution studies, either deprotonation at chiral carbon followed by rehydration or keto-enol tautomer form of has been cited as mechanism of such occurence.[6] However, structural characterization of the products or formation of this type of hexanuclear architecture through racemization has not been reported.

Addition of 1 equiv. LiOH to LiHL and resultant racemization studies showed that the extent of racemization depends on solvent, base as well as temperature. This explains the observation of optical rotation and CD spectrum in **1b**, synthesized at low temperature. The chiral excess in **1b** retains the possibiliy of isolation of enantiopure cage for chiral recognition in future.

References

1. M. –D. Tsai, H. J. R. Weintraub, S. R. Byrn, C.-j. Chang and H. G. Floss, *Biochemistry*, 1978, **17**, 3183.

2. V. M. Belikov, Y. N. Belokon, V. A. Karginov, N. S. Martinkova, and M. B. Saporovskaya, *Izv. Akad. Nauk SSSR, Ser. Khim.*, 1976, **6**, 1276.

3. Y. N. Belokon, A. S. Melikyan, V. I. Bakhmutov, S. V. Vitt and V. M. Belikov, *Inorg. Chim. Acta*, 1981, **55**, 117.

4. Y. N. Belokon, V. M. Belikov, V. A. Maksakov, and V. I. Tararov, *Izv. Akad. Nauk SSSR, Ser. Khim.*, 1978, **10**, 2276.

5. D. E. Metzler, M. Ikawa and E. E. Snell, *J. Am. Chem. Soc.*, 1954, **76**, 648.

6. G. N. Weinstein, M. J. O'connor and R. H. Holm, *Inorg. Chem*., 1970, **9,** 2104.

7. (a) C.-Y. Chu, D. Hwang, S.-K. Wang and B.-J. Uang, *Chem. Commun.*, 2001, 980; (b) R. Ando, H. Inden, M. Sugino, H. Ono, D. Sakaeda, T. Yagyu and M. Maeda, *Inorg. Chim. Acta*, 2004, **357**, 1337; (c) S. Kumar, D. N. Dhar and P. N. Saxena, *J. Sci. Ind. Res.*, 2009, **68**, 181; (d) Z. H. Chohan, M. Arif and M. Sarfraz, *Appl. Organomet. Chem.*, 2007, **21**, 294; (e) R. C. Das, M. K. Mishra and S. K. Mohanty, *Acta Chim. Hung.*, 1983, **112**, 377; (f) L. Tian, J. Tian, T. Li, G. Li, S. Bi, E. Gao and S. Liu, *Huaxue Shiji*, 1996, **18**, 114.

8. (a) T. Ueki, T. Ashida, Y. Sasada and M. Kakudo, *Acta Crystallogr.*, 1967, **22**, 870; (b) T. Ueki, T. Ashida, Y. Sasada and M. Kakudo, *Acta Crystallogr., Sect. B: Struct. Sci., Cryst. Eng. Mater.*, 1969, **B25**, 328; (c) S.A. Warda, P. Dahlke, S. Wocadlo, W. Massa, C. Friebel, *Inorg. Chim. Acta*, 1998, **268**, 117; (d) Y. H. Xing, J. Han, G. H. Zhou, Z. Sun, X. J. Zhang, B. L. Zhang, Y. H. Zhang, H. Q. Yuan and M. F. Ge, *J. Coord. Chem.*, 2008, **61**, 715; (e) S. Mondal, S. P. Rath, K. K. Rajak and A. Chakravorty, *Inorg. Chem.*, 1998, **37**, 1713; (f) G. C. Wang, J. Xiao, Y. N. Lu, L. Yu, H. B. Song, J. S. Li, J. R. Cui, R. Q. Wang, F. X. Ran and H. G. Wang, *Appl.*

Organometal. Chem., 2005, **19**, 113; (g) Y. Zou, Y. Z. Jiang and W. Z. Wang, *Acta Crystallogr., Sect. E: Crystallogr. Commun.*, 2010, **66**, m455.

9. (a) A. Nakahara, *Bull. Chem. Soc. Jpn.*, 1959, **32**, 1195; (b) M. Kishita, A. Nakahara and M. Kubo, *Aust. J. Chem.*, 1964, ***17,*** 810; (c) M. R. Wagner and F. A. Walker, *Inorg. Chem.*, 1983, **22**, 3021; (d) R. C. Burrows and J. C. Bailar, Jr., *J. Am. Chem. Soc.*, 1966, **88**, 4150; (e) J. C. Pessoa, I. Cavaco, I. Correia, M. T. Duarte, R. D. Gillard, R. T. Henriques, F.J. Higes, C. Madeira, I. Tomaz, *Inorg. Chim. Acta*, 1999, **293**, 1.

10. (a) V. P. Garcia, R. O. Latorre, E. Spodine, *Polyhedron*, 2004, **23**, 1869; (b) J. Vanco, Z. Travnicek, J. Marek, R. Herchel, *Inorg. Chim. Acta*, 2010, **363**, 3887.

11. (a) S. Shit, M. Nandy, G. M. Rosair, M. S. El Fallah, J. Ribas, E. Garribba and S. Mitra, *Polyhedron*, 2013, **52**, 963; (b) P. Talukder, S. Shit, A. Sasmal, S. R. Batten, B. Moubaraki, K. S. Murray and S. Mitra, *Polyhedron*, 2011, **30**, 1767; (c) Y. Lan, G. Novitchi, R. Clérac, J.-K. Tang, N. T. Madhu, I. J. Hewitt, C. E. Anson, S. Brooker and A. K. Powell, *Dalton Trans.*, 2009, 1721.

12. (a) M. A. Alam, M. Nethaji and M. Ray, *Angew. Chem., Int. Ed.*, 2003, **42**, 1940; (b) D. H. Leung, R. G. Bergman and K. N. Raymond, *J. Am. Chem. Soc.*, 2007, **129**, 2746; (c) J. S. Seo, D. Whang, H. Lee, S. I. Jun, J. Oh, Y. J. Jeon and K. Kim, *Nature*, 2000, **404**, 982; (d) E. Lee, J. Kim, J. Heo, D. Whang and K. Kim, *Angew. Chem., Int. Ed.*, 2001, **40**, 399; (e) J. M. Rivera, T. Martin and J. Rebek Jr., *Science*, 1998, **279**, 1021; (f) S. G. Kim, K. H. Kim, J. Jung, S. K. Shin and K. H. Ahn, *J. Am. Chem. Soc.*, 2002, **124**, 591; (g) S. Tashiro, Y. Ogura, S. Tsuboyama, K. Tsuboyama and M. Shionoya, Inorg. Chem., 2011, 50, 4; (h) Y. Inokuma, M. Kawano and M. Fujita, *Nat. Chem.*, 2011, **3**, 349; (i) S. C. Sahoo and M. Ray, *Chem. – Eur. J.*, 2010, **16**, 5004.

13. (a) S. A. Warda, *Z. Kristallogr. - New Cryst. Struct.*, 1998, **213**, 771; (b) S. A. Warda, *Acta Crystallogr., Sect. C: Struct. Chem.*, 1998, **54**, 304; (c) S. A. Warda, *Z. Kristallogr. - New Cryst. Struct.*, **214**, 1999, 77; (d) G. Plesch, C. Friebel, S. A. Warda, J. Sivy and O. Svajlenova, *Transition Met. Chem.*, **22**, 1997, 433; (e) A. G.

Raso, J. J. Fiol, A. L. p. Zafra, I. Mata, E. Espinosa and E. Molins, *Polyhedron*, 2000, **19** , 637.

14. (a) J. E. Davies, *Acta Crystallogr., Sect. C: Cryst. Struct. Commun.*, 1984, **40**, 903; (b) B. Das and K. O. Medhi, *Spectrochim. Acta, Part A.*, 2013, **104**, 352; (c) R. Hamalainen, U. Turpeinen, M. Ahlgren and M. Rantala, *Acta Chem. Scand. Ser. A.*, 1978, **A32**, 549.

15. C. M. Rajesh and M. Ray, *Dalton Trans.*, 2014, **43**, 12952.

16. (*a*) CrysAlis CCD and CrysAlis RED. Oxford Diffraction Ltd, Yarnton, Oxfordshire, England. Oxford Diffraction, 2009; (*b*) G. M. Sheldrick, Acta Crystallogr., Sect. A: Fundam. Crystallogr., 2008, A64, 112

17. M. N. Burnett and C. K. Johnson, ORTEP-III: Oak Ridge Thermal Ellipsoid Plot Program for Crystal Structure Illustrations, Oak Ridge National Laboratory Report ORNL-6895, 1996.

18. C.-G. Zhu, Synth. React. Inorg. Met.-Org., *Nano-Met. Chem.*, 2013, **43**, 886; (b) Y.-G. Li, D.-H. Shi, H.-L. Zhu, H. Yan and S. W. Ng, *Inorg. Chim. Acta*, 2007, **360**, 2881; (c) Z. Zhang, X. Li, C. Wang, C. Zhang, P. Liu, T. Fang, Y. Xiong and W. Xu, *Dalton Trans.*, 2012, **41**, 1252.

19. D. Heinert and A. E. Martell, *J. Am. Chem. Soc.*, 1962, **84**, 3257; (b) ref for uv of lisalala

20. Molar conductance (ohm−1 cm2 mol−1) range for 1 : 1 electrolyte in MeOH: 80–115. W. J. Geary, *Coord. Chem. Rev.*, 1971, **7**, 81.

21. X.-S. Gao, Y.-M. Wan, Q. Zhou, Y.-X. Shi and J.-T. Wang, *Acta Crystallogr., Sect. E: Crystallogr. Commun.*, 2007, **63**, m1417.

22. G. Miiller, G.-M. Maier and M. Lutz, *Inorg. Chim. Acta*, 1994, **218**, 121.

23. The amount of distortion was calculated from the structural data where the value of τ should be 0 for the perfect square-pyramidal geometry and 1 for the perfect trigonal

bipyramidal structure; A. W. Addision, T. N. Rao, J. Reedijk, J. van Rijn and G. C. Verschoor, *J. Chem. Soc., Dalton Trans*., 1984, 1349.

24. Hydroxo-bridged Cu(II)trinuclear complexes: (a) H.-D. Bian, J.-Y. Xu, W. Gu, S.-P. Yan, P. Cheng, D.-Z. Liao and Z.-H. Jianga, *Polyhedron*, 2003, **22**, 2927; (b) B. Sarkar, M. Sinha Ray, M. G. B. Drew, A. Figuerola, C. Diaz and A. Ghosh, *Polyhedron*, 2006, **25**, 3084; (c) P. Mukherjee, M. G. B. Drew, M. Estrader, C. Diaz and A. Ghosh, *Inorg. Chim. Acta*, 2008, **361**, 161; (d) B. L. Guennic, S. Petit, G. Chastanet, G. Pilet, D. Luneau, N. Ben Amor and V. Robert, *Inorg. Chem.*, 2008, **47**, 572; (e) C. Biswas, M. G. B. Drew, A. Figuerola, S. Gómez-Coca, E. Ruiz, V. Tangoulis and A. Ghosh, *Inorg. Chim. Acta*, 2010, **363**, 846; (f) Y.-B. Cai, L. Liang, J. Zhang, H.-L. Sunc and J.-L. Zhang, *Dalton Trans*., 2013, **42**, 5390.

25. (a) B. J. Hathaway, in *Comprehensive Coordination Chemistry*, ed. G. Wilkinson, R. D. Gillard and J. A. McCleverty, Pergamon Press, London, 1987, vol. 5, p. 533; (b) A. W. Addison and E. Sinn, *Inorg. Chem.*, 1983, **22**, 1225; (c) M. Bonamico, G. Dessy, A. Mugnoli, A. Vaeiago and L. Zambonelli, *Acta Crystallogr*., 1965, **19**, 886; (d) Y. Agus, R. Louis and R. Weiss, *J. Am. Chem. Soc*., 1979, **101**, 3381.

26. C. Knight and G. A. Voth, Acc. Chem. Res., 2012, **45**, 101.

27. IR of coordinated imine, ref (a) S. Thakurta, J. Chakraborty, G. Rosair, J. Tercero, M. S. E. Fallah, E. Garribba and S. Mitra, *Inorg. Chem.*, 2008, **47**, 6227; (b) K. Nakamoto, Infrared and Raman Spectra of Inorganic and Coordination Compounds, Theory and Applications in Inorganic Chemistry, 5th ed., John Wiley and Sons Inc., New York, 1997.

28. M. R. Wagner and F. A. Walker, *Inorg. Chem.*, 1983, **22**, 3021 and references therein; (b) N. Arulsamy and P. S. Zacharias, *Transition Met. Chem.*, 1991, **16**, 255; (c) A. B. P. Lever, *'Inorganic Electronic Spectroscopy'*, 2nd ed., Elsevier, New York, 1984.

29. (a) W. E. Hatfield and R. Whyman, *Transition Met. Chem.*, 1969, **47**, 5; (b) A. Earnshaw, 'An Introduction to Magnetochemistry', Academic, London, 1968; (c) F.

E. Mabbs and D. J. Machin, 'Magnetism and Transition Metal Complexes', Chapman and Hall, London, 1973; (d) C. J. OConnor, *Prog. Inorg. Chem.*, 1982, **29**, 203.

30. (A) H. Yokoi, A. W. Addison, *J. Chem. Soc., Dalton Trans*., 1977, **16**, 1341; (B) U. Sakaguchi, A. W. Addison, *J. Chem. Soc., Dalton Trans.*, 1979, 600; (C) E. Garribba, G. Micera, *J. Chem. Education*, 2006, **83**, 1229; (D) B. R. McGarvey, in 'Electron Spin Resonance of Transition Metal Complexes', ed. R. L. Carlin, Dekker, New York, 1966, vol. 3, p. 89

31. (a) M. P. Suh, M. Y. Han, J. H. Lee, K. S. Min and C. Hyeon, J. Am. Chem. Soc., 1998, **120**, 3819; (b) H.-D. Bian, J.-Y. Xu, W. Gu, S.-P. Yan, P. Cheng, D.-Z. Liao and Z.-H. Jiang, Polyhedron, 2003, **22**, 2927.

32. The program package JulX was used for spin-Hamiltonian simulations and fittings of the data by a full-matrix diagonalization approach (E. Bill, unpublished results).

33. W. E. Hatfield, in Magneto-Structural Correlations in Exchange Coupled Systems, ed. R. D. Willett, D. Gatteschi and O. Kahn, NATO-ASI Series, Reidel, Dordrecht, 1985, p. 555, and references therein.

34. M. Fondo, N. Ocampo, A. M. Garcìıa-Deibe, M. Corbella, M. R. Bermejoc and J. Sanmartìn, *Dalton Trans.*, 2005, 3785.

Chapter III

C-C cleavage of threonine side arm in salicylidene-L- threoninate Schiff base and formation of Cu(II) hexanuclear complex

In the last chapter, our interest in synthesizing chiral assembly of metal complexes using simple amino acid derived Schiff base lead to isolation of a μ_3-hydroxo bridged trinuclear Cu(II) complex, a previously unreported type of architecture using this of type ligands. The characterization of the complex showed racemization occurred during complexation. Racemization of Schiff bases, derived from amino acid, salicylaldehyde and pyridoxal as well as their substituted analogs under various conditions, had been studied to a great extent by others due to its relevance to vitamin B_6 chemistry.[1] Pyridoxal 5'-phosphate (PLP) is the active form of Vitamin B_6 . Synthetic models of PLP amino acid Schiff bases under basic condition and in presence of metal ions are known to undergo deprotonation of the alpha proton forming a quinonoid intermediate, which regenerates the amino acid upon protonation (Scheme **1A**). As the protonation occurs at a sp2 carbon in the quinonoid intermediate, amino acid formed is racemic in nature. Source of proton is water. From the literature[2,1e] we have also learned that in synthetic models of PLP Schiff bases of L-threonine, L-serine and L-cysteine, show loss of amino acid side arm from the quinonoid intermediates (Scheme **1B**) generating glycine derivative in case of threonine. We could not find any report where similar reaction has been occurred with salicylaldehyde. Salicylaldehyde derivatives are expected to be less reactive than pyridoxal due to the absence of pyridine nitrogen, which participate in stabilization of the quinonoid intermediate. Because of this, the 4-nitro derivatives of salicylaldehyde were chosen in model systems.[3,1b] In this chapter we choose to explore reactions of Schiff bases of L-threonine and L-serine of salicylaldehyde in presence of base and copper(II) salt. While we maintained the reaction conditions as close as possible to the last chapter, we tried few other variations in order to obtain crystals.

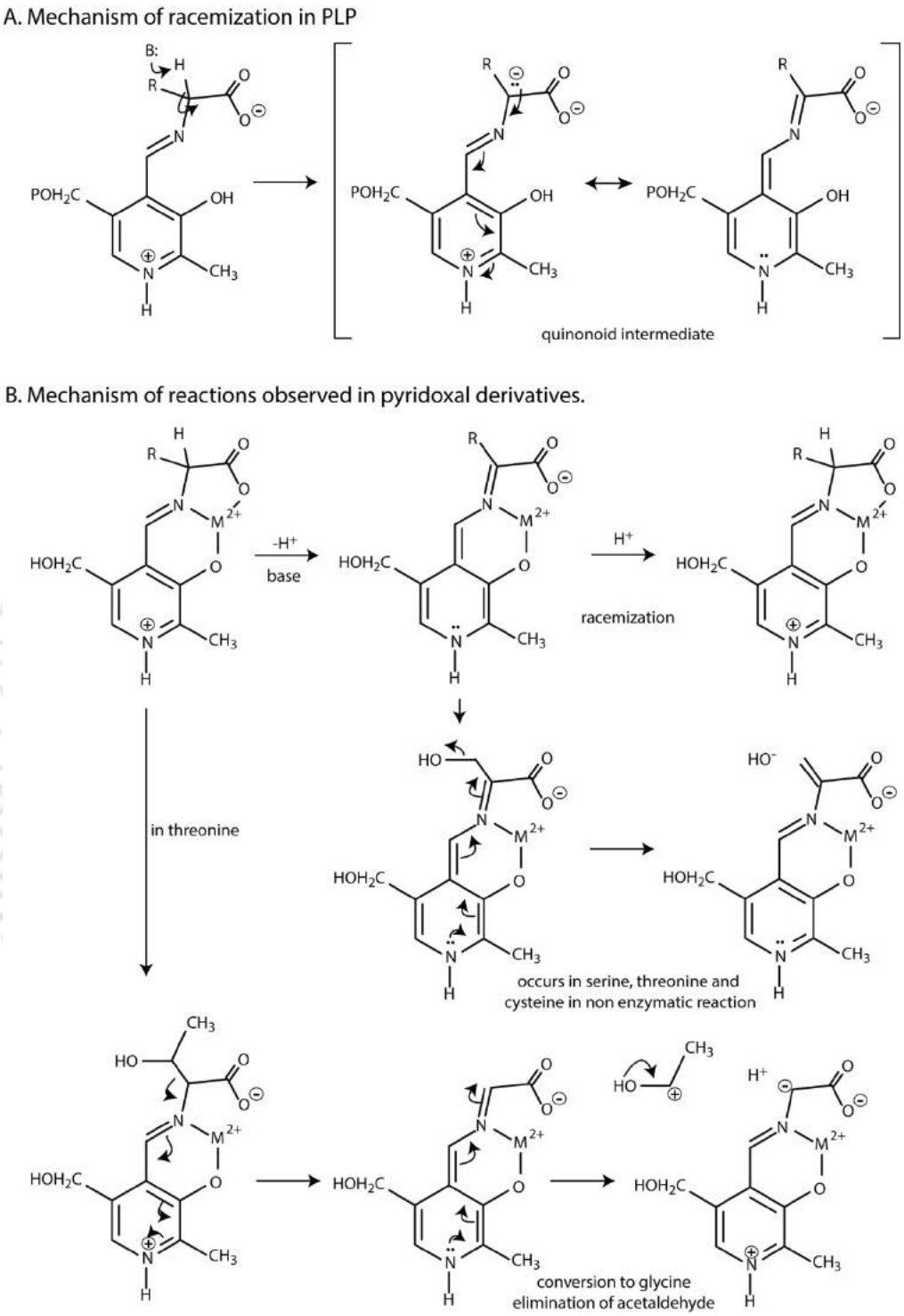

Scheme 3.1. Reported mechanism for amino acid transformations based on solution phase studies, scheme B redrawn from the reference 1a. P in figure denotes phosphate.

3.1 Experimental section

3.1.1 Materials and methods

Materials and methods used in this chapter are same as in the last chapter unless specifically mentioned. Glycine, L-threonine and L-serine were purchased from Sisco Research Laboratories Pvt. Ltd. (SRL), India, and used as received.

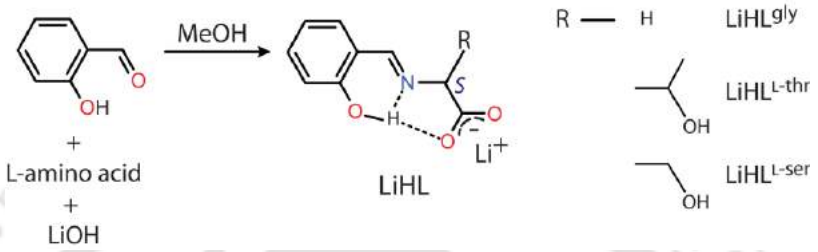

Scheme 3.2. The synthesis of the ligands.

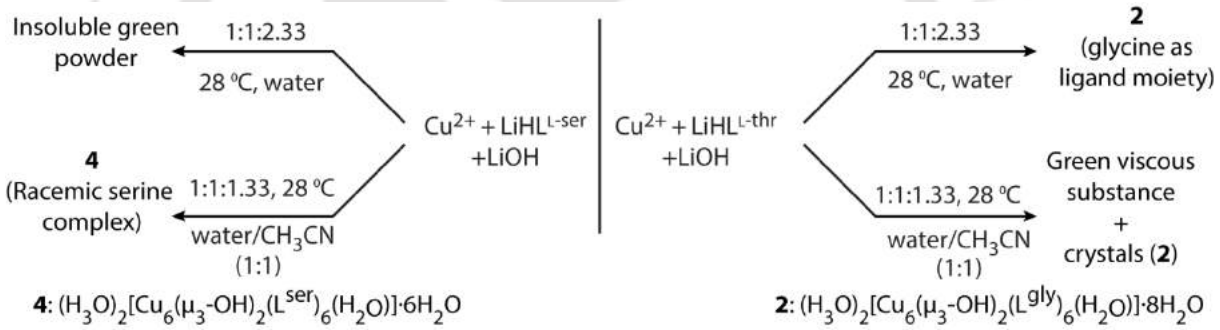

Scheme 3.3. The synthesis of the complexes.

3.2 Syntheses and characterization

3.2.1 $LiHL^{L\text{-}thr}$

$LiOH{\bullet}H_2O$ (0.705 g, 16.8 mmol) was added as solid in small quantities to a 10 min stirred suspension of L-threonine (2.00 g, 16.8 mmol) in 20 mL of MeOH and stirred continuously for 30 min. The resulting turbid solution was filtered through a frit and to the clear colorless filtrate salicylaldehyde (2.06 g, 16.9 mmol) was added in drops to give a pale brownish yellow solution. This solution was stirred for another 2 h. The volume of the reaction mixture was reduced to $1/4^{th}$ by rotary evaporation under vacuum and the resulting concentrated reaction mixture was cooled to room temperature, to which 10-15 mL of ethyl

acetate was added in small volumes and kept aside for 10-15 min to give a pale yellow precipitate. The precipitate was filtered off, washed with ethyl acetate (4 x 3 mL) and dried under vacuum. Yield 3.28 g (85%). %). ^{1}H NMR (400MHz, CD_3OD, ppm): 8.36 (imine, s, 1H), 7.32-7.26 (Ph-H, m, 2H), 6.79 (Ph-H, d, 1H, J = 8.4 Hz), 6.74 (Ph-H, t, 1H, J = 7.6 Hz), 4.16 (C-$H_{side\ arm}$, m, 1H, J = 6.4 Hz), 3.76 (C-H_{chiral}, d, 1H, J = 6.0 Hz), 1.26 (CH_3, d, 3H, J = 6.4 Hz). ESI-MS ($[M\text{-}Li+2H]^+$): calcd 224.2332; found 224.1875. $[\alpha]_D^{25}$ = +20^o in MeOH, c = 0.5. UV/Vis (MeOH): λ_{max}, nm (ε, M^{-1} cm^{-1}): 214 (17000), 220sh, 258 (9000), 280sh, 315 (2700), 404 (2000). IR (KBr, cm^{-1}): 3570(w), 1630(s), 1596(s), 1410(s), and 1272(m). Λ_M (ohm^{-1} cm^2 mol^{-1}): 41 in MeOH.

3.2.2 $LiHL^{gly}$

$LiOH{\bullet}H_2O$ (0.558 g, 13.3 mmol) was added as solid in small quantities to a 10 min stirred suspension of glycine (1.00 g, 13.3 mmol) in 20 mL of MeOH and stirred continuously for 30 min. To the resulting turbid solution, salicylaldehyde (1.64 g, 13.4 mmol) was added dropwise. A yellow precipitate was formed immediately and the reaction mixture was allowed to stir for another 1.5 h. The yellow precipitate was filtered off, washed with diethyl ether (4 x 3 mL) and dried under vacuum. Yield 2.11 g (86%). ^{1}H NMR (300MHz, CD_3OD, ppm): 8.36 (imine, s, 1H), 7.32 (Ph-H, d, 2H), 6.71- 6.81 (Ph-H, m, 2H), 4.24 (-CH_2, s, 2H). ESI-MS ($[M\text{-}H]^-$): calcd 184.0978; found 184.1669. UV/Vis (MeOH): λ_{max}, nm (ε, M^{-1} cm^{-1}): 215 (19000), 254 (9000), 278sh, 316 (2700), 402 (2000). IR (KBr, cm^{-1}): 3454(w), 1655(s), 1622(s), 1522(s) and 1393(s). Λ_M (ohm^{-1} cm^2 mol^{-1}): 42 in MeOH.

3.2.3 $LiHL^{L\text{-}ser}$

$LiOH{\bullet}H_2O$ (1.97 g, 0.047 mol) was added as solid in small quantities to a 10 min stirred white slurry of L-serine (5.00 g, 0.048 mol) in 30 mL of MeOH and stirred continuously for 30 min. The resulting turbid solution was filtered through a frit and to the clear colorless filtrate salicylaldehyde (5.74 g, 0.047 mol) was added dropwise to give a brownish yellow solution. This solution was stirred for another 2 h and then, the solvent was completely evaporated by rotary evaporation under vacuum to give a yellowish brown oily substance. To this 4-5 mL of EtOH was added and dissolved the oily substance. To this 8-10 mL of diethyl ether was added to precipitate the compound. The resulting yellow lumps were

made in to fine powder by stirring for about 20 min and filtered off (4.560 g). The filtrate was completely evaporated to give an oily substance, which was dried under high vacuum to give a yellow powder (0.900 g). Both the yellow powders were washed with diethyl ether (10 x 5 mL) and weighed after drying under vacuum. Yield 5.460 g (54%). ^{1}H NMR (400MHz, CD_3OD, ppm): 8.38 (imine, s, 1H), 7.32-7.26 (Ph-H, m, 2H), 6.79 (Ph-H, d, 1H, J = 8.4 Hz), 6.73 (Ph-H, t, 1H, J = 7.4 Hz), 4.05-4.01 ($CH_{2side\ arm}$, m, 2H, J = 6.4 Hz), 3.83 (C-H_{chiral}, dd, 1H, J = 12.0 & 9.0 Hz). ESI-MS ($[M\text{-}Li+2H]^+$): calcd 210.2066; found 210.1720. $[\alpha]_D^{25} = 0^o$ (Optical rotation: starts with an initial value of 0.050 and ends with zero within 1 h) in MeOH, c = 0.5. UV/Vis (MeOH): λ_{max}, nm (ε, M^{-1} cm^{-1}): 215 (17800), 256 (9200), 275sh, 316 (2800), 403 (2200). IR (KBr, cm^{-1}): 3443(br), 1646(s), 1610(s), 1531(m), 1463(m) and 1384(m). Λ_M (ohm^{-1} cm^2 mol^{-1}): 41 in MeOH.

3.2.4 $(H_3O)_2[Cu_6(\mu_3\text{-}OH)_2(L^{gly})_6(H_2O)]\bullet 8H_2O$ (2)

$LiOH\bullet H_2O$ (0.130 g, 3.10 mmol) was added as solid in small quantities to a 5 min stirred yellow solution of $LiHL^{L\text{-}thr}$ (0.300 g, 1.31 mmol) in 2 mL of H_2O and stirred continuously for 30 min to give a pale yellow solution. A solution of $Cu(ClO_4)_2\bullet 6H_2O$ (0.485 g, 1.31 mmol) in 3 mL of H_2O was added dropwise to the above solution, which immediately gave a turbid green solution. To this 3 mL acetone was added and stirred continuously for 1.5 h, resulting in almost a clear green solution. The reaction mixture was filtered and slow evaporation of the filtrate gave fine blue micro crystals after 3-4 days. The precipitate after filtration was negligible. The crystals were isolated, washed with water and acetone mixture (1:2) and dried under vacuum. Yield 0.190 g (51%). Anal. Calcd. for $(H_3O)_2[Cu_6(\mu_3\text{-}OH)_2(L^{gly})_6(H_2O)]\bullet 8H_2O$: C, 38.64; H, 4.08; N, 5.01; found C, 38.55; H, 3.96; N, 5.10. UV/Vis (MeOH): λ_{max}, nm (ε, M^{-1} cm^{-1} /Cu_6 unit): 223 (114000), 242 (115000), 268 (68000), 368 (26000), 657 (600). IR (KBr, cm^{-1}): 3443(br), 1643(s), 160(s), 1545(m), 147(m), 1446(s), 1420(w), 1369(m), 1292(m), 1200(m), 1153(m), 937, 798, 778 and 576. ESI-MS ($[Cu_3(\mu_3\text{-}OH)(L^{gly})_3]^-$): calcd 739.1158; found 739.7448. μ_{eff} (powder, 298K): 1.76μ_B/Cu. Λ_M (ohm^{-1} cm^2 mol^{-1}): 116 in MeOH. EPR in DMF at 298K: g_{av} 2.102, A_{av} 86 G.

Alternatively complex **(2),** can be synthesized directly from the complexation reaction of $LiHL^{gly}$ with $Cu(ClO_4)_2\bullet 6H_2O$ **(3)**. A solution of $LiOH\bullet H_2O$ (0.060 g, 1.43 mmol) in 1 mL of H_2O was added dropwise to a stirring yellow solution of $LiHL^{L\text{-}gly}$ (0.200 g, 1.08 mmol) in

3 mL of H_2O. The resulting yellow solution was stirred continuously for 10-15 min and to this a solution of $Cu(ClO_4)_2$•$6H_2O$ (0.320 g, 0.864 mmol) in 2 mL of H_2O was added dropwise to to give a turbid green solution. A green precipitate was formed after 30 min and the reaction mixture was allowed to stir continuously for another 1.5 h. The green precipitate was filtered off, and the precipitate was washed first with water (3 x 2 mL) and then with acetone (2 x 3 mL). The precipitate was dried under vacuum and weighed (0.160 g). The filtrate was kept in air, and after 2-3 days gave blue micro crystals (under microscope). The crystals were isolated, washed with water and acetone mixture (1:2) and dried under vacuum (0.010 g). Yield 0.160 g (70%). Anal. Calcd. for $(H_3O)_2[Cu_6(\mu_3\text{-}OH)_2(L^{gly})_6\ (H_2O)]$•$8H_2O$: C, 38.64; H, 4.08; N, 5.01; found C, 38.46; H, 3.93; N, 5.10. UV/Vis (MeOH): λ_{max}, nm (ε, $M^{-1}\ cm^{-1}$ /Cu_6 unit): 223 (126000), 242 (126000), 268 (74000), 367 (28000), 658 (600). IR (KBr, cm^{-1}): 3450(br), 1644(s), 1600(s), 1546(m), 1471(m), 1446(s), 1420(w), 1369(m), 1292(m), 1200(m), 1153(m), 937, 798, 778 and 576. ESI-MS ($[Cu_3(\mu_3\text{-}OH)(L^{gly})_3]^-$): calcd 739.1158; found 739.7648. μ_{eff} (powder, 298K): 1.82 μ_B/Cu. Λ_M ($ohm^{-1}\ cm^2\ mol^{-1}$): 101 in MeOH. EPR in DMF at 298K: g_{av} 2.102, A_{av} 89 G.

3.2.5 $(H_3O)_2[Cu_6(\mu_3\text{-}OH)_2(L^{ser})_6(H_2O)]$•$6H_2O$ (4)

LiOH•H_2O (0.026 g, 0.620 mmol) was added as solid in small quantities to a 5 min stirred yellow solution of $LiHL^{L\text{-}ser}$ (0.100 g, 0.465 mmol) in 3 mL of H_2O and stirred for another 10 min. To this, 3 mL of acetonitrile was added and stirred for another 15 min. A solution of $Cu(ClO_4)_2$•$6H_2O$ (0.172 g, 0.464 mmol) in 1 mL of H_2O was added dropwise to the yellow solution to give a turbid green solution. To this 1 mL acetonitrile was added and stirred continuously for another 1.5 h. Then, the reaction mixture was filtered and the precipitate was washed first with water (3 x 2 mL) and then with acetone (2 x 3 mL). The precipitate was dried under vacuum and weighed (0.027 g). Slow evaporation of the filtrate gave fine blue micro crystals after 3-4 days. The crystals were isolated, washed with water and acetone mixture (1:2) and dried under vacuum. Yield 0.045 g (33%). Anal. Calcd. for $(H_3O)_2[Cu_6(\mu_3\text{-}OH)_2(L^{ser})_6(H_2O)]$•$6H_2O$: C, 39.54; H, 4.20; N, 4.61; found C, 39.72; H, 4.09; N, 4.78. UV/Vis (MeOH): λ_{max}, nm (ε, $M^{-1}\ cm^{-1}$ /Cu_6 unit): 223 (113000), 242 (120000), 268 (70000), 367 (28000), 653 (600). IR (KBr, cm^{-1}): 3417(br), 1634(s), 1599(s), 1540(m), 1469(m), 1444(s), 1410(w), 1383(w), 1345(m), 1292(m), 1200(m), 1153(m), 1068(m), 910,

801, 783 and 552. μ_{eff} (powder, 298K): 1.86 μ_B/Cu. Λ_M (ohm^{-1} cm^2 mol^{-1}): 128 in MeOH. EPR in DMF at 298K: g_{av} 2.102, A_{av} 90 G.

3.3 X-ray Data Collection, Structure Solution and Refinement

The crystal structures of **LiHL^{gly}**, **2**, **3** and **4** were obtained by using single crystal X-ray diffraction method. Single crystal of **LiHL^{gly}** was obtained from a mixture of methanol and diethyl ether solution of the ligand by slow evaporation. Single crystals of **2**, **3** and **4** were obtained by slow evaporation of the filtrate of their corresponding reaction mixtures.

All geometric and intensity data for **1** was collected at room temperature using a Bruker SMART APEX CCD diffractometer, equipped with a fine focus 1.75 kW sealed tube Mo-K X-ray source, with increasing (width of 0.3 per frame) at a scan speed of 3 s/frame. The SMART software was used for data acquisition and the SAINT software for data extraction. Absorption corrections were not performed. The structures were solved and refined using SHELX97.[4] Single crystal X-ray structural studies of **LiHL^{gly}**, **3** and **4** were performed on a CCD Oxford Diffraction XCALIBUR-S diffractometer. The intensities of the X-ray reflections were collected at room temperature [296(2) K] using graphite-monochromated Mo Kα radiation (λα = 0.71073 Å). The strategy for the intensity data collection was evaluated by using the CrysAlisPro CCD software. The intensities data were recorded by the standard φ–ω scan techniques, and were scaled and reduced using CrysAlisPro RED software.[5] The structures were solved and refined using SHELX97.[4] All non-hydrogen atoms were refined anisotropically. The hydrogen atoms were located from the difference Fourier maps and were refined isotropically. Selected crystallographic data are given in Table 3.1. Perspective view of the complex was obtained by ORTEP.[6]

3.4 Results and discussion

3.4.1 Ligand synthesis and crystal structure

The zwitterionic amino acids glycine, L-threonine and L-serine were deprotonated with one equiv. LiOH•H_2O in MeOH to form the free amine, which undergoes condensation with salicylaldehyde to form the corresponding amino acid Schiff bases (Scheme **3.2**). The ligands were isolated as monolithium salt from the reaction medium by adding appropriate precipitant

to precipitate the ligand and were filtered off, washed with diethyl ether and dried under vacuum. All the ligands are yellow in color. Yield of $LiHL^{L\text{-}thr}$ and $LiHL^{gly}$ are about 85% and $LiHL^{L\text{-}ser}$ is about 55%.

Immediate appearance of yellow color in the reaction medium after addition of salicylaldehyde indicates the formation of imine bond. UV-vis spectral study of $LiHL^{L\text{-}thr}$, $LiHL^{L\text{-}ser}$ and $LiHL^{L\text{-}gly}$ gave two characteristic imine absorption bands between 300 and 410 nm in MeOH and water (Figure **3.10**). The imine stretching frequency between 1630 and 1655 cm^{-1} in the FT-IR spectra and the appearance of imine proton as a singlet between 8.36 and 8.38 ppm in ^{1}H-NMR experiment confirms the formation of the Schiff bases. Detailed assignments based on both position and integration has been provided in experimental section.

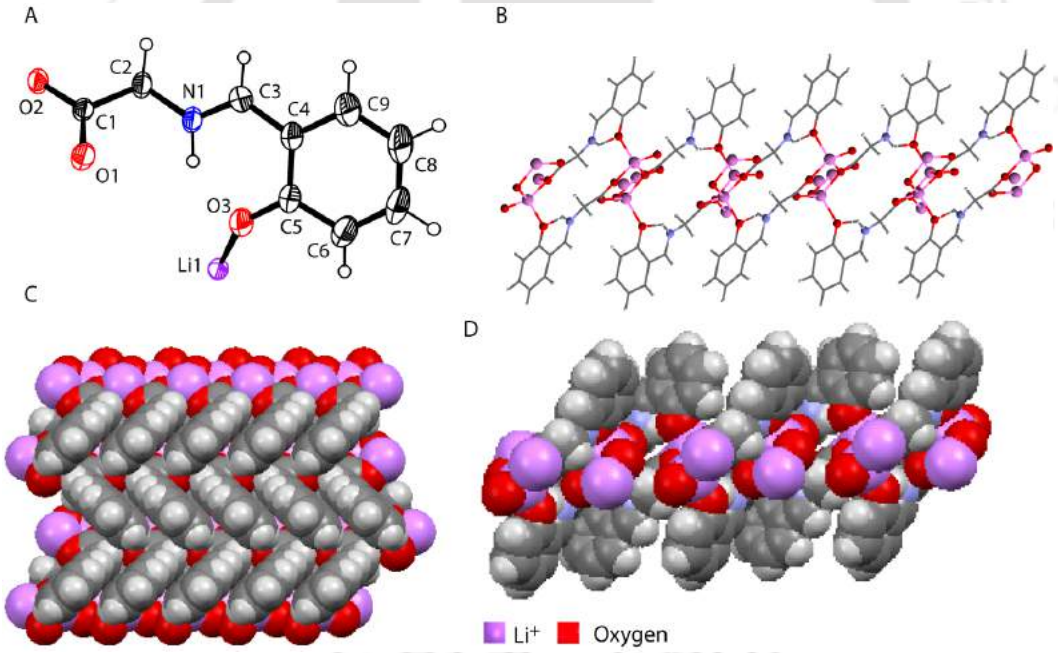

Figure 3.1. (A) ORTEP diagram of the asymmetric unit of $LiHL^{gly}$ with thermal ellipsoids set to 40% probability, (B) Two-dimensional coordination network formed by $LiHL^{gly}$, (C) and (D) Space filling models of the coordination network along different axes.

Among the three ligands, only $LiHL^{gly}$ has formed crystals suitable for structural characterization. It was crystallized from a mixture of methanol and ether solution (1:1). The crystal was solved in an achiral space group of *C*2/c in the monoclinic crystal system.

Table 3.1 Selected crystallographic data for **LiHL^{gly}**, **2**, **3** and **4.**[a]

Compounds	**LiHL^{gly}**	**2**	**3**	**4**
Empirical formula	$C_9H_8Li\,NO_3$	$C_{54}H_{68}Cu_6N_6O_{31}$	$C_{54}H_{68}Cu_6N_6O_{31}$	$C_{60}H_{76}Cu_6N_6O_{35}$
M	185.10	1678.41	1678.41	1822.54
Wavelength (Å)	0.71073	0.71073	0.71073	0.71073
Crystal system	Monoclinic	Trigonal	Trigonal	Trigonal
Space group	*C*2/c	$R\bar{3}$	$R\bar{3}$	$R\bar{3}$
a/Å	31.278(3)	16.2661(6)	16.1568(18)	16.3204(9)
b/Å	5.0066(3)	16.2661(6)	16.1568(18)	16.3204(9)
c/Å	11.8096(10)	22.725(2)	22.476(5)	22.6886(12)
α/°	90.00	90.00	90.00	90.00
β/°	103.412(13)	90.00	90.00	90.00
γ/°	90.00	120.00	120.00	120.00
V/Å^3	1798.9(3)	5207.2(7)	5081.1(18)	5233.6(7)
Z	8	3	3	3
ρ/g cm^{-3}	1.367	1.642	1.683	1.716
μ/mm^{-1}	0.101	1.900	1.947	1.895
Flack parameter	-	-	-	-
Reflections collected	5939	15804	4788	4327
Independent reflections	2335	2216	2904	2964
Goodness of fit	1.036	1.031	0.951	0.964
Final *R* indices [$I > 2\sigma(I)$]	*R*1 = 0.0479	*R*1 = 0.0500	*R*1 = 0.1011	*R*1 = 0.0616
	*wR*2 = 0.1171	*wR*2 = 0.1358	*wR*2 = 0.2256	*wR*2 = 0.1332
R indices (all data)	*R*1 = 0.0652	*R*1 = 0.0604	*R*1 = 0.2642	*R*1 = 0.1039
	*wR*2 = 0.1301	*wR*2 = 0.1486	*wR*2 = 0.3473	*wR*2 = 0.1480

[a] Refinement method: full-matrix least-squares on F^2.

Table 3.2 Selected bond distances (Å) and angles (°) for **2**, **3** and **4**.

Complex-2		**Complex-3**		**Complex-4**	
Bond length (Å)		Bond length (Å)		Bond length (Å)	
Cu1-O2	1.940(5)	Cu1-O2	1.941(8)	Cu1-O2	1.929(3)
Cu1-O3	1.917(5)	Cu1-O3	1.928(7)	Cu1-O4	1.920(3)
Cu1-O4	1.981(3)	Cu1-O4	1.976(5)	Cu1-O5	1.976(2)
Cu1-N1	1.904(6)	Cu1-N1	1.910(10)	Cu1-N1	1.920(4)
Cu1-O3_i	2.44(7)	Cu1-O3_i	2.41(1)	Cu1-O4_i	2.479(3)
Bond angle (°)		Bond angle (°)		Bond angle (°)	
O2-Cu1-O4	95.1(2)	O2-Cu1-O4	95.8(4)	O2-Cu1-O4	177.88(15)
O3-Cu1-O4	87.0(2)	O3-Cu1-O4	86.7(3)	O5-Cu1-O4	87.20(16)
N1-Cu1-O4	167.2(2)	N1-Cu1-O4	168.3(4)	N1-Cu1-O5	165.34(17)
O3-Cu1-O2	177.9(3)	O3-Cu1-O2	177.4(4)	O2-Cu1-O5	94.64(17)
N1-Cu1-O2	84.4(3)	N1-Cu1-O2	84.3(4)	N1-Cu1-O2	84.66(16)
N1-Cu1-O3	93.7(2)	N1-Cu1-O3	93.3(3)	N1-Cu1-O4	93.82(15)
N1-Cu1-O3_i	118.9(2)	N1-Cu1-O3_i	117.2(4)	N1-Cu1-O4_i	121.4(2)
O4-Cu1-O3_i	73.9(2)	O4-Cu1-O3_i	74.5(4)	O4-Cu1-O4_i	73.2(2)
Cu1-O4-Cu1	105.4(2)	Cu1-O4-Cu1	105.2(4)	Cu1-O4-Cu1	106.36(18)

Table 3.3 H-bonding distances (Å) and angles (°) for **2**, **3** and **4**.

D-H…A	*d*(D-H) (Å)	*d*(H…A) (Å)	*d*(D…A) (Å)	∟D-H…A (°)
		Complex-2		
[a]O4…O5	-	-	2.72(1)	-
[a]O5…O6	-	-	2.74(1)	-
[a]O6…O1	-	-	2.72(1)	-
[a]O8…O3	-	-	3.09(5)	-
		Complex-3		
[a]O4…O5	-	-	2.70(2)	-
[a]O5…O6	-	-	2.67(2)	-
[a]O6…O1	-	-	2.68(3)	-
[a]O8…O3	-	-	3.08	-
		Complex-4		
O5-H11…O6	0.87(9)	1.85(9)	2.72(1)	180(2)
O3-H7A…O3_viii	0.82	2.37	2.72(2)	106
[a]O6…O7	-	-	2.77(7)	-
[a]O7…O1	-	-	2.76(8)	-
[a]O8…O4	-	-	3.04(4)	-

[a] Hydrogen on O4, O5, O6, O7 and O8 could not be found from difference Fourier map.

The asymmetric unit contains lithium salt of the ligand. The bond N1–C3 with a length of 1.277(2) Å is shorter due to its double bond nature. The hydrogen attached with N1 was located from difference Fourier map. Forcible attachment of this to oxygen leads to an increase in the R-value. Thus attachment of this hydrogen with N1 is justified (Section **2.4.2**). The phenolate oxygen atom forms an intramolecular hydrogen bond with the protonated imine nitrogen and is of 2.57(2) Å. In the crystal lattice lithium ion is tetrahedrally coordinated to three bridging carboxylate oxygens and one phenolate oxygen. Both the tetrahedral coordination of lithium ion and the carboxylate acting as bridges between the lithium ions form a 2D coordination network (Figure **3.1**) of the ligand in the crystal lattice. A view along a-axis shows a zig-zag chain network and in the each 2D layer, the hydrophilic core formed by the lithium coordination is sandwiched between the hydrophobic aromatic rings (Figure **3.1**).

3.4.2 Complexation of $LiHL^{L\text{-}thr}$ with Cu(II) (C-C cleavage of threonine side arm)

Complexation of $LiHL^{L\text{-}thr}$ with Cu(II) in presence of 2.33 equiv. $LiOH{\bullet}H_2O$ in water (Scheme **3.3**) yielded crystals of complex **2**. Complex **2** was synthesized by mixing $LiHL^{L\text{-}thr}$, $LiOH{\bullet}H_2O$ and $Cu(ClO_4)_2{\bullet}6H_2O$ in the ratio 1:2.33:1 respectively, in water (Scheme **3.3**). Initially the reaction gave a turbid green solution and at the end it turned almost into a green solution. The filtrate, after 3-4 days gave blue block shaped crystals (under microscope) of diffraction quality, upon keeping in air.

Crystal structure of complex **2** was characterized by X-ray crystallography. The structure of **2** was solved in an achiral space group of $R\bar{3}$ in the trigonal crystal system. Molecular structure of complex **2** showed the absence of threonine's side arm in the ligand moiety of the complex, indicating the occurrence of C-C cleavage during the reaction. Similar type of C-C cleavages were reported in pyridoxiledene aminoacidato (L-threonine and L-serine) complexes in presence of base,[2] whereas none was reported with salicylidene aminoacidato complexes. The overall structure is nearly identical with that of complex **1** in chapter 2. The asymmetric unit contains one sixth of the molecule (Figure **3.2**). Complex **2** has two trinuclear Cu(II) units which are oriented face to face with a water molecule at the centre forming a hexanuclear Cu(II) cage (Figure **3.2**).

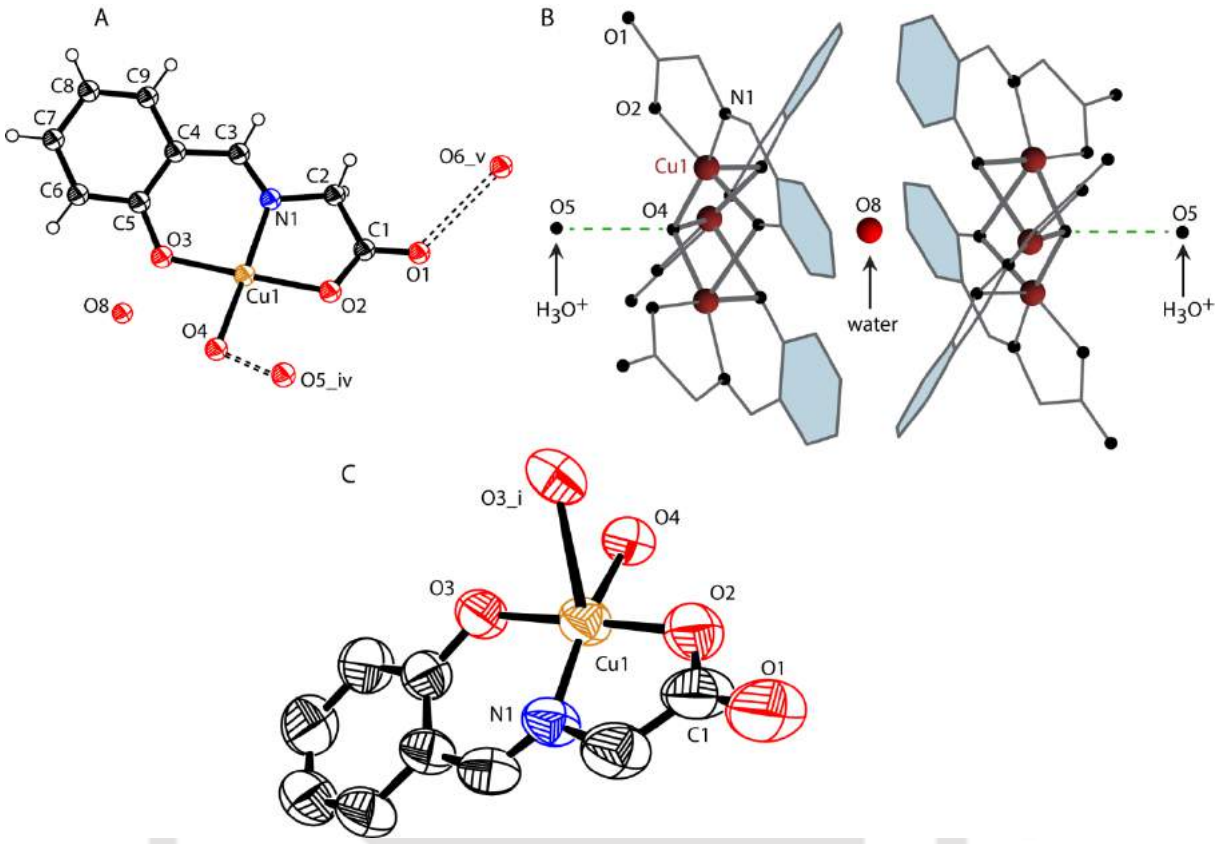

Figure 3.2. (A) ORTEP diagram of the asymmetric unit of **2** with thermal ellipsoids set to 40% probability. The atoms O5_iv and O6_v were generated using the symmetry operation (x, y, 1+z), (B) Schematic representation of the hexanuclear molecule of **2**, and (C) ORTEP diagram showing the pentacoordinated Cu(II) in **2,** with thermal ellipsoids set to 40% probability. The atom O3_i was generated using the symmetry operation (1-x+y, 1-x, z).

Each trinuclear Cu(II) unit consist of three, five coordinated Cu(II) bound to a single terminal hydroxo bridge. Each Cu(II) is coordinated by one tridentate L^{2-}, hydroxo bridge (O4) and phenolate oxygen (O3_i) from the next Cu(II) in the axial position (Figure **3.2C**). The geometry at Cu(II) is slightly a distorted square pyramidal for **2** (τ 0.178).[7] The in-plane bond length ranges from 1.917(5) Å for phenolate (O3) to 1.981(3) Å for bridging hydroxide (O4). It has considerably a longer axial bond length of 2.440(7) Å for the phenolate bridge. The longer axial bond length is probably due to the Jahn–Teller effect, common for Cu(II).[8] The selected bond lengths and angles are given in (Table **3.2**). The lengths and angles are comparable to other hydroxo-bridged trinuclear Cu(II) complexes.[9] The trapped water

molecule within the hexanuclear cage **2** is at a distance of 3.098(5) Å (O8…O3) from the six phenolate oxygen atoms.

The structure has a notable H-bonding arrangement. The oxygen atom O5 (hydronium) is within H-bonding distances of O4 (bridging hydroxide) and three O6 (solvent water) (Table **3.3**). The three O6 are arranged in a *C*3 symmetric fashion around O5 through which the *C*3 axis passes and also through O4 (Figure **3.3B**). The atom O6 is further H-bonded to the carboxylate (O1) from the neighboring unit. H's on O4, O5 and O6 could not be found from the difference Fourier map. The charge balance on the two $[Cu_3L_3OH]^-$ units require two cations. Since no other cation could be found, tentatively O5 was assigned as a hydronium ion as it is within H-bonding distance of three O6, symmetrically. This assignment augurs well with the charge of the trinuclear half. Alternatively, it is possible that one proton per trinuclear unit is disordered over O5 and three O6. The known examples of hydronium ion within crystals usually bind to three water molecules with short H-bond distances ~2.5 Å without any possibility of a fourth H-bond on oxygen.[10] Thus a total of four H-bonds on O5 is difficult to explain. Thus it is not possible to pinpoint the location of the protons either on O5 or on O6.

The lattice also contains a pocket, formed between six of the O6, which are in-between the two hexanuclear cage (Figure **3.3B**). The electron density inside the pocket was refined as an oxygen atom (O7) and it is highly disordered symmetrically over six positions. Thermogravimetric analysis (TGA) of **2**, between 30 and 140 °C showed a weight loss of 12.20%, which could be accounted for 11 H_2O molecules (calc. weight loss of 11.90%) (Figure **3.9**). Thus TGA supports the assignment of O7 as water. However, the large thermal ellipsoids of O7 and the short O7–O7 distance (2.27(9) Å) indicate disorder at this position.

The complex **3** was synthesized directly by using $LiHL^{gly}$, instead of $LiHL^{L\text{-}thr}$ in the complexation reaction. It was synthesized by mixing $LiHL^{gly}$, $LiOH{\bullet}H_2O$ and $Cu(ClO_4)_2{\bullet}(H_2O)_6$ in the ratio 1:1.33:0.85 respectively, in water. During the reaction it gave a green precipitate. The filtrate, after 3-4 days gave blue block shaped crystals (under microscope) of diffraction quality, upon keeping in air. The FT-IR spectrum of the green precipitate is nearly identical with that of the mounted crystal (**3**). The powder-XRD pattern of the green precipitate and the one which was simulated from the X-ray crystallographic

analysis of the crystal (**3**) were compared and found to be consistent with each other (Figure **3.4A**). Hence the above results indicate that, the green powder, which was precipitated from the reaction and the crystals which were isolated from the filtrate are the same compound. The complex is soluble in MeOH, however use of 1 equiv. Cu(II) in the synthesis of **3** gives a green precipitate, of which some of it dissolves in MeOH and the rest remains undissolved indicating the formation of some other by-product during the reaction.

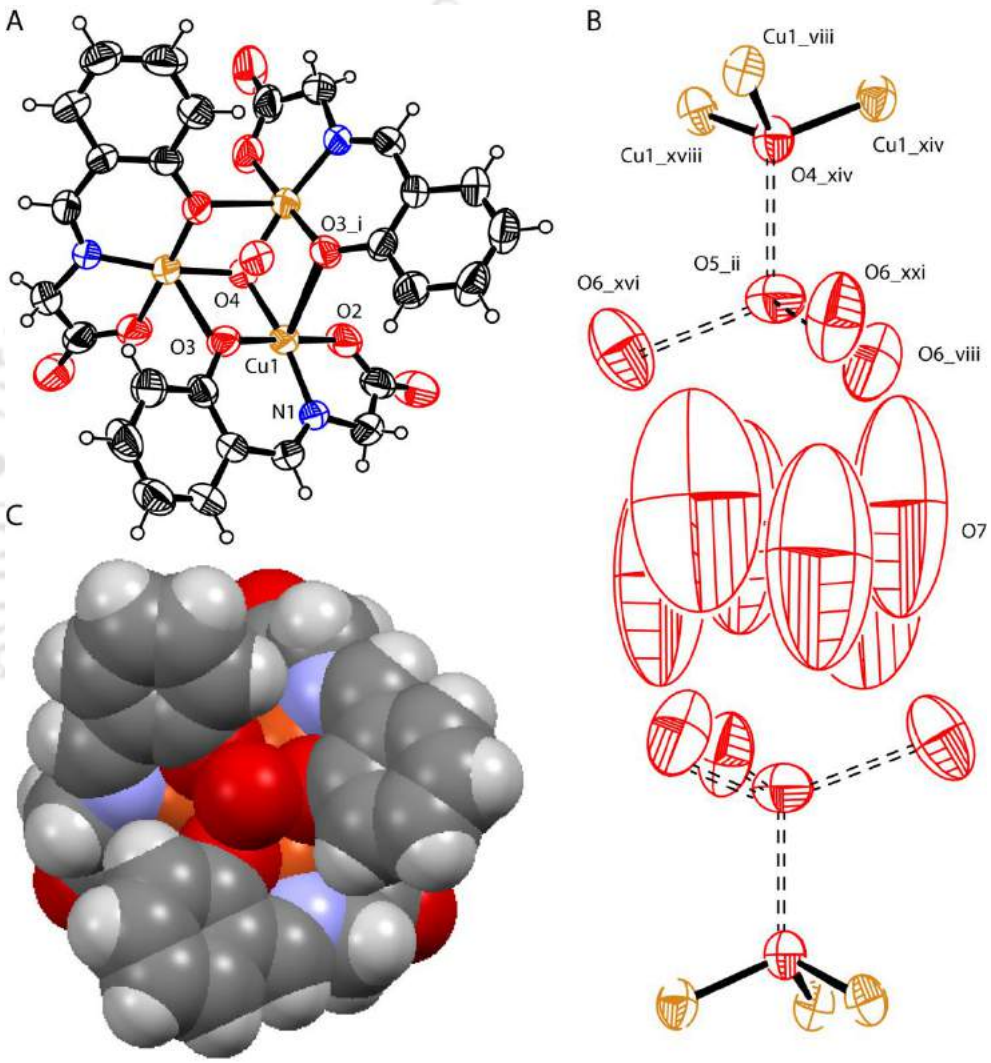

Figure 3.3. (A) ORTEP diagram of the trinuclear half of **2** with thermal ellipsoids set to 40% probability. The atom O3_i was generated using the symmetry operation (1-x+y, 1-x, z), (B) The pocket formed between two hydronium ions occupied by a symmetrically disordered water molecule (O7). The atoms Cu1_xviii, Cu1_viii, Cu1_xiv, O4_xiv, O5_ii, O6_xvi, O6_viii and O6_xxi were generated using the symmetry operations (1/3-x+y, 2/3-x, -1/3+z),

(-2/3+x, -1/3+y, -1/3+z), (1/3-y, -1/3+x-y, -1/3+z), (-2/3+x, -1/3+y, -1/3+z), (-2/3+x, -1/3+y, 2/3+z), (1-x, 1-y, 1-z), (-1+y, -x+y, 1-z) and (x-y, -1+x, 1-z), respectively, and (C) Space filling model of **2** showing the *C*3 symmetric cavity.

Since C-C cleavage was observed in threonine's side arm in the synthesis of **2**, complexation of $LiHL^{L\text{-}thr}$ with Cu(II) in relatively lesser quantity of base (1.33 equiv. $LiOH{\bullet}H_2O$) (Scheme **3.3**) was tried to isolate heaxanuclear Cu(II) complex with threonine's side arm intact in the ligand moiety as crystals. The complexation gave a green viscous substance along with few crystals of **2**, indicating a lesser amount of cleavage in lesser quantity of base. The FT-IR of crystals of **2** isolated from the reaction involving lesser quantity (1.33 equiv. $LiOH{\bullet}H_2O$) of base is identical with that of the **2** isolated from the reaction involving relatively higher quantity (2.33 equiv. $LiOH{\bullet}H_2O$) of base. A possible reason for few crystals of **2** in lesser quantity of base could be formation of R-threonine, and R- and S-allo-threonine Schiff base Cu(II) complexes in the reaction mixture due to racemization of either of the two chiral centers in L-threonine.

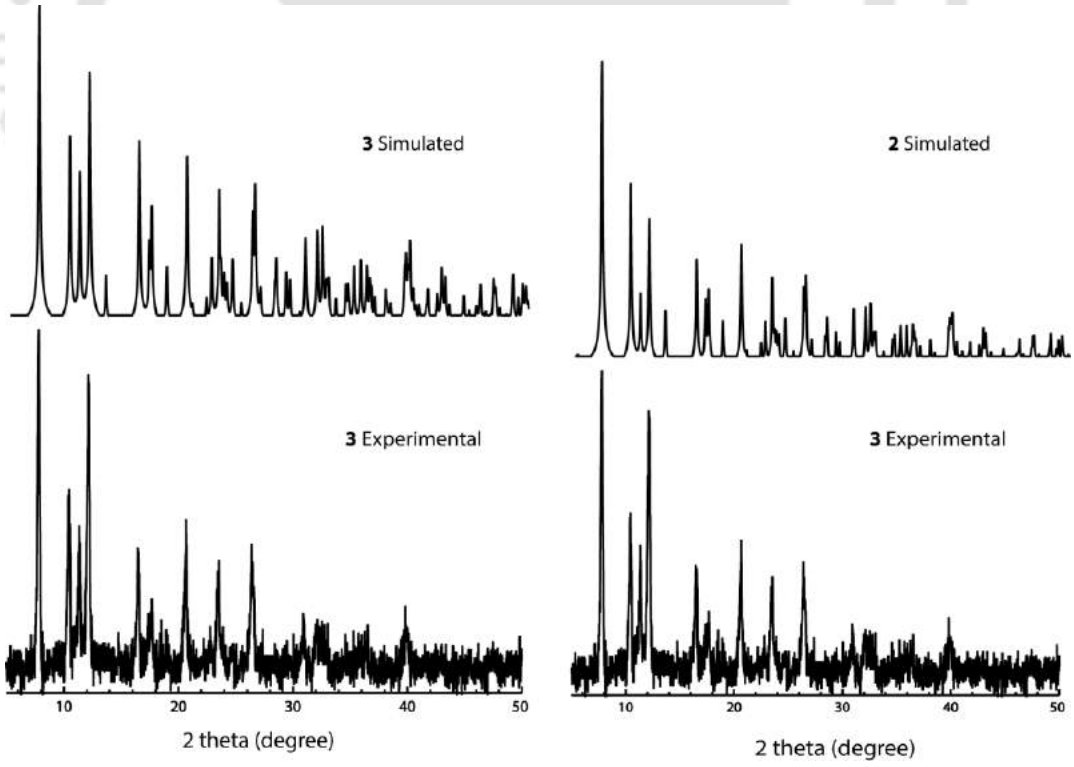

Figure 3.4. (A) Simulated and experimental powder-XRD pattern of **3** and (B) comparison of simulated and experimental powder-XRD pattern of **2** and **3**, respectively.

3.4.3 Complexation of $LiHL^{L\text{-}ser}$ with Cu(II)

Complexation of $LiHL^{L\text{-}ser}$ with Cu(II) in presence of 2.33 equiv. $LiOH{\bullet}H_2O$ (Scheme **3.3**) in water gave a green precipitate, which is insoluble in DMF, DMSO, MeOH, H_2O and acetonitrile. Except FT-IR experiment, the powder was not characterized with any other technique. FT-IR spectrum of the green powder was found to be different from that of the crystals of **2** (Figure **3.5**). This indicates that, unlike $LiHL^{L\text{-}thr}$, in the case of $LiHL^{L\text{-}ser}$ a different reaction might have occurred to give a product that is different from **2**.

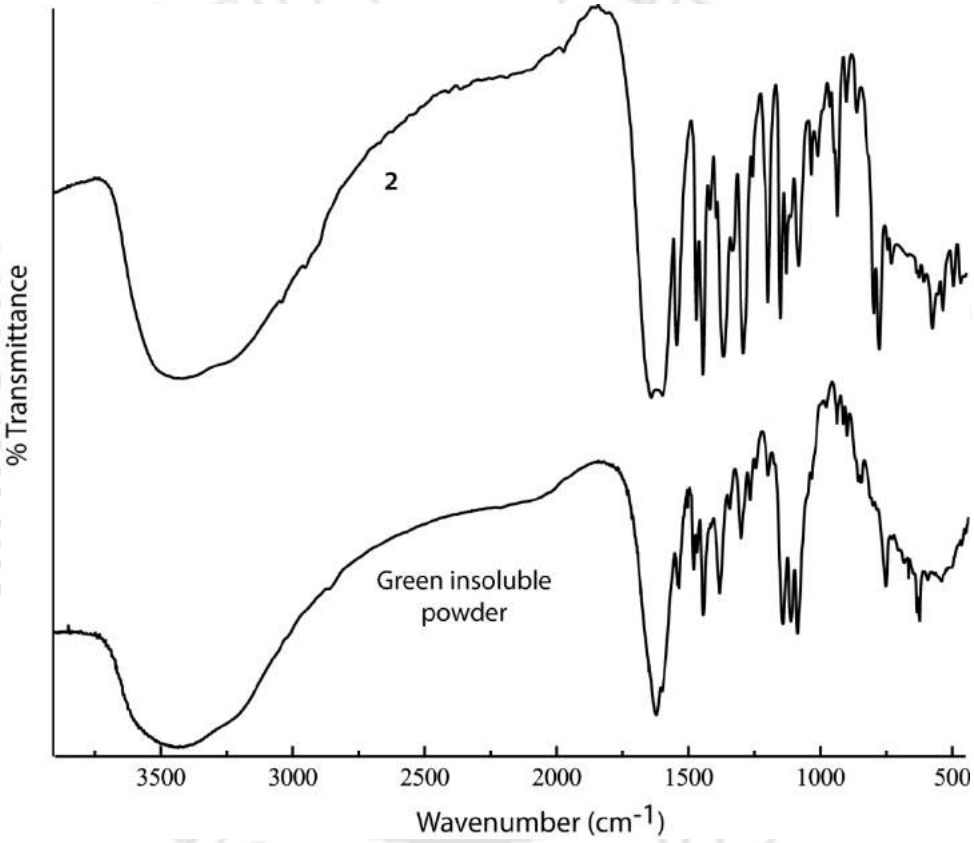

Figure 3.5. Comparison of the FT-IR spectrum of **2** and the green insoluble powder.

Complexation of $LiHL^{L\text{-}ser}$ with Cu(II) in relatively lesser quantity of base (1.33 equiv. $LiOH{\bullet}H_2O$) (Scheme **3.3**) yielded crystals of complex **4**. Complex **4** was synthesized by mixing $LiHL^{L\text{-}ser}$, $LiOH{\bullet}H_2O$ and $Cu(ClO_4)_2{\bullet}6H_2O$ in the ratio 1:1.33:1 respectively, in water and acetonitrile (1:1) mixture (Scheme **3.3**). The reaction gave a turbid green solution. The filtrate, after 3-4 days gave fine blue crystals of diffraction quality, upon keeping in air.

Crystal structure of complex **4** was characterized by X-ray crystallography. The structure of **4** was solved in an achiral space group of $R\bar{3}$ in the trigonal crystal system (Table **3.1**). Molecular structure of complex **4** showed that the side arm of serine is intact in the ligand moiety of the complex, whereas the starting L-isomer of serine in the ligand racemized to give a racemic Cu(II) hexanuclear cage during the reaction. The asymmetric unit contains one sixth of the molecule (Figure **3.6**). The hexanuclear cage consist of two trinuclear units, while one unit has all L-serine, the other unit has all D-serine in the ligand moiety of the complex. The two trinuclear units are oriented face to face occupying a water molecule in the hexanuclear cage. Each Cu(II) is coordinated by one tridentate L^{2-}, hydroxo bridge (O5) and phenolate oxygen (O4_i) from the next Cu(II) in the axial position (Figure **3.6C**).

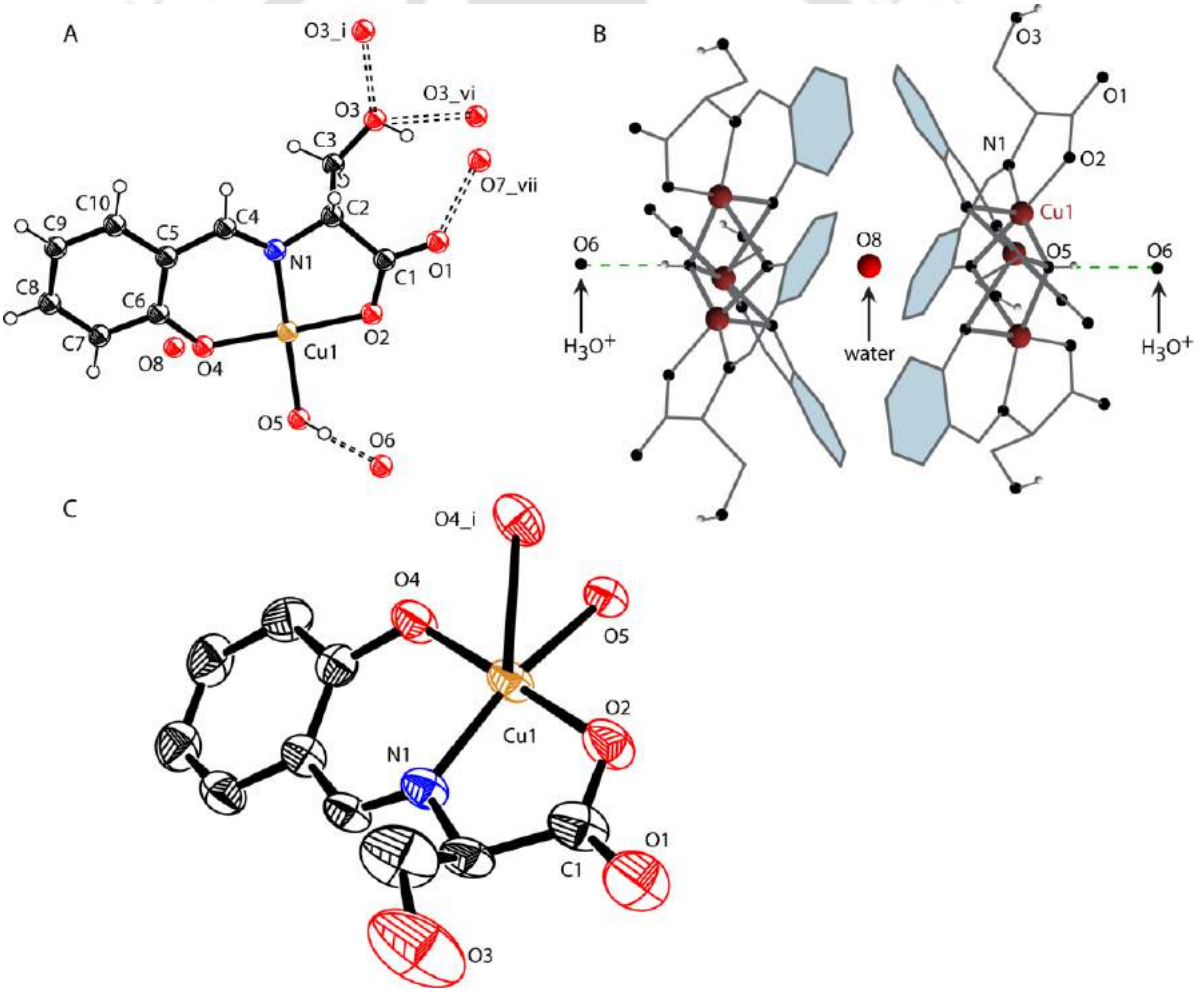

Figure 3.6. (A) ORTEP diagram of the asymmetric unit of **4** with thermal ellipsoids set to 40% probability. The atoms O3_i, O3_vi and O7_vii were generated using the symmetry

operations (-2/3+y, -1/3-x+y, 1.66-z), (1/3+x-y, 2/3+x, 1.66-z) and (-1+y, -x+y, 1-z), respectively, (B) Schematic representation of the hexanuclear molecule of **4**, and (C) ORTEP diagram showing the pentacoordinated Cu(II) in **4**, with thermal ellipsoids set to 40% probability. The atom O4_i was generated using the symmetry operation (-x+y, 1-x, z).

Complex **4** has similar structural features as that of **2** and **3** except, one interesting complementary hydrogen bonding pattern between the hydroxyl groups of the serine side arm (Figure **3.7** and **3.8**). The geometry at Cu(II) is slightly a distorted square pyramidal for **4** (τ 0.209).[7] The in-plane bond length ranges from 1.920(3) Å for phenolate (O4) to 1.976(2) Å for bridging hydroxide (O5). It has considerably a longer axial length of 2.479(3) Å for the phenolate bridge. The selected bond lengths and angles are given in (Table **3.2**). The trapped water molecule within the hexanuclear cage is at a distance of 3.045(4) Å (O8…O4) from the six phenolate oxygen atoms.

Structure **4** also has a pocket between the hexanuclear cages. Six trinuclear units lying in a plane in an alternatively inverted fashion around the pocket between the hexanuclear cages, creates an interesting complementary hydrogen bonding (2.716(2) Å) between the six hydroxyl groups of the six trinuclear halves. This hydrogen bonding pattern forms a hexagon of hydroxyl oxygen atoms in the pocket (Figure **3.8**). The pocket does not have any solvent molecule in it. Thermogravimetric analysis (TGA) of **4**, between 30 and 135 °C showed a weight loss of 9.0%, which could be accounted for 9 H_2O molecules (calc. weight loss of 8.8%) (Figure **3.9**), supporting the absence of solvent molecules inside the pocket.

The discussion of the results of the synthesis and structural characterization of **2** and **4** indicates that, the ligand, $LiHL^{L\text{-}thr}$ undergoes C-C cleavage in threonine's side arm during the synthesis of **2,** whereas no such cleavage of serine's side arm in the ligand $LiHL^{L\text{-}ser}$ was observed in the synthesis of **2**. By applying the reaction conditions of **2** and **4** to the ligands $LiHL^{L\text{-}ser}$ and $LiHL^{L\text{-}thr}$, respectively (Scheme **3.3**), $LiHL^{L\text{-}ser}$ gave a green precipitate, which is insoluble in DMF, DMSO, MeOH and H_2O, and $LiHL^{L\text{-}thr}$ gave a green viscous substance and few crystals of **2** from the filtrate upon evaporation. Overall, the above discussions reveal that the reactions are sensitive to base ($LiOH{\bullet}H_2O$) quantity.

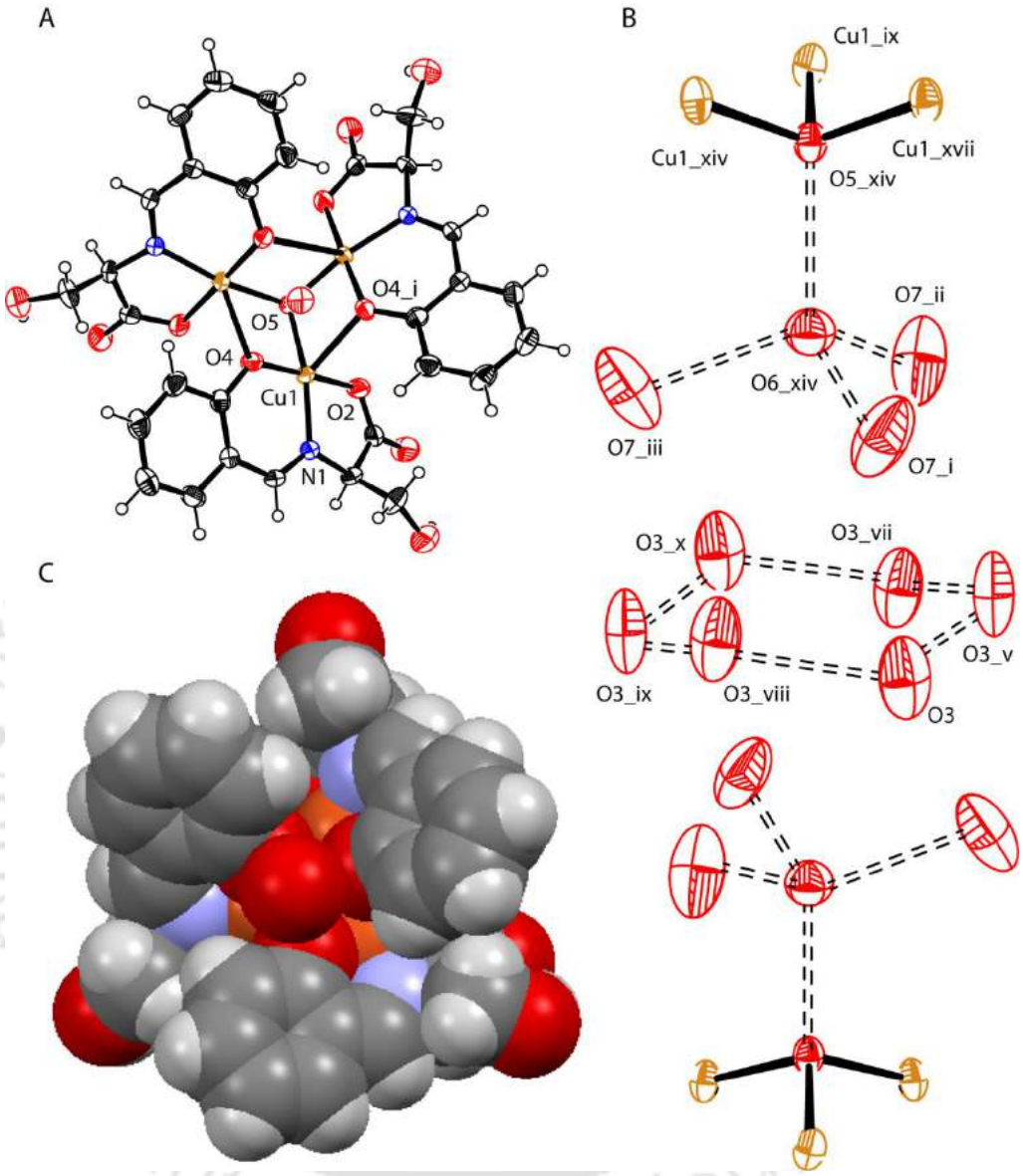

Figure 3.7. (A) ORTEP diagram of the trinuclear half of **4** with thermal ellipsoids set to 40% probability. The atom O4_i was generated using the symmetry operation (-x+y, 1-x, z), (B) The pocket formed between two hydronium ions, showing the complementary H-bonding between the six hydroxyl oxygens (O3) of serine. The atoms Cu1_xiv, Cu1_ix, Cu1_xvii, O5_xiv, O6_xiv, O7_i, O7_ii, O7_iii, O3_viii, O3_vii, O3_v, O3_ix and O3_x were generated through the symmetry operations (-2/3+y, -1/3-x+y, 1.66-z), (1/3-x, 2/3-y, 1.66-z), (1/3+x-y, -1/3+x, 1.66-z), (1/3-x, 2/3-y, 1.66-z), (1/3-x, 2/3-y, 1.66-z), (1/3-x, 2/3-y, 2/3-z), (-2/3+y, -1/3-x+y, 2/3-z), (1/3+x-y, -1/3+x, 2/3-z), (-2/3+y, -1/3-x+y, 1.7-z), (1/3+x-y, 2/3+x,

1.7-z), (-y, 1+x-y, z), (-2/3-x, 2/3-y, 1.7-z) and (-1-x+y, -x, z), respectively and (C) Space filling model of **4** showing the *C*3 symmetric cavity.

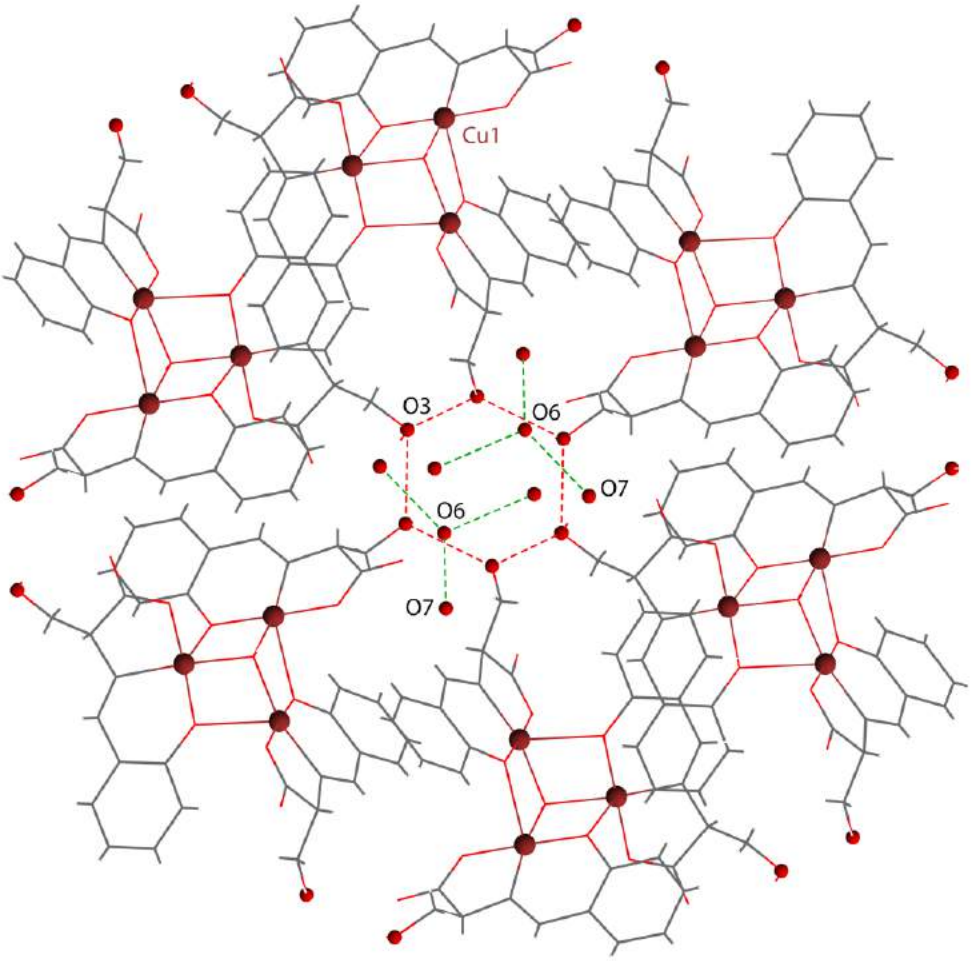

Figure 3.8. Schematic representation of the six complementary hydrogen bonding between the hydroxyl groups (O3) of the serine in **4**.

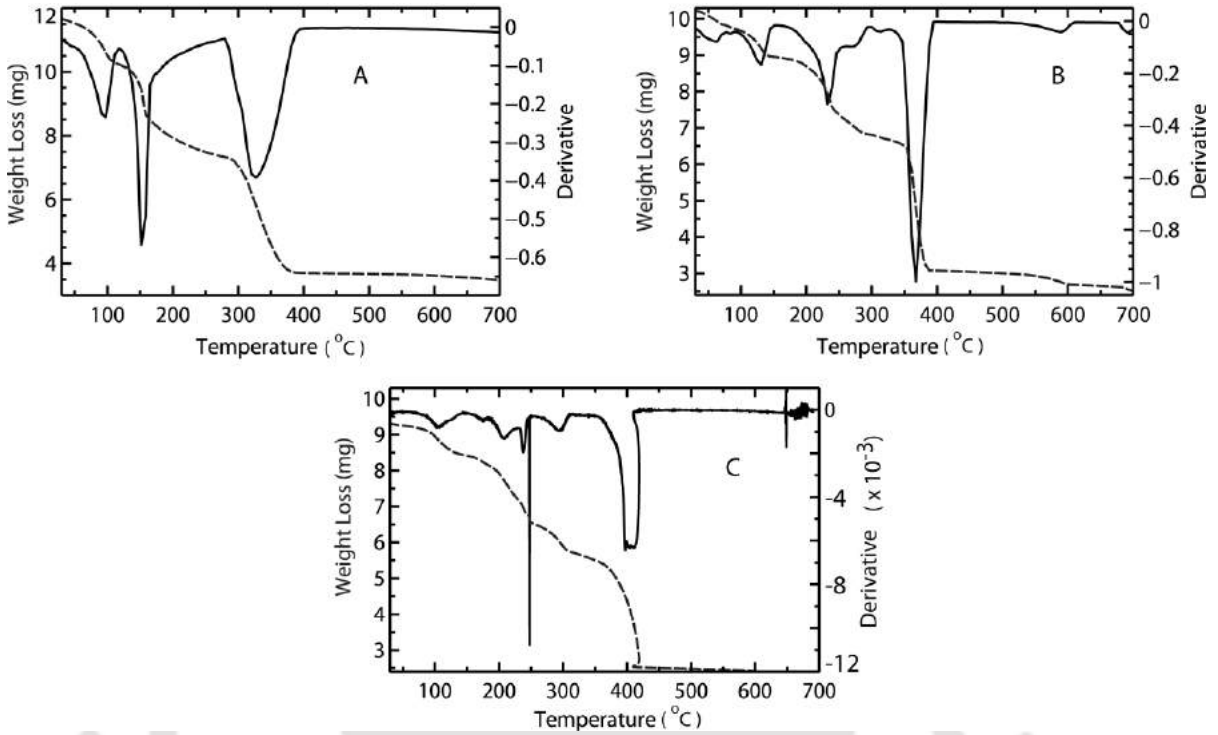

Figure 3.9. (A), (B) and (C) are the TGA and DTA plots of **2**, **3** and **4**, respectively.

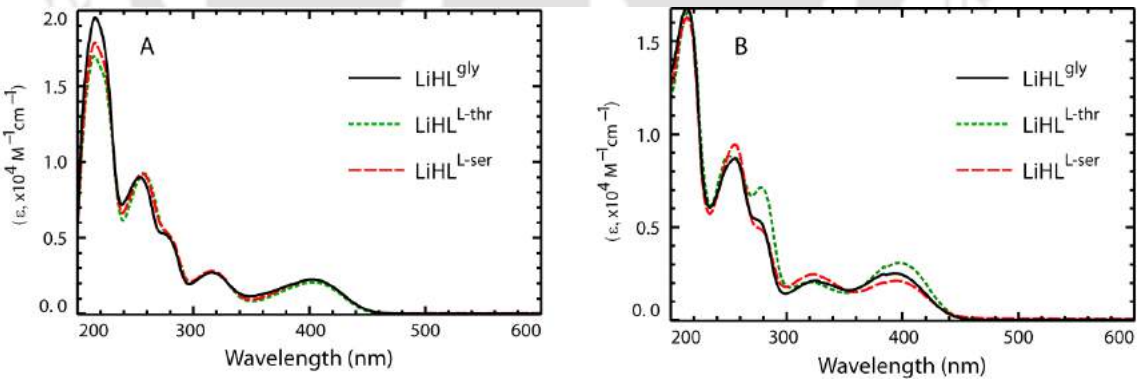

Figure 3.10. (A) and (B) are UV-vis spectra of LiHL$^{L\text{-}gly}$, LiHL$^{L\text{-}thr}$ and LiHL$^{L\text{-}ser}$ in MeOH and water, respectively.(5.57 x 10^{-5} M, 4.54 x 10^{-5} M and 4.84-4.98 x 10^{-5} M, respectively)

All the complexes were characterized by FT-IR, UV-vis, room temperature magnetic susceptibility and solution state EPR at room temperature (experimental section). The FT-IR spectra of all the complexes show a strong and sharp imine stretching frequency between 1630 and 1650 cm^{-1}. Complexes **1** and **1a** gives the imine stretching frequency at 1644 cm^{-1}, and **2** at 1634 cm^{-1}. The imine stretching frequencies in the complexes moved about 10 cm^{-1} towards lower wavenumber when compared to the free imine, which is typical for the coordinated imine's to the metal centre.[11] Electronic spectra of all the complexes show essentially five absorption bands between 200 and 700 nm. Complexes **1** and **1a** show a broad band at 657 and 658 nm, and **2** at 653 nm (Figure **3.11**). These bands are assigned for d-d transition, usual for amino acid Schiff base Cu(II) complexes.[12] The remaining four absorption bands between 200 and 370 nm are of ligand origin (experimental section). Room temperature magnetic susceptibility of all the complexes is in the range 1.76-1.86 μ_B [13]

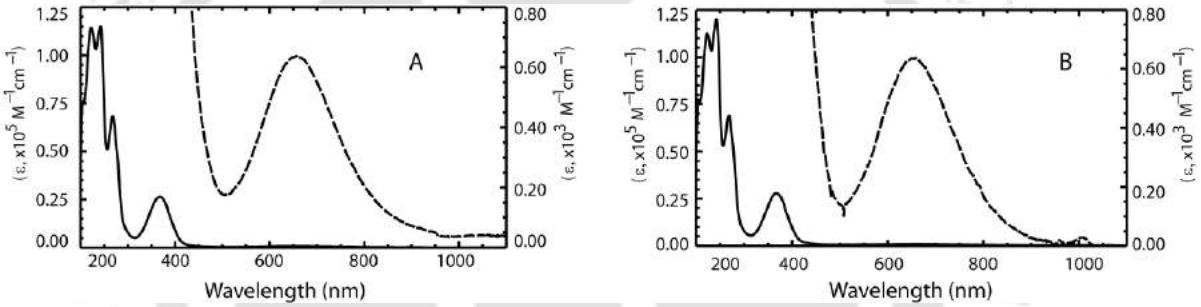

Figure 3.11. (A) and (B) are the UV-vis spectra of **2** and **4** in MeOH. [**2**- (----6.26 x 10^{-5} M / Cu_6 unit) and (—— 6.26 x 10^{-6} / Cu_6 unit), **4** - .[(---5.70 x 10^{-5} M / Cu_6 unit) and (—— 5.70 x 10^{-6} / Cu_6 unit)]

3.4.4 Characterization of the Solution state behavior of the ligands in presence of base

X-ray structural analysis of **2**, revealed the occurrence of C-C cleavage in threonine's side arm during the synthesis of **2**. Solution state experiments of the ligands were performed to determine whether the cleavage has happened before or after the addition of Cu(II) salt. The solution state behavior of the ligands $LiHL^{L\text{-}thr}$ and $LiHL^{L\text{-}ser}$ were characterized using UV-vis, ^{1}H-NMR and Circular dichroism (CD) experiments in presence and absence of base (2 equiv. $LiOH{\bullet}H_2O$) in water and MeOH.

3.4.4.1 UV-vis experiment

UV-vis spectral study of $LiHL^{L\text{-}thr}$, $LiHL^{L\text{-}ser}$ and $LiHL^{gly}$ gave the imine absorption band at 397, 395 and 394 nm in water, respectively. In MeOH it was observed at 404, 403 and 402 nm, respectively (Table 3.4, Figure 3.10). Both, $LiHL^{L\text{-}thr}$ and $LiHL^{L\text{-}ser}$ with 2 equiv. of $LiOH{\bullet}H_2O$ in water gave an absorption band at 377 nm, a blue shift when compared to the absorption in water without base (Figure **3.14, 3.12B and 3.13B)**. UV-vis spectra were monitored continuously over a period of about 3 h for $LiHL^{L\text{-}thr}$ and about 7 h for $LiHL^{L\text{-}ser}$ in water, and for about 7 h in MeOH for both the ligands (Figure **3.12 & 3.13**).

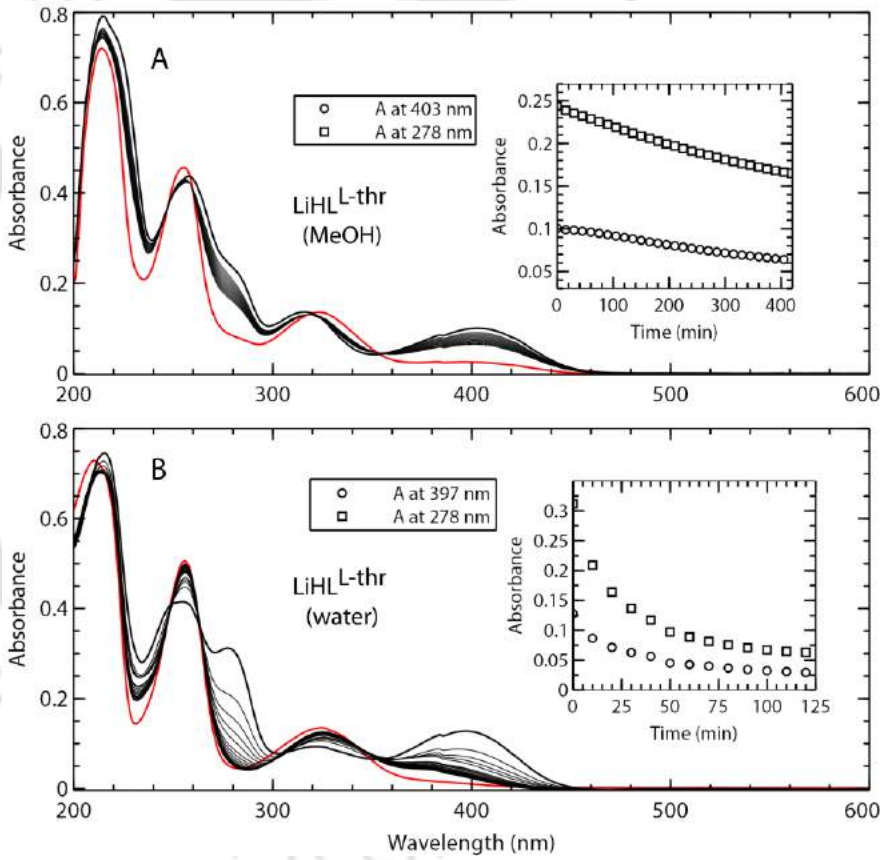

Figure 3.12. (A) UV-vis spectra of $LiHL^{L\text{-}thr}$ in MeOH monitored continuously for about 7 h (black line) and (red) after about 48 h (4.54×10^{-5} M) and (B) UV-vis spectra of $LiHL^{L\text{-}thr}$ in water monitored continuously for about 3 h (black) and (red) after about 16 h (4.54×10^{-5} M). The inset is the absorbance vs. time plot.

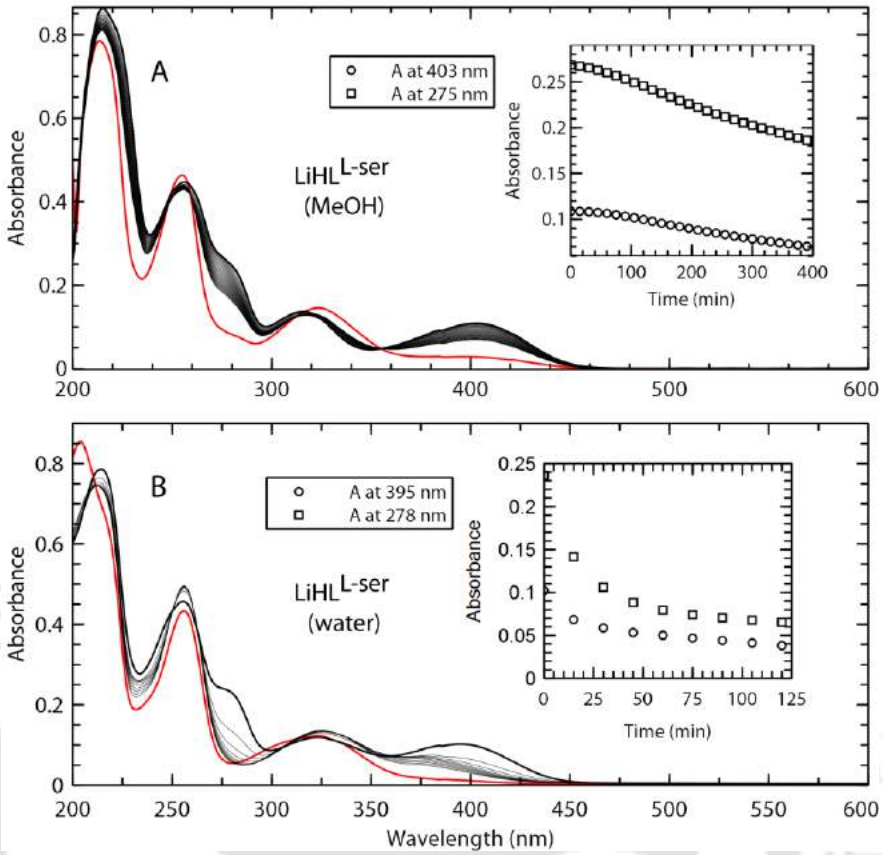

Figure 3.13. (A) UV-vis spectra of $LiHL^{L\text{-}ser}$ in MeOH monitored continuously for about 7 h (black line) and (red) after about 46 h (4.84×10^{-5} M) and (B) UV-vis spectra of $LiHL^{L\text{-}ser}$ in water monitored continuously for about 7 h (black) and (red) after about 16 h (4.84×10^{-5} M). The inset is the absorbance vs. time plot.

From the spectra it was observed that the characteristic ligand bands disappear over a period of time and eventually gives a spectrum, which is almost similar to the spectra of salicylaldehyde in water and MeOH for the ligands ($LiHL^{L\text{-}thr}$ and $LiHL^{L\text{-}ser}$) in these corresponding solvents (Figure **3.12, 3.13 & 3.15**).

UV-vis spectra of $LiHL^{L\text{-}thr}$ and $LiHLL^{L\text{-}ser}$ with two equiv. of $LiOH{\bullet}H_2O$ in water were monitored continuously for about 7 h (Figure **3.14**). Spectra of salicylaldehyde with $LiOH{\bullet}H_2O$ in water matches the spectra of the ligands with two equiv. of $LiOH{\bullet}H_2O$ in water (Figure **3.14 & 3.15**). During these changes in the spectra different isosbestic points were also observed. The above UV-vis spectral studies of the ligands indicate that the dissociation of the imine bond takes place both in the absence and presence of base in MeOH and water.

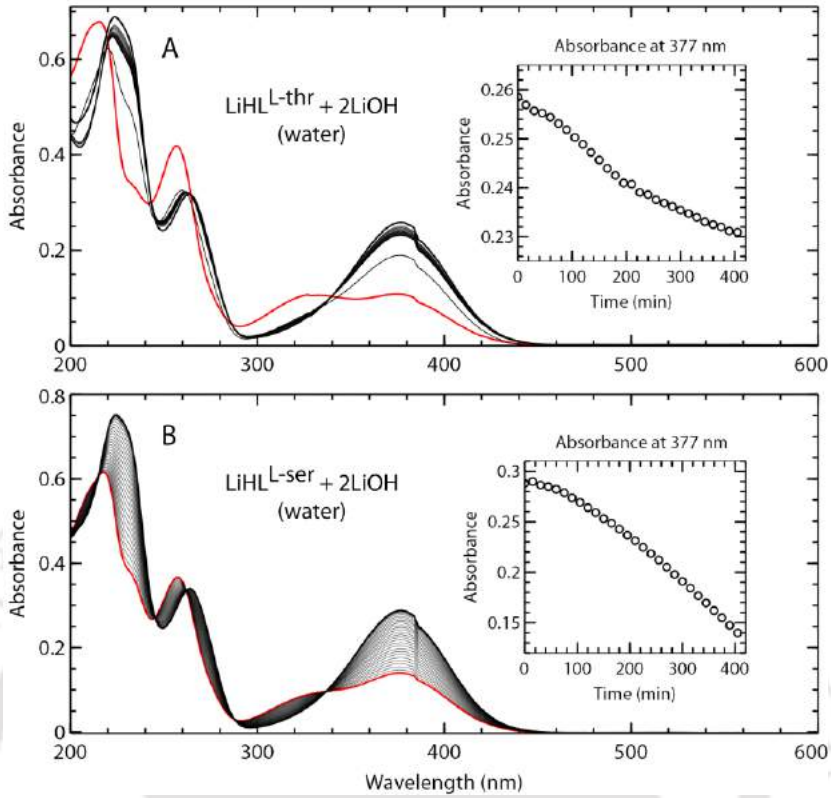

Figure 3.14. (A) UV-vis spectra of $LiHL^{L\text{-}thr}$ in presence of $LiOH{\bullet}H_2O$ monitored continuously for about 7 h (black line) and (red) after about 36 h in water (4.54×10^{-5} M) and (B) UV-vis spectra of $LiHL^{L\text{-}ser}$ in presence of $LiOH{\bullet}H_2O$ monitored continuously for about 7 h (black to red) in water (4.98×10^{-5} M). The inset is the absorbance vs. time plot.

The data obtained from UV-vis experiments of the ligands were used to form an absorbance vs. time plot, to compare the speed of dissociation of the imine bond in the ligands, qualitatively. From the kinetic plot, (Figure **3.16**) it was observed that there was ~ 9% and 68% (average) decrease of initial absorbance in 2 h for both $LiHL^{L\text{-}thr}$ and $LiHL^{L\text{-}ser}$ in MeOH and water, respectively. For both the ligands, the dissociation was faster at initial stage, but it gradually slows down with time in water. In MeOH, the speed of dissociation was almost same for both the ligands (Figure **3.16**). The above results indicate that the imine bond dissociation in water is faster than that in MeOH. In the case of imine bond dissociation of the ligands in presence of two equiv. of $LiOH{\bullet}H_2O$ in water, ~ 10% and 50% decrease of initial absorbance in 7 h for $LiHL^{L\text{-}thr}$ and $LiHL^{L\text{-}ser}$ were observed, respectively, indicating relatively a faster dissociation in $LiHL^{L\text{-}ser}$ than in $LiHL^{L\text{-}thr}$ (Figure **3.16**).

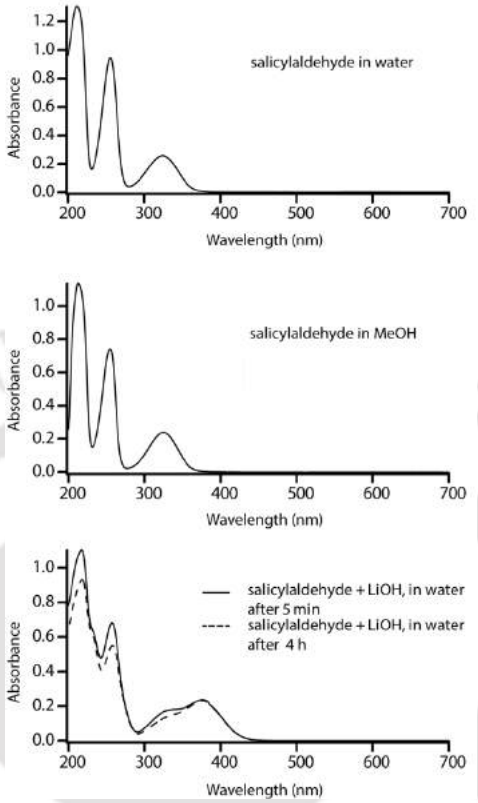

Figure 3.15. UV-vis spectra of salicylaldehyde in water (top), in MeOH (middle) and with one equiv. of $LiOH•H_2O$ in water (bottom), (6.26×10^{-5} M).

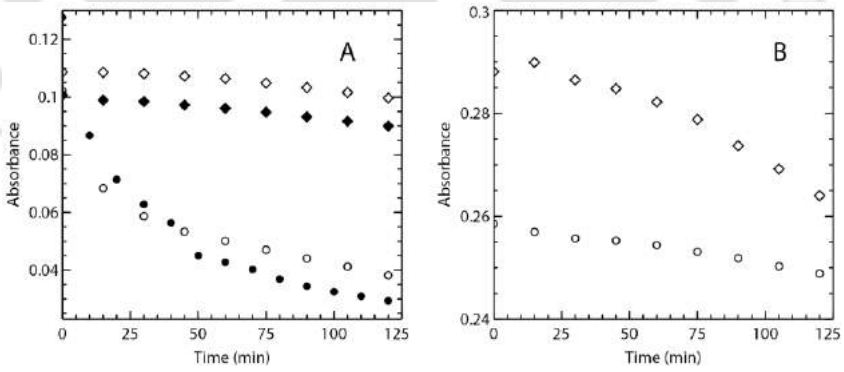

Figure 3.16. (A) Absorbance vs. time plot comparison of $LiHL^{L\text{-}thr}$ (solid black) and $LiHL^{L\text{-}ser}$ (hollow) in MeOH (diamond symbol) and water (circle symbol) and (B) Absorbance vs. time plot comparison of $LiHL^{L\text{-}thr}$ (circle symbol) and $LiHL^{L\text{-}ser}$ (diamond symbol) with 2 equiv. of $LiOH•H_2O$ in water.

Table 3.4. UV-vis spectral data of the ligands and salicylaldehyde in MeOH and water, and in presence of $LiOH•H_2O$ in water.

Compound	Concentration	Solvent	$\lambda_{max,}$ nm (ε, $M^{-1}cm^{-1}$)
			$LiHL^{gly}$
$LiHL^{gly}$	$5.57x10^{-5}$ M	MeOH	402 (2000), 316 (2700), 278 sh, 254 (9000), 215 (19000)
		Water	394 (2500), 326 (2000), 278 sh, 255 (8500), 214 (16500)
			$LiHL^{L\text{-}thr}$
$LiHL^{L\text{-}thr}$	4.54×10^{-5} M	MeOH	404 (2000), 315 (2700), 280sh, 258 (9000), 220 sh, 214 (17000)
		Water	397 (3000), 321 (2000), 278 (7000), 250 (8800), 215 (16500)
$LiHL^{L\text{-}thr}$ + 2 LiOH		Water	377 (5500), 263 (6800), 230 sh, 224 (14800)
			$LiHL^{L\text{-}ser}$
$LiHL^{L\text{-}ser}$	4.84×10^{-5} M	MeOH	403 (2200) , 316 (2800), 275sh, 256 (9200), 215 (17800)
		Water	395 (2100), 323 (2400), 277 sh, 256 (9400), 214 (16200)
$LiHL^{L\text{-}ser}$ + 2 LiOH	4.98×10^{-5} M	Water	377 (5700), 264 (6800), 224 (15000)
			Salicylaldehyde
Salicylaldehyde	6.26×10^{-5} M	MeOH	325 (3800), 255 (11700), 213 (18000)
Salicylaldehyde		Water	324 (4000), 256 (15000), 212 (20,000)
Salicylaldehyde + LiOH		Water	375 (3700), 330 sh, 257 (10800), 231 sh, 217 (17600)

3.4.4.2 ^{1}H-NMR experiment

^{1}H-NMR experiment of $LiHL^{L\text{-}thr}$ in presence of base was performed to check the effect of base on the ligand. ^{1}H-NMR spectrum of $LiHL^{L\text{-}thr}$ with $LiOH{\bullet}H_2O$ (2 equiv.) in D_2O, supports the results of the UV-vis study of the ligands. The imine proton, which generally appears in a range of 8-9 ppm was not observed, instead a singlet at 9.9 ppm was observed. This is a region for aldehydes. A peak at 1.2 ppm, which is assigned for the methyl protons of the side arm of threonine indicate that the side arm is intact within the reaction condition before the addition of Cu(II) salt (Figure **3.17**). Hence, UV-vis and ^{1}H-NMR study proves that imine bond dissociation is taking place in presence of base but not the C-C cleavage in threonine's side arm in $LiHL^{L\text{-}thr}$. Thus in turn, it proves that the C-C cleavage in threonine's side arm in $LiHL^{L\text{-}thr}$ occurs after complexation with Cu(II) salt. This implies, that the role of metal salt [Cu(II)] is essential for such cleavages.

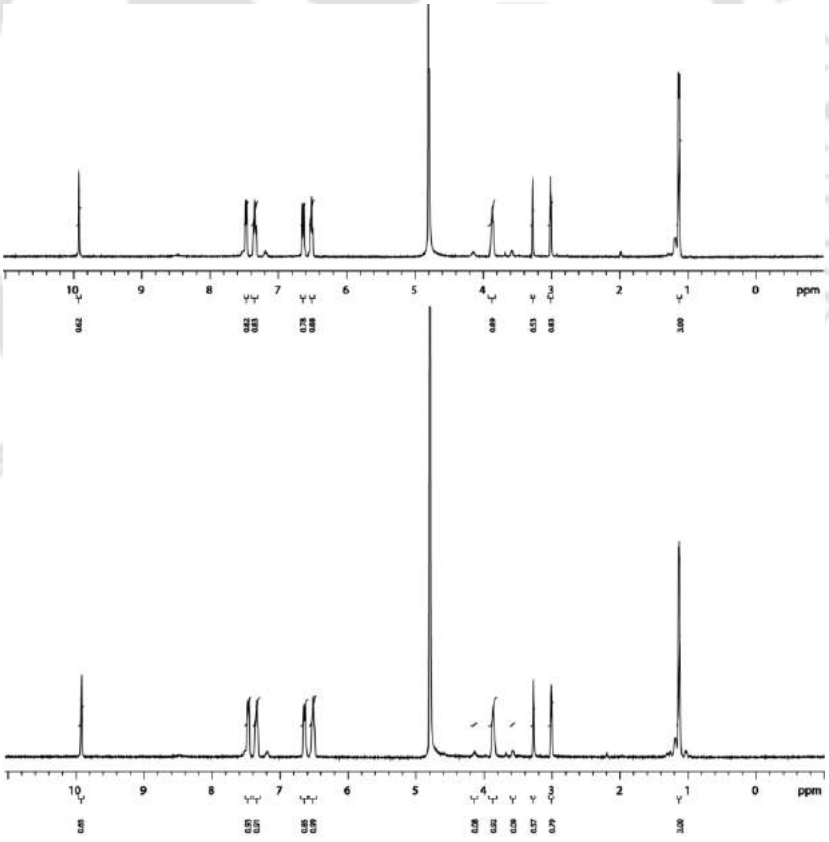

Figure 3.17. ^{1}H-NMR spectra of $LiHL^{L\text{-}thr}$ with 2 equiv. of $LiOH{\bullet}H_2O$ in D_2O. [after 30 min (above) and after 20 h (below)]

3.4.4.3 Circular dichroism experiment

Circular dichroism study of the ligands was performed to check the effect of base on the chirality of amino acid moieties in the ligands. The CD spectra of the ligands in MeOH showed negative cotton. It was observed that addition of one equiv. of LiOH•H_2O to the ligands in MeOH reduces the cotton effect with respect to time (Figure **3.18 & 3.19**).

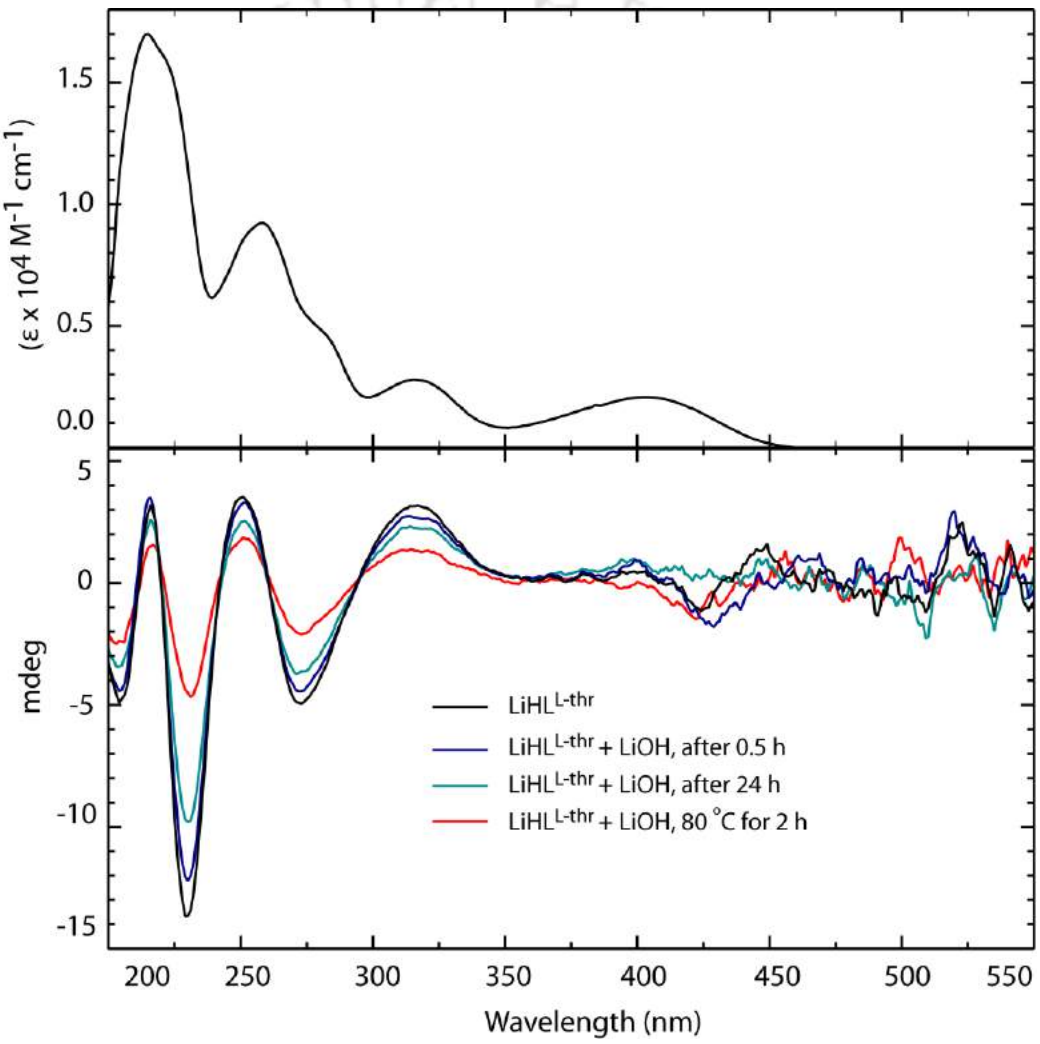

Figure 3.18. UV-vis spectrum of $LiHL^{L\text{-}thr}$ in MeOH (4.54×10^{-5} M) (above) and CD spectra of $LiHL^{L\text{-}thr}$ recorded at RT, in presence and absence of LiOH•H_2O in MeOH (below). (6.55×10^{-4} M, for all CD spectra)

Spectra of the ligands in presence of $LiOH•H_2O$ were recorded after 0.5 and 24 h. From the spectra it was observed that the ligands racemize slowly in presence of base in MeOH at RT over a period of 24 h. When the ligand $LiHL^{L\text{-}ser}$ in presence of base in MeOH was heated at 80 ^oC for 2 h, it undergoes complete racemization, which was observed by a straight line in the CD spectra (Figure **3.19**), whereas for the ligand $LiHL^{L\text{-}thr}$ at the same condition complete racemization was not observed (Figure **3.18**).

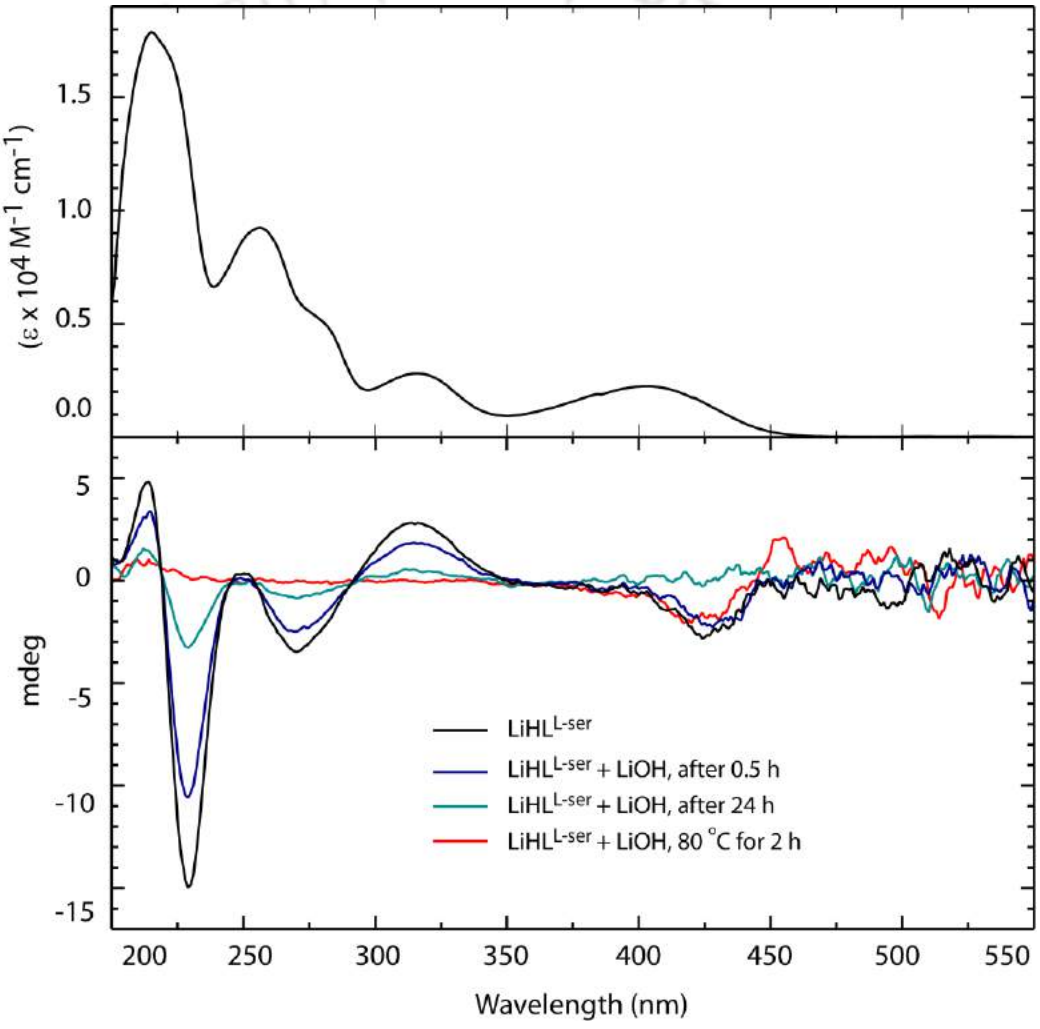

Figure 3.19. UV-vis spectrum of $LiHL^{L\text{-}ser}$ in MeOH (4.84×10^{-5} M) (above) and CD spectra of $LiHL^{L\text{-}ser}$ recorded at RT, in presence and absence of $LiOH•H_2O$ in MeOH (below). (6.98×10^{-4} M, for all CD spectra)

Following the CD experiments of the ligands in MeOH, the CD experiments of the ligands in presence and absence of base (2 equiv. $LiOH•H_2O$) in water were also performed. The CD spectra showed a minimal negative cotton effect for the ligands in water. In presence of base (2 equiv. $LiOH•H_2O$) it was found that the cotton effect was disappeared almost within 0.5 h (Figure **3.20 & 3.21**). This implies that in presence of base the ligands undergo almost complete racemization within 0.5 h in water at RT.

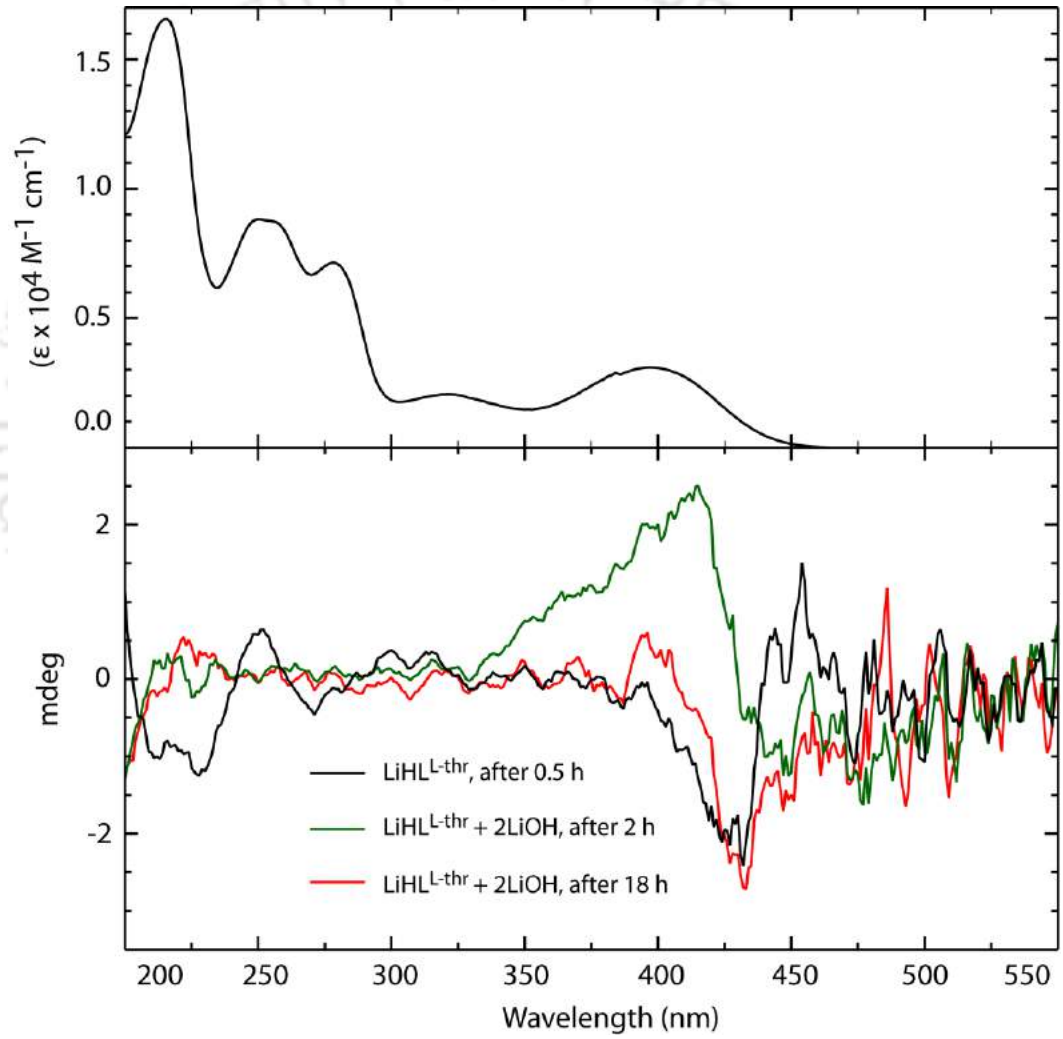

Figure 3.20. UV-vis spectrum of $LiHL^{L\text{-}thr}$ in water (4.54×10^{-5} M) (above) and CD spectra of $LiHL^{L\text{-}thr}$ recorded at RT, in presence and absence of $LiOH•H_2O$ in water (below). (6.55×10^{-4} M, for all CD spectra)

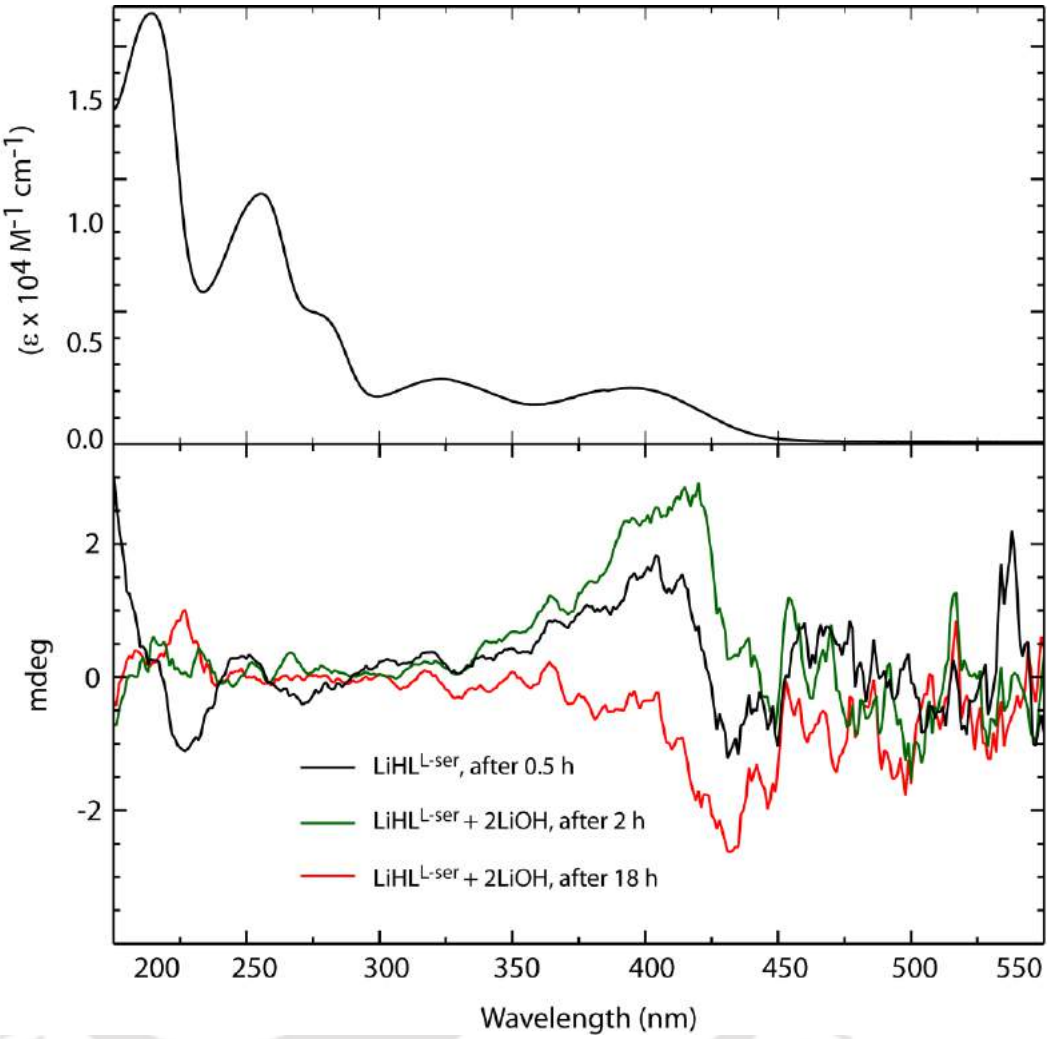

Figure 3.21. UV-vis spectrum of $LiHL^{L\text{-}ser}$ in water (4.84×10^{-5} M) (above) and CD spectra of $LiHL^{L\text{-}ser}$ taken at RT, in presence and absence of $LiOH{\bullet}H_2O$ in water (below). (6.98×10^{-4} M, for all CD spectra)

In summary, the results of UV-vis and Circular dichroism experiments of the Schiff bases of hydroxy amino acids in presence and absence of base ($LiOH{\bullet}H_2O$) in water and MeOH reveals that the Schiff bases undergo dissociation and racemization with respect to time. The ^{1}H-NMR experiment of $LiHL^{L\text{-}thr}$ in presence of base in D_2O reveals that there is no sign of C-C cleavage in the side arm of threonine whereas dissociation of the Schiff base was observed.

Conclusions

We have successfully synthesized and characterized two new Cu(II) hexanuclear cages of salicylidene Schiff bases of glycine and serine. Complexation of $LiHL^{L\text{-}thr}$, with 2.33 equiv. $LiOH{\bullet}H_2O$ and Cu(II), gives the Cu(II) hexanuclear cage (**2**), having salicylidene glycinate as the ligand indicating the occurrence of C-C cleavage in threonine side arm of $LiHL^{L\text{-}thr}$. However, **2** can also be synthesized directly from the complexation of $LiHL^{L\text{-}gly}$. Complexation of $LiHL^{L\text{-}ser}$, with 2.33 equiv. $LiOH{\bullet}H_2O$ and Cu(II), gives an insoluble green powder, rendering it difficult for complete characterization.

Complexation of $LiHL^{L\text{-}thr}$, with 1.33 equiv. $LiOH{\bullet}H_2O$ and Cu(II), gives few crystals of **2**. Complexation of $LiHL^{L\text{-}ser}$, with 1.33 equiv. $LiOH{\bullet}H_2O$ and Cu(II), gives a racemic Cu(II) hexanuclear cage having salicylideneserinate as the ligand. The overall structure of all the complexes and the H-bondings are similar to each other except, the interesting complementary H-bonding between the hydroxyl (O3) groups of the serine side arm in **4**.

Solution state studies of the ligand $LiHL^{L\text{-}thr}$ and $LiHL^{L\text{-}ser}$ with 2 equiv. of $LiOH{\bullet}H_2O$ through UV-vis and CD experiments reveal that the ligands undergo imine bond dissociation and racemization. ^{1}H-NMR study of the $LiHL^{L\text{-}thr}$ in presence of ~2 equiv. of $LiOH{\bullet}H_2O$ shows the occurrence of imine bond dissociation, but no sign of C-C cleavage in threonine's side arm in $LiHL^{L\text{-}thr}$, indicating the importance of the Cu(II) in the C-C cleavage.

References

1. (A) D. E. Metzler, M. Ikawa and E. E. Snell, *J. Am. Chem. Soc.*, 1953, **76**, 648; (B) G. N. Weinstein, M. J. O'connor and R. H. Holm, *Inorg. Chem.*, 1970, **9,** 2104; (C) Y. N. Belokon, V. M. Belikov, V. A. Maksakov, and V. I. Tararov, *Izv. Akad. Nauk SSSR, Ser. Khim.*, 1978, **10**, 2276; (D) M. –D. Tsai, H. J. R. Weintraub, S. R. Byrn, C.-j. Chang and H. G. Floss, *Biochemistry*, 1978, **17**, 3183; (E) A. E. Martell, *Acc. Chem. Res.*, 1989, **22**, 115.

2. (A) D. E. Metzler, J. B. Longenecker and E. E. Snell, *J. Am. Chem. Soc.*,1953, **75**, 2786; (B) D. E. Metzler, J. B. Longenecker and E. E. Snell, *J. Am. Chem. Soc.*, 1954, **76**, 639.

3. M. Ikawa and E. E. Snell, *J. Am. Chem. Soc.*, 1954, **76**, 653.

4. G. M. Sheldrick, Acta Crystallogr., Sect. A: Fundam. Crystallogr., 2008, A64, 112.

5. CrysAlis CCD and CrysAlis RED. Oxford Diffraction Ltd, Yarnton, Oxfordshire, England. Oxford Diffraction, 2009.

6. M. N. Burnett and C. K. Johnson, ORTEP-III: Oak Ridge Thermal Ellipsoid Plot Program for Crystal Structure Illustrations, Oak Ridge National Laboratory Report ORNL-6895, 1996.

7. The amount of distortion was calculated from the structural data where the value of τ should be 0 for the perfect square-pyramidal geometry and 1 for the perfect trigonal bipyramidal structure; A. W. Addision, T. N. Rao, J. Reedijk, J. van Rijn and G. C. Verschoor, *J. Chem. Soc., Dalton Trans*., 1984, 1349.

8. (a) B. J. Hathaway, in *Comprehensive Coordination Chemistry*, ed. G. Wilkinson, R. D. Gillard and J. A. McCleverty, Pergamon Press, London, 1987, vol. 5, p. 533; (b) A. W. Addison and E. Sinn, *Inorg. Chem.*, 1983, **22**, 1225; (c) M. Bonamico, G. Dessy, A. Mugnoli, A. Vaeiago and L. Zambonelli, *Acta Crystallogr.*, 1965, **19**, 886; (d) Y. Agus, R. Louis and R. Weiss, *J. Am. Chem. Soc.*, 1979, **101**, 3381.

9. Hydroxo-bridged Cu(II)trinuclear complexes: (a) C. M. Rajesh and M. Ray, *Dalton Trans.*, 2014, **43**, 12952; (b) B. Sarkar, M. Sinha Ray, M. G. B. Drew, A. Figuerola, C. Diaz and A. Ghosh, *Polyhedron*, 2006, **25**, 3084; (c) P. Mukherjee, M. G. B. Drew, M. Estrader, C. Diaz and A. Ghosh, *Inorg. Chim. Acta*, 2008, **361**, 161; (d) B. L. Guennic, S. Petit, G. Chastanet, G. Pilet, D. Luneau, N. Ben Amor and V. Robert, *Inorg. Chem.*, 2008, **47**, 572; (e) C. Biswas, M. G. B. Drew, A. Figuerola, S. Gómez-Coca, E. Ruiz, V. Tangoulis and A. Ghosh, *Inorg. Chim. Acta*, 2010, **363**, 846; (f) Y.-B. Cai, L. Liang, J. Zhang, H.-L. Sunc and J.-L. Zhang, *Dalton Trans*., 2013, **42**, 5390.

10. C. Knight and G. A. Voth, *Acc. Chem. Res.*, 2012, **45**, 101.

11. a) S. Thakurta, J. Chakraborty, G. Rosair, J. Tercero, M. S. E. Fallah, E. Garribba and S. Mitra, *Inorg. Chem.*, 2008, **47**, 6227; (b) K. Nakamoto, Infrared and Raman Spectra of Inorganic and Coordination Compounds, Theory and Applications in Inorganic Chemistry, 5th ed., John Wiley and Sons Inc., New York, 1997.

12. M. R. Wagner and F. A. Walker, *Inorg. Chem.*, 1983, **22**, 3021 and references therein; (b) N. Arulsamy and P. S. Zacharias, *Transition Met. Chem.*, 1991, **16**, 255; (c) A. B. P. Lever, *'Inorganic Electronic Spectroscopy'*, 2nd ed., Elsevier, New York, 1984.

13. (a) W. E. Hatfield and R. Whyman, *Transition Met. Chem.*, 1969, **47**, 5; (b) A. Earnshaw, 'An Introduction to Magnetochemistry', Academic, London, 1968; (c) F. E. Mabbs and D. J. Machin, 'Magnetism and Transition Metal Complexes', Chapman and Hall, London, 1973; (d) C. J. OConnor, *Prog. Inorg. Chem.*, 1982, **29**, 203.

Chapter IV

C-C bond formation between salicylideneglycinate units through nucleophilc addition and formation of a Cu(II) complex

While exploring different conditions to isolate crystallizable Cu(II) complexes with amino acid derived Schiff bases, we have tried the use of three alkali metal hydroxides individually ($LiOH•H_2O$, NaOH and KOH) with lithium salicylideneglycinate, Cu(II) and anhydrous $CaCl_2$ with different ratios with respect to each other. In one of the reaction we have isolated a crystal which is different from the trinuclear complexes described in the earlier chapters. Structural analysis of the complex revealed the formation of a new organic molecule through C-C bond formation between two salicylideneglycinate units in *in situ* within the reaction conditions employed. In this chapter we present the isolation and structural characterization of a Cu(II) mononuclear complex of a new organic molecule which has been formed *in situ*.

4.1 Experimental section

4.1.1 Materials and methods

Materials and methods used in this chapter are same as in the last chapter unless specifically mentioned. NaOH and anhydrous $CaCl_2$ were purchased from Sisco Research Laboratories Pvt. Ltd. (SRL), India, and used as received.

4.2 Syntheses and characterization

4.2.1 $LiHL^{gly}$ The ligand was synthesized by following the procedure given in chapter 3.

4.2.2 $Ca[CuL]_2•9H_2O$ (5) Solid NaOH (0.108 g, 2.70 mmol) was added in small quantities to a 5 min stirred yellow solution of $LiHL^{gly}$ (0.500 g, 2.70 mmol) in 15 mL of MeOH and stirred continuously for 30 min. To the resulting clear yellow solution 10 mL of acetonitrile was added and stirred for 5 min. A solution of $Cu(ClO_4)_2•6H_2O$ (0.500 g, 1.35 mmol) in 5 mL of acetonitrile was added dropwise to give a green solution, and stirred continuously for another 45 min. The reaction mixture was kept in air, and after 3-4 days most of the solvent was evaporated to give a green concentrated solution. To this anhydrous $CaCl_2$ (0.300 g, 2.70 mmol) in 3 mL of H_2O was added dropwise to give a pale green precipitate, followed by addition of 3 mL of acetonitrile. Then, the reaction mixture was heated at 65-70 ^oC to give a bluish green solution along with some precipitate. The reaction mixture was filtered and the filtrate was kept in air. After 3-4 days, blue crystals were formed in the solution along with some pale green fluffy precipitate. The solution was decanted and the crystals were washed

with a mixture of water and acetonitrile (1:2) solution and dried under vacuum. Yield 0.060 g (8.55%). Anal. Calcd. for $Ca[CuL]_2 \bullet 9H_2O$: C, 41.74; H, 4.28; N, 5.41; found C, 41.57; H, 4.10; N, 5.12. UV/Vis (H_2O): λ_{max}, nm (ε, M^{-1} cm^{-1} /Cu_2 unit): 215 (65500), 237 (45000), 271 (37700), 358 (10800), 608 (300), 966 (60). IR (KBr, cm^{-1}): 3419, 1627(s), 1596(s), 1536(m), 1460(m), 1445(m), 1424(w), 1384(m), 1304(m), 1192(w), 992, 758(m) and 585. μ_{eff} (powder, 298K): 1.76 μ_B/Cu. Λ_M (ohm^{-1} cm^2 mol^{-1}): 120 in H_2O.

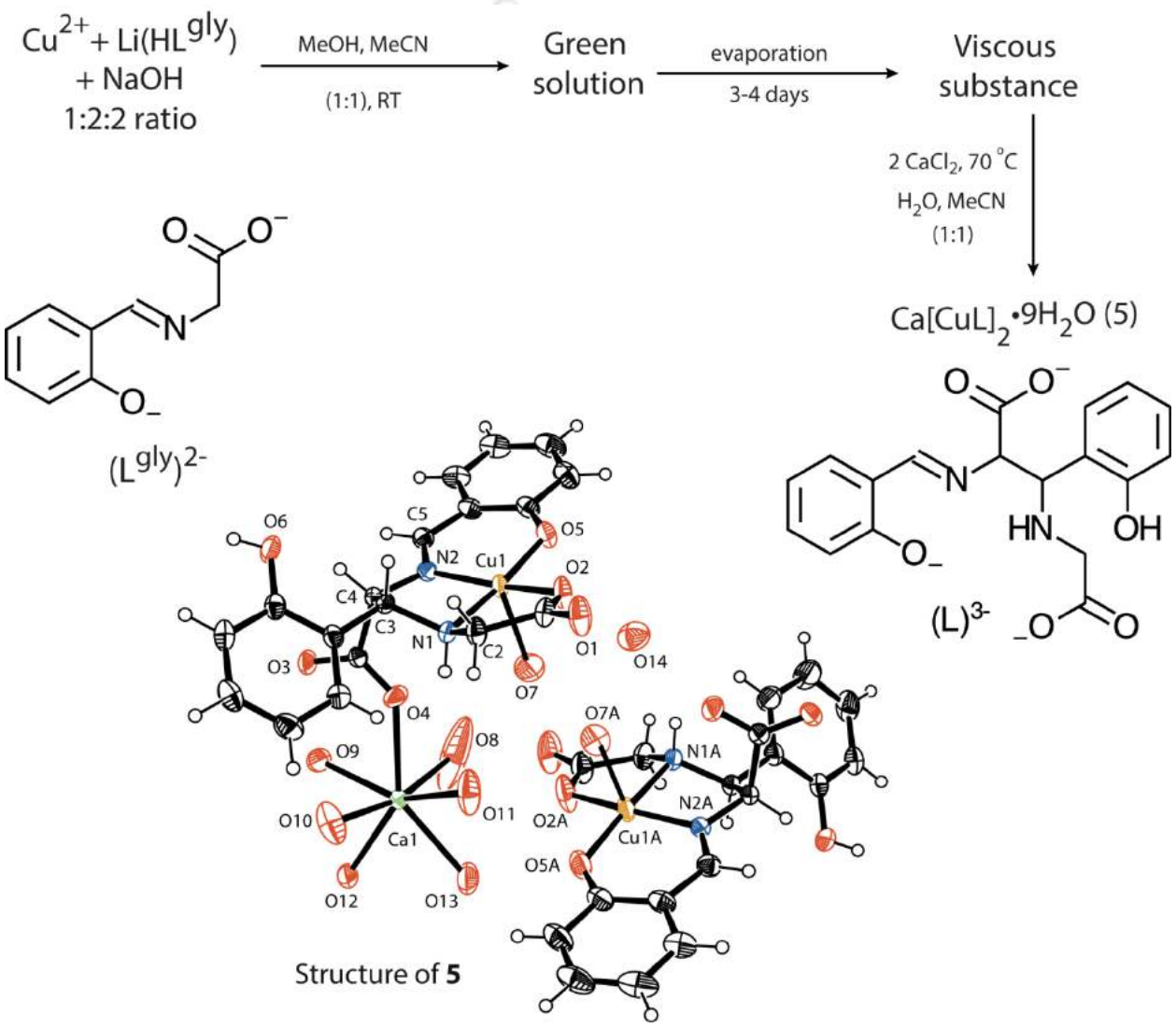

Figure 4.1. Scheme for the synthesis of complex **5** containing the new ligand (L^{3-}) formed during complexation and the ORTEP diagram of the complex with thermal ellipsoids set to 40%.

4.3 X-ray Data Collection, Structure Solution and Refinement

Single crystal X-ray structural study of **5** was performed on a CCD Oxford Diffraction XCALIBUR-S diffractometer. The intensities of the X-ray reflections were collected at room temperature [296(2) K] using graphite-monochromated Mo Kα radiation (λα = 0.71073 Å). The strategy for the intensity data collection was evaluated by using the CrysAlisPro CCD software. The intensities data were recorded by the standard φ-ω scan techniques, and were scaled and reduced using CrysAlisPro RED software.[1] The structures were solved by direct methods using SHELXS-97 and refined by full-matrix least-squares with SHELXL-97, refining on F^2.[2] All non-hydrogen atoms were refined anisotropically. Selected crystallographic data are summarized in (Table **4.1**). Perspective view of the complex was obtained by ORTEP.[3]

4.4 Results and Discussion

4.4.1 Synthesis, Characterization and Solid state structure

The complex **5** was synthesized by mixing $LiHL^{gly}$, NaOH and $Cu(ClO_4)_2 \cdot 6H_2O$ in the ratio 2:2:1 respectively, in MeOH and acetonitrile (1:1) mixture (Figure **4.1**). The reaction gave a green solution and the reaction mixture was kept for slow evaporation, after 3-4 days, the solution was concentrated to give a green colloid or viscous substance. To this two equivalents of anhydrous $CaCl_2$ with respect to $Cu(ClO_4)_2 \cdot 6H_2O$ in water was added, which resulted in a pale green precipitate. To this equal volume of acetonitrile was added and heated for 5-10 min at 65-70 ^oC to give a bluish green solution. The reaction mixture was filtered, and the filtrate after 3-4 days gave blue crystals upon slow evaporation.

Crystal structure of complex **5** was structurally characterized by X-ray crystallography.The structure of **5** was solved in an achiral space group of $P\bar{1}$ in the triclinic crystal system. The asymmetric unit has two mononegative ions of the complex with one Ca(II) neutralizing the charge (Figure **4.1**). Two mononegative ions of the asymmetric unit are oriented in such a way that the axial water (O7 & O7A) molecules face each other and they are within hydrogen bonding distance of 2.788(6) Å. The geometry around Cu(II) is slightly a distorted square pyramidal (τ 0.146)[6]. The Cu(II) is coordinated with a carboxylate oxygen, a phenolate oxygen and two nitrogen atoms, one from the imine and the other from

the amine, forming the in-plane coordination. Axial coordination of a water molecule completes the fifth coordination. The in-plane bond length ranges from 1.898(2) Å for phenolate oxygen (O5) to 2.016(3) Å for amine nitrogen (N1). The structure of **5** has considerably a longer axial length of 2.316(3) Å for the water oxygen (O7). Ca(II) is hepta coordinated with six water molecules and one carboxylate oxygen. The C3-C4, C2-N1, C3-N1 and C=N bonds at 1.554(4), 1.483(4), 1.493(4) and 1.293(4) respectively, support the formation of new ligand in *in situ*. The selected bond lengths and angles are given in (Table **4.1**).

The ligand has a phenolate, a phenol, an imine, an amine and two carboxylate coordinating groups. Out of the two carboxylates, one is coordinated with Cu(II) and the other with Ca(II). Phenolate oxygen is coordinated with Cu(II), whereas the phenol oxygen remains uncoordinated. The other molecule which is opposite to the Ca(II) bound complex also has similar coordination environment around Cu(II), except one carboxylate remaining uncoordinated. In the crystal lattice the uncoordinated carboxylate oxygen's O3A and O4A are oriented towards two coordinated water molecules O12 and O13 of Ca(II), respectively and they are within hydrogen bonding distances of each other (Figure **4.2**).

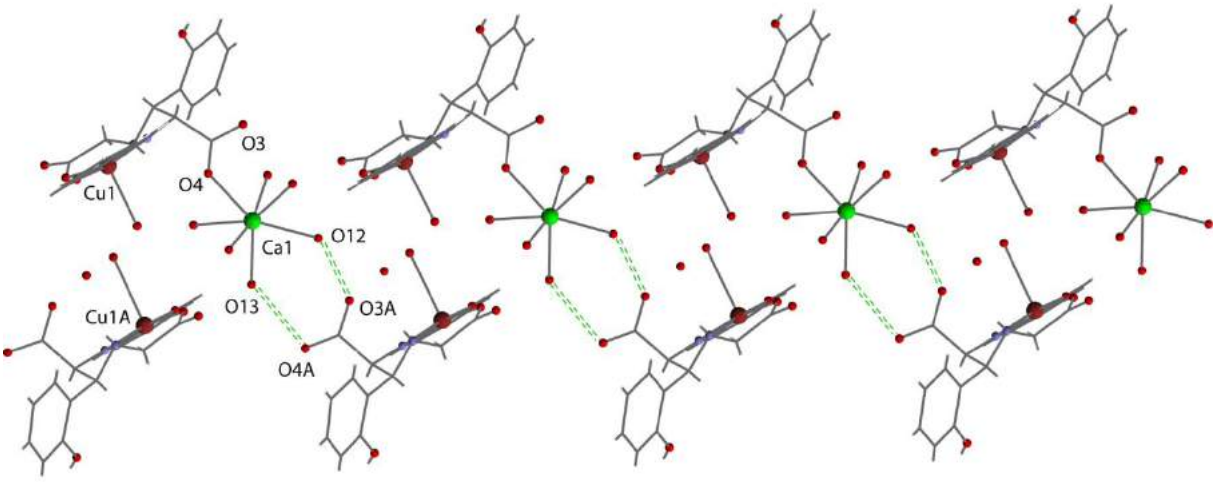

Figure 4.2. Schematic presentation of the Packing diagram showing the orientation of uncoordinated carboxylate towards water molecules coordinated to Ca(II) and the hydrogen bonding between them. Other hydrogen bonding and labeling of other atoms are not shown for clarity.

Table 4.1 Selected crystallographic data [a], bond distances and angles for complex **5**

Complex-**5**	
Empirical formula	$C_{36}H_{32}CaCu_2N_4O_{21}$
M	1023.82
Wavelength (Å)	0.71073
Crystal system	Triclinic
Space group	$P\bar{1}$
a/Å	10.3252(6)
b/Å	13.5239(7)
c/Å	16.7435(10)
α/°	103.136(5)
β/°	91.134(5)
γ/°	103.687(5)
V/Å^3	2205.5(2)
Z	2
ρ/g cm^{-3}	1.539
μ/mm^{-1}	1.165
Flack parameter	-
Reflections collected	18173
Independent reflections	11375
Goodness of fit	1.029
Final R indices [$I > 2\sigma(I)$]	*R1* = 0.0543
	wR2 = 0.1425
R indices (all data)	*R1* = 0.0693
	wR2 = 0.1564

Complex-**5**			
Bond length (Å)		Bond angle (°)	
Cu1-O2	1.959(2)	O2-Cu1-N1	83.75(10)
Cu1-O5	1.898(2)	N1-Cu1-N2	84.97(11)
Cu1-N1	2.016(3)	N2-Cu1-O5	95.75(11)
Cu1-N2	1.925(3)	O5-Cu1-O2	93.50(10)
Cu1-O7	2.316(3)	O2-Cu1-N2	162.72(11)
Ca1-O4	2.437(3)	O5-Cu1-N1	171.46(11)
Ca1-O9	2.414(3)	N1-Cu1-O7	95.82(12)
Ca1-O11	2.483(3)	O5-Cu1-O7	92.53(12)
Ca1-O12	2.360(3)	N2-Cu1-O7	97.52(12)
Ca1-O13	2.432(4)	O2-Cu1-O7	96.61(13)
Ca1-O8	2.312(5)		
Ca1-O10	2.405(3)		
C3-C4	1.554(4)		
C3-N1	1.493(4)		
C2-N1	1.483(4)		
C5-N2	1.293(4)		
C7-O5	1.320(4)		

[a] Refinement method: full-matrix least-squares on F^2.

Table 4.2 H-bonding distances (Å) and angles (°) for the complex **5**

D-H…A	*d*(D-H) (Å)	*d*(H…A) (Å)	*d*(D…A) (Å)	∟D-H…A (°)
		Complex-5		
		Intermolecular H-bonding distances		
O6-H6AA…O3	0.82	1.88	2.68(4)	165
O6A-H7AA…O4A	0.82	1.88	2.70(4)	169
N1A-H1…O14	0.91	2.24	3.03(5)	144
[a]O7…O7A	-	-	2.79(6)	-
		Intramolecular H-bonding distances		
N1-H1AA…O4	0.91	2.32	2.91(4)	122
N1-H1…O3A	0.91	2.36	2.92(4)	120
[a]O9-O3	-	-	2.68(4)	-

[a] Hydrogen on O7 and O9 could not be found from difference Fourier map.

The complex has several inter-molecular and two intra-molecular hydrogen bonding. The water molecules coordinated to Ca(II) are within hydrogen bonding distances to the neighboring carboxylates, phenolates, axial and solvent water molecules. The phenol is within hydrogen bonding distance of 2.684(4) Å (O6…O3) to the neighboring carboxylate. The two intramolecular hydrogen bonding are between, (1) the amine –NH (N1-H1AA) and the coordinated carboxylate oxygen (O3), (2) the water (O9) coordinated to the Ca(II) and the coordinated carboxylate oxygen (O3) (Table **4.1**).

Complex **5** was characterized by FT-IR and UV-vis experiments. The FT-IR spectrum of the complex show strong and sharp imine and carboxylate stretching frequencies between 1630 and 1300 cm^{-1}. The complex is soluble only in water and insoluble in methanol, ethanol, DMF and acetonitrile. Electronic spectra of the complex show essentially five absorption bands between 200 and 700 nm in water, and a small hump at 966 nm. The broad band at 608 nm is assigned for the d-d transition, usual for distorted square pyramidal geometry around Cu(II) (Figure **4.3**).[7] The remaining four absorption bands between 200 and 360 nm are of ligand origin (experimental section).

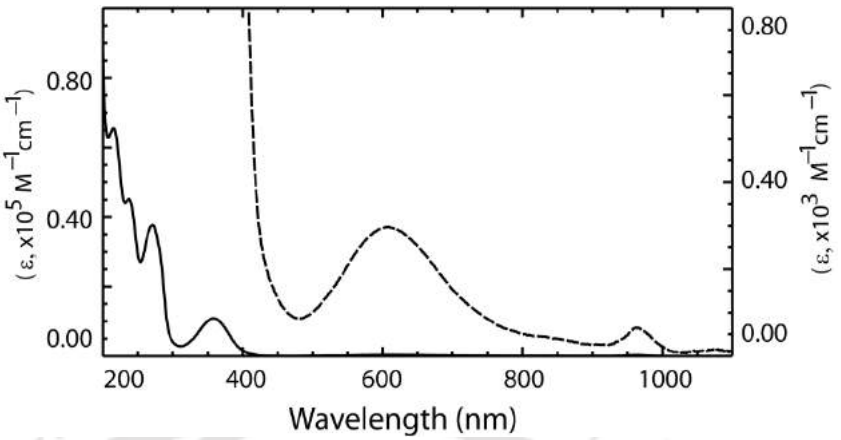

Figure 4.3. UV-vis spectra of **5** in water. (---- 1 x 10^{-4} M and —— 1 x 10^{-5} M)

The reaction was found to be very much sensitive to the reaction condition. The following are the observations which are noted during optimization of the reaction condition. When LiOH•H_2O and KOH were used instead of NaOH, the yield of **5** was found to be less, along with the formation of a pale yellow by-product. Slow evaporation of the reaction mixture (green solution) for 3-4 days to give a green viscous or colloidal substance was found to be a necessary step in the reaction sequence. Addition of anhydrous $CaCl_2$ after the complete addition of Cu(II) salt to a solution of the ligand and NaOH in methanol-acetonitrile mixture did not give complex **5**. Use of acetonitrile in the reaction was found to be essential for the formation of the complex.

4.4.2 C-C bond formation between salicylideneglycinate units

Molecular structure of **5** reveals the presence of a different new ligand in **5** instead of $LiHL^{gly}$. The new ligand has been formed by the C-C bond formation between the salicylideneglycinate units in *in situ* within the reaction conditions. Several other C-C bond formation between transition metal [Cu(II), Ni(II) and Co(III)] complexes of salicylideneglycinate ligands, and aldehydes, ketones and activated olefins were reported in literature[4] (Scheme **4.1**), whereas none was reported between two salicylideneglycinate ligands.

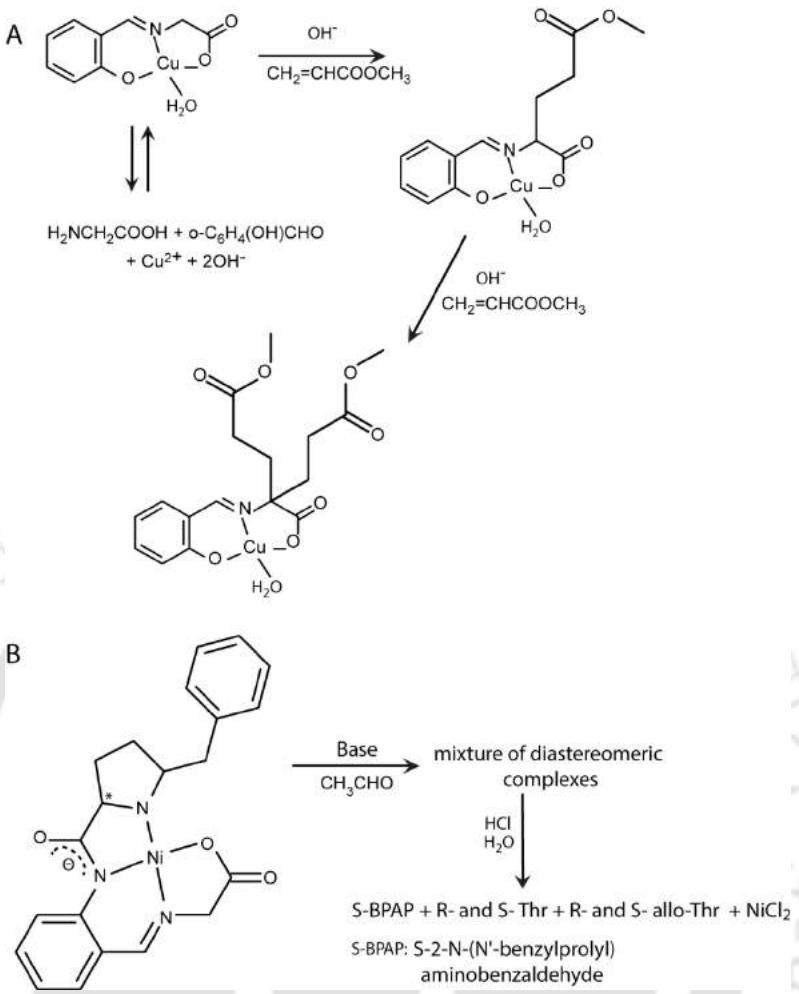

Scheme 4.1. (A) C-C bond formation between Cu(II)-salicylideneglycinate complex and methyl acrylate in presence of base. Scheme redrawn from the reference 4A and (B) C-C bond formation between glycine derived chiral Schiff base Ni(II) complex and acetaldehyde in presence of base. The scheme was redrawn from the reference 4D.

Mechanism for such C-C bond formation reaction was proposed and reported in literature.[5] According to literature; the α-proton of the amino acid moiety in the Schiff base transition metal complex is deprotonated in an alkaline reaction medium and forms a carbanion, which undergoes stabilization through delocalization with the conjugated ligand system. Then, the carbanion undergoes nucleophilic addition to aldehydes, ketones and activated olefins to form corresponding products. This type C-C bond formation reactions were applied in the synthesis of amino acids (glutamic acid, serine and threonine) and

substituted amino acids (β and γ- substituted glutamic acid, β-substituted-β-hydroxy amino acids and α-methyl-α-amino acids).[4]

In the present case, the α-proton of one molecule of the starting ligand ($LiHL^{gly}$) is deprotonated within the reaction condition and forms a carbanion, which can undergo stabilization through delocalization with the π-bonds of the imine and phenyl ring. This carbanion attacks the imine carbon of another molecule of ligand ($LiHL^{gly}$) to form the new ligand in *in situ* (Scheme **4.2**).

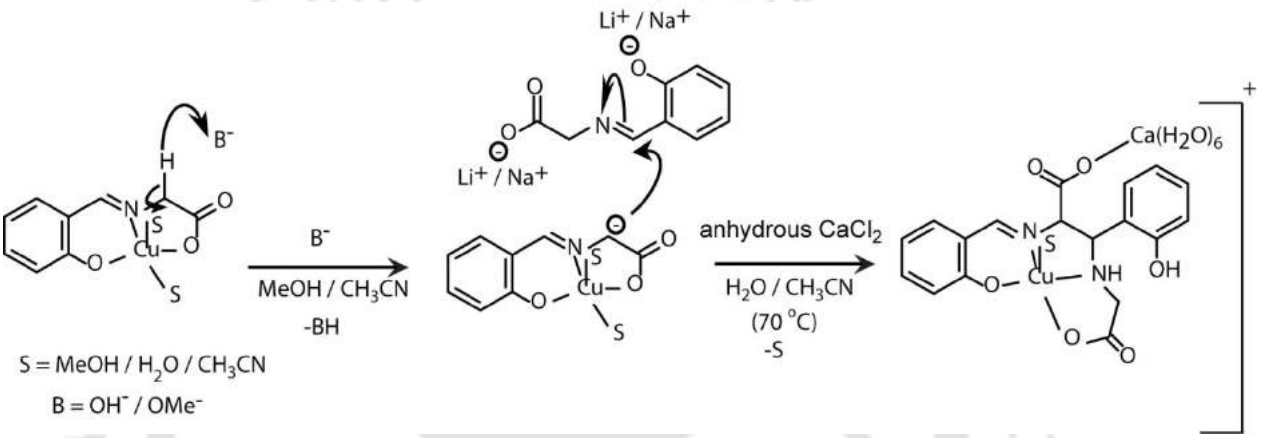

Scheme 4.2. Plausible mechanism for the formation of the new ligand *in situ* in the complexation reaction.

Conclusions

In this chapter we have been able to isolate a mononuclear Cu(II) complex containing a different new ligand and characterized structurally. By exploiting the α-C-H acidity of the glycine derived Schiff base a new ligand was formed *in situ* by nucleophilic addition of carbanion to the carbonyl carbon of imine. The ligand has both the amine and imine functional groups along with carboxylate and phenol groups.

References

1. CrysAlis CCD and CrysAlis RED. Oxford Diffraction Ltd, Yarnton, Oxfordshire, England. Oxford Diffraction, 2009.

2. G. M. Sheldrick, Acta Crystallogr., Sect. A: Fundam. Crystallogr., 2008, A64, 112.

3. M. N. Burnett and C. K. Johnson, ORTEP-III: Oak Ridge Thermal Ellipsoid Plot Program for Crystal Structure Illustrations, Oak Ridge National Laboratory Report ORNL-6895, 1996.

4. (A) Y. N. Belokon, V.M. Belikov, N.I. Kuznetsova and M. M. Dolgaya, *Izv. Akad. Nauk SSSR, Ser. Khim.*, 1972, **6**, 1338; (B) Y. N. Belokon, N. I. Kuznetsova, V. M. Belikov and R. L. Murtazin, *Izv. Akad. Nauk SSSR, Ser. Khim.*, 1972, **10**, 2288; (C) Y. N. Belokon, N. I. Kuznetsova, R. M. Murtazin, M. M. Dolgaya, T. B. Korchemnaya and V. M. Belikov, *Izv. Akad. Nauk SSSR, Ser. Khim.*, 1972, **12**, 2772; (D) Y. N. Belokon, N. I. Chernoglazova, K. A. Kochetkov, N. S. Garbalinskaya, M. G. Ryzhov, V. I. Bakhmutov, M. B. Saporovskaya, E. A. Paskonova,V. I. Maleev, S. V. Vitt and V. M. Belikov, *Izv. Akad. Nauk SSSR, Ser. Khim.*, 1984, **4**, 804; (E) Y. N. Belokon, N. I. Chernoglazova, N. S. Garbalinskaya, M. B. Saporovskaya, K. A. Kochetkov and V. M. Belikov, *Izv. Akad. Nauk SSSR, Ser. Khim.*, 1986, **10**, 2340; (F) Y. N. Beloko, A. G. Bulychev, M. G. Ryzhov, S. V. Vitt, A. S. Batsanov, Y. T. Struchkov, V. I. Bakhmutov and V. M. Belikov, *J. Chem. Soc. Perkin Trans.*, 1986, 1865.

5. (B) A. E. Martell, *Acc. Chem. Res.*, 1989, **22**, 115; (B) D. E. Metzler, M. Ikawa and E. E. Snell, *J. Am. Chem. Soc.*, 1953, **76**, 648.

6. The amount of distortion was calculated from the structural data where the value of τ should be 0 for the perfect square-pyramidal geometry and 1 for the perfect trigonal bipyramidal structure; A. W. Addision, T. N. Rao, J. Reedijk, J. van Rijn and G. C. Verschoor, *J. Chem. Soc., Dalton Trans*., 1984, 1349.

7. M. R. Wagner and F. A. Walker, *Inorg. Chem.*, 1983, **22**, 3021 and references therein; (b) N. Arulsamy and P. S. Zacharias, *Transition Met. Chem.*, 1991, **16**, 255; (c) A. B. P. Lever, *'Inorganic Electronic Spectroscopy'*, 2nd ed., Elsevier, New York, 1984.

Publications

1. C. M. Rajesh and M. Ray, *Dalton Trans.*, 2014, **43**, 12952.
2. Two manuscripts based on chapter 3 and 4 are to be submitted.

Conferences and Symposia

1. MTIC-XV, 13-16 Dec., 2013, held at Indian Institute of Technology Roorkee, Roorkee - **Poster presentation**.
2. Frontiers in Chemical Science (FICS-2014), held at Indian Institute of Technology Guwahati, Guwahati - **Poster presentation**.